Developing a One-Dimensional, Two-Phase Fluid Flow Model in Simulink

James Edward Yarrington

Thesis submitted to the faculty of the Virginia Polytechnic Institute and State University in partial fulfillment of the requirements for the degree of

Master of Science

In

Mechanical Engineering

Alan A. Kornhauser, Chair

Yang Liu

Robert E. Masterson

12/9/2013

Blacksburg, Virginia

Keywords: Simulink, One-Dimensional, CFD, Two-Phase

Developing a One-Dimensional, Two-Phase Fluid Flow Model in Simulink

James Edward Yarrington

ABSTRACT

In this thesis, a one-dimensional, two-fluid model is developed in MATLAB-Simulink. The model features a mass, momentum, and energy balance for each fluid—an ideal gas and an incompressible liquid. The simulation may model a straight pipe section, or a pipe section that involves a cross-sectional area change. Rough models of interphase heat transfer and interphase friction are included. Currently, phase change is not modeled in the simulation

Also, a single-fluid model was developed before the two-fluid model, as an intermediate step in developing the two-fluid model. The single-phase simulation applies a mass, momentum, and energy balance for the single fluid, and ideal gas.

The single-fluid model was validated by incompressible flow, Fanno flow, and isentropic flow models. The incompressible model demonstrated the simulations ability to properly balance pressure and frictional forces. The Fanno flow model showed that the simulation could capture compressibility effects. The isentropic flow model validation verified that the simulation could model area change properly.

The two-fluid model was validated using the Homogeneous Equilibrium Model (HEM). An analytical model of HEM flow with frictional pressure drop was developed to compare against the simulation results. To achieve the HEM, interphase effects were tuned so that the liquid and gas phases had similar temperatures and velocities. Under these conditions, the simulation matched the analytical model.

The thesis goal is to create a solid foundation for an open-source, one-dimensional, two-fluid model that is easier to use and modify than current nuclear system analysis software.

Table of Contents

List of Figures

List of Tables

Introduction

One-Dimensional, Two-Fluid Models

One-dimensional, two-fluid modelling packages, such as RELAP (Idaho National Laboratory, 2005), TRAC (Liles, 1988), and TRACE (United States Nuclear Regulatory Commission, 2012), model fluid flow for the purposes of nuclear reactor analysis. The simulations discretize the simulated flow path into control volumes, which balance the mass, momentum, and energy flowing across their boundaries. Time is also discretized, where each time step brings a new state for each control volume in the system. For each time step, each control volume uses information from adjacent control volumes to determine how much mass, momentum, and energy transfers across each boundary. One-dimensional models simplify fluid flow by limiting the mass, momentum, and energy balance equations to one axis. While a three-dimensional model would capture the intricacies of three-dimensional movement, like travelling through a pipe bend, or contracting through a nozzle, one-dimensional models represent these effects by incorporating empirical correlations into their balance equations.

Two-fluid models employ a mass, momentum, and energy balance for both fluids, effectively dividing each control volume in two—one for each fluid. Two-fluid simulations transfer information, mass, momentum, and energy, not only between adjacent control volumes, but between the fluids within the same control volume. The resulting simulation: two fluids flow through the same medium, affected by the constraints placed on the system as well as the interactions between the fluids. Homogenous equilibrium models (HEM) represent two fluids flowing through the same medium, but are not true two-fluid models; HEMs only model one fluid with the properties of the two-fluid mixture.

Motivation

Though several one-dimensional, two-fluid models exist, these models involve some deficiencies. For one, the source code behind the simulations is often unavailable due to proprietary restrictions. This presents the user from knowing the exact mechanisms of the program. For instance, if a piece of simulation software allows the user to adjust a friction factor, without the source code, the user may poorly define the parameter and incorrectly model their system.

Furthermore, while some factors can be modified by users, several correlations are locked into the original state. This reduces flexibility, preventing the user from creating more customized models.

Finally, many current one-dimensional models lack an intuitive front-end that allows the user to interact with their system. Rather than change values within a text file to adjust the model, a user should be able to interact with a graphical user interface to easily find (and change) any desired parameters. An improved user interface would lessen the burden on the user manual to provide usage instructions.

Addressing Concerns

The new simulation developed in this thesis will address these three concerns. The user's simulation will be done through MATLAB-Simulink. Simulink allows the user to graphically arrange and connect pieces of code to build a model. Once the model is created, Simulink provides several ordinary differential equation solvers to simulate the system, time-step by time-step. This provides a perfect environment in which to simulate a one-dimensional fluid model.

The Simulink interface remedies the three concerns I presented in the Motivation section. With the fluid model components developed, the user can easily arrange the components to create a series of connected control volumes. System constraints can be changed directly on the front-end; the simulation does not require a large text file with lists of settings for each component. If the user wishes to examine and modify the source code of a certain part of the simulation, simply double-clicking the component reveals the desired information.

Model Overview

This section contains a brief overview of how the simulation functions. For a complete explanation, including the governing equations, please see "Single-Phase Simulation" on page 7 and "Two-Phase Model" on page 22.

The new software employs alternating "junction" and "volume" blocks to simulate the flow of fluid along a pipe—dividing the work of the control volumes explained in the "One-Dimensional, Two-Fluid Models" section. Each volume block calculates the state of the fluids contained in its boundaries, solving the time derivative of the flow across its boundaries. Each junction performs the space-derivatives of the simulation, taking the state of adjacent volume blocks to determine the flow rates between them. **Figure 1** shows the transfer of information between the volumes and junctions. Junction blocks require the state of the fluids in the adjacent blocks at the previous time step to determine flow rates. Volume blocks use those flow rates—along with the initial conditions—to determine the total mass, momentum, and energy contained within the volume. The volume blocks then determine density, velocity, and temperature from the mass, momentum and energy totals, passing this information to the neighboring junction blocks for the next time step's calculations. The cycle of volume and junction blocks exchanging information perpetuates until the simulation reaches the preset stopping time

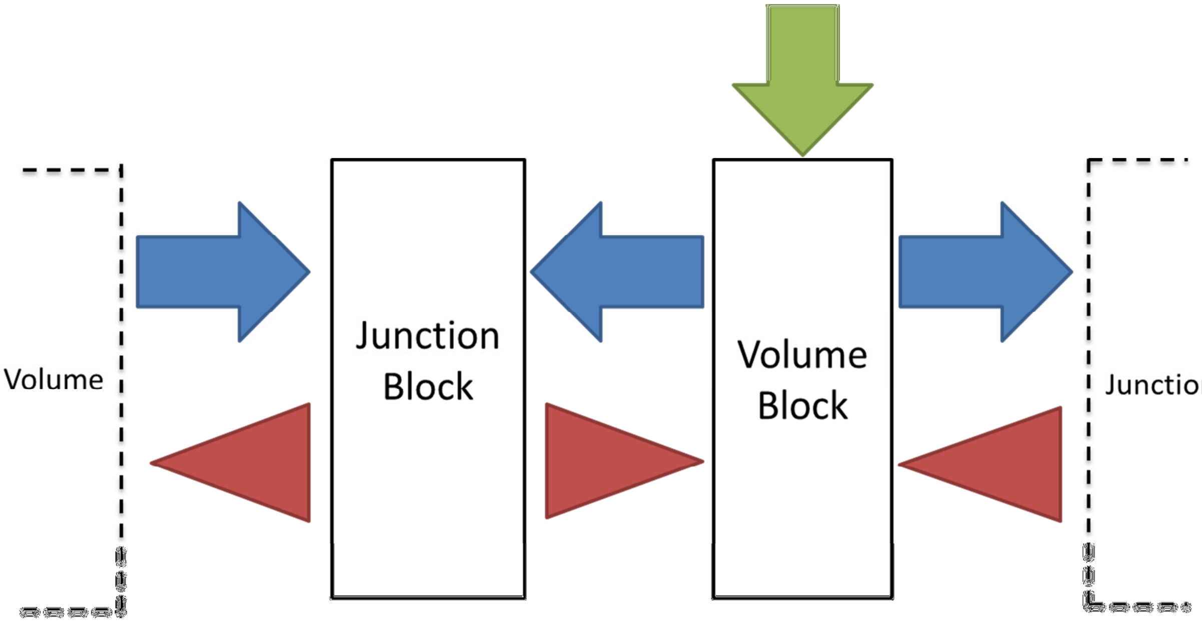

Figure 1. The transfer of information between simulation components. The horizontal arrows represent volume data, including geometry, fluid state, and velocity, which pass to adjacent junction blocks at each iteration. The triangles contain junction data, including friction and various flow rates, which pass to adjacent volume blocks. The vertical arrow represents the initial conditions of a volume block. The vertical arrow contains the same type of information as the horizontal arrows, except that the information is only used once at the beginning of the simulation.

At the start of the simulation, each volume block receives information describing the geometry of that section of the pipe: the cross-sectional area; the length; and the angle above horizontal. Adjusting the geometric settings of each volume block allows the user to model expansion, contraction, upward flow, downward flow, or a combination of any of those four. **Figure 2** shows several volumes connected that use different areas, lengths, and angles. Along with the geometry, the volume blocks receive the initial condition of the fluids within their boundaries. This information allows the volume blocks to calculate the starting point for the total mass, momentum, and energy they each contain.

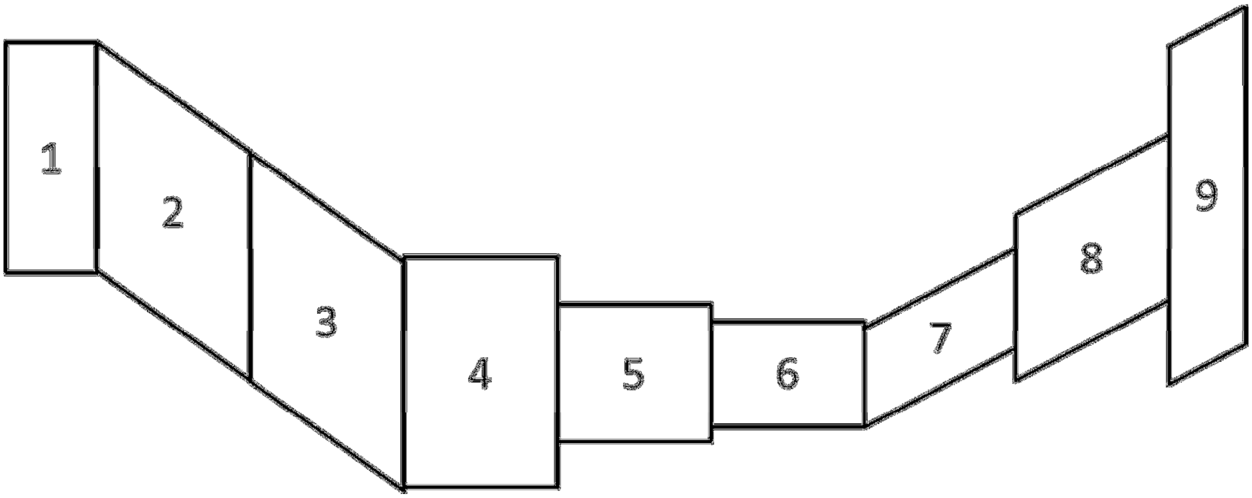

Figure 2. Representation of a possible simulation setup. The nine shapes represent the discretization of a pipe section that contracts, expands, falls, and climbs. To accomplish this, the pipe is divided into sections that have varying angle, cross-sectional area, and length. Sections 2 and 3 have negative angles relative to the horizontal, while sections 7, 8, and 9 have positive angles. Contraction occurs between sections 4 through 6, as each successive section has a smaller cross-sectional area. Sections 7 through 9 expand, increasing the cross-sectional area. Finally, sections 1 and 9 have shorter lengths than the other sections.

Initially, a single-phase model was developed, using only an ideal gas as the simulation fluid. This simple model was used as an intermediate point during development of the two-phase model. In the single-phase model, the junction blocks calculate the mass, momentum, and energy flow rates of the ideal gas (space derivatives), while the volume blocks determine the state of the ideal gas, using the mass, momentum, and energy stored within the volume, along with the ideal gas law (time derivatives). To appropriately constrain the system, the simulation requires an inlet temperature and density, as well as an outlet pressure. This is equivalent to a pressure drop across the pipe plus the state of the source fluid. To facilitate change of direction, the temperature and density are defined on both boundaries; however, only the pressure (calculated from temperature and density using the equation of state) is used on the exit boundary.

The two-phase model adds an incompressible liquid phase to the ideal gas-phase. Developed after the single-phase model, the two-phase model employs the same structure as the original, with a few exceptions. The junction blocks transmit two sets of flow data; one mass, momentum, and energy flow rate for each phase. Likewise, the volume blocks perform an extra set of balances to manage the additional fluid.

At each time step, the volume each fluid occupies fluctuates, so the ideal gas relationship cannot initially be used. Because the liquid phase has a constant density, the volume it occupies can be found from the total liquid mass within the volume block. The remaining volume belongs to the gas phase, and is used for the ideal gas equation of state calculations. Liquid pressure equals the gas pressure derived from the ideal gas relationship.

Furthermore, the two fluids interact with one another within the volume block. Momentum transfers from one phase to the other due to friction driven by a velocity difference. Energy transfers due to heat transfer driven by a temperature difference.

With the second set of balance equations added for the liquid, three additional constraints must be added to the system—in addition to the inlet gas density, inlet gas temperature, and outlet pressure. First, as the liquid is incompressible, the fluid density is predefined at the start of the simulation. Then the addition of inlet void fraction and inlet liquid temperature completely define the state of the two fluids entering the system.

Literature Review

This literature review briefly covers the history of one-dimensional, two-fluid modelling. It also highlights the origins of several concepts employed by this thesis. This section also introduces previously developed models; however, the section “Comparison to Previous Work” contains more details on how these models compare to the model described by this thesis.

One of the earliest two-fluid modelling schemes was developed by (Martinelli & Nelson, 1948). This oft-cited work represents two-fluid flow by applying an empirically derived correction factor to a single-fluid model. As explained by (Todreas & Kazimi, 2012), the application of two-fluid models to nuclear systems began later in the 1960s. This led to the accepted convention of models applying balances across control volumes, as in (Collier & Thome, 1994). Further evolution led to the more recent method of local instant formulation, by (Ishii & Takashi, 2011), which solves for properties at centers of volumes with unknown boundaries.

Within the past 25 years, several one-dimensional models have been developed. This thesis compares these models with the new simulation developed in this thesis in the Comparison to Previous Work section. (Scheuerer & Scheuerer, 1992) developed a one-dimensional, two fluid model utilizing mass and momentum balance equations. (Herrán-González, De La Cruz, De Andrés-Toro, & Risco-Martín, 2009) developed one dimensional models for Simulink to simulate natural gas distribution pipelines, accounting for elevation change, but also neglected the energy equation. (Davis & Campbell, 2007) created a one-dimensional fluid flow model utilizing mass, momentum and energy balance equations, utilizing the REFPROP database to determine fluid states. Davis’s simulation models two fluids by assuming homogenous equilibrium, treating the two fluids as a single substance. Other, more unique methods of simulating fluid flow include (Alamian, Behbahani-Nejad, & Ghanbarzadeh, 2012), who solved the governing equations as state-space equations.

The standard of comparison for the simulation created in this thesis, RELAP (Idaho National Laboratory, 2005), models one- and two-dimensional flow using volumes and the junctions that connect them. The section “RELAP Comparison” contains more information on the underlying equations balance equation that govern RELAP. Other commercial software, such as TRAC (Liles, 1988), also model the thermal-hydraulics of nuclear systems. Later, TRACE combined the functionality of RELAP and TRAC (United States Nuclear Regulatory Commission, 2012).

Several resources proved to be vital in the development of the simulation. As the simulation was created in the MATLAB-Simulink environment, the associated documentation, (The MathWorks, Inc, 2012), helped immensely. The integral form of the balance equations found in (Potter & Foss, 1982) provided a check to ensure that the simulation followed the governing equations properly. The extrapolation methods explained in (Hirsch, 1990) were employed at the boundaries of the system. A modification of the smooth-pipe correlation presented in (Incropera, DeWitt, Bergman, & Lavine, 2007) was used to programmatically determine friction factor from Reynolds number. To validate the simulation, the Fanno and Isentropic gas tables from (Keenan & Kaye, 1948), provided a starting point, though not used in the final validation calculations; the validation equations were provided by (Munson, Young, & Okiishi, 1998).

Single-Phase Simulation

The one-dimensional, single-phase simulation models the flow of an ideal gas within a pipe section. The independent variables of the simulation include the total mass, momentum, and energy contained within control volumes. The volume blocks, which perform calculations on their respective control volumes, use the ideal gas law to determine the state (velocity, temperature, density) of the fluid from the independent variables. Connecting the volume blocks, junction blocks receive the state information to determine the mass, momentum, and energy flow rates between volume blocks. In the next time step, the volume blocks use the flow rates to determine the new quantities of mass, momentum, and energy stored in their control volumes. This section details the calculations of the junction and volume blocks.

Junction Calculations

As seen in **Figure 1**, the function of junction blocks is to provide mass, momentum, and energy flow rates to adjacent volume blocks. This information describes how much of a quantity (mass, momentum, or energy) passes from one volume to another. The junction blocks accomplish this by averaging the properties of adjacent volumes, then calculating mass, momentum, and energy flow rates according to the averaged properties.

Property Averaging

To calculate a junction property, the simulation finds the length-weighted average,

$$X = \frac{X_{+\frac{1}{2}}L_{-\frac{1}{2}}+X_{-\frac{1}{2}}L_{+\frac{1}{2}}}{L_{+\frac{1}{2}}+L_{-\frac{1}{2}}} \tag{1}$$

where X is the property being averaged, L is the length, and the subscripts $+\frac{1}{2}$ and $-\frac{1}{2}$ refer to the right and left adjacent volumes, respectively. **Figure 3** below illustrates the subscript nomenclature for when a junction is the focus. Moving to the next junction either increases (right) or decreases (left) the subscript by one. When moving to an adjacent volume the increase or decrease is one-half.

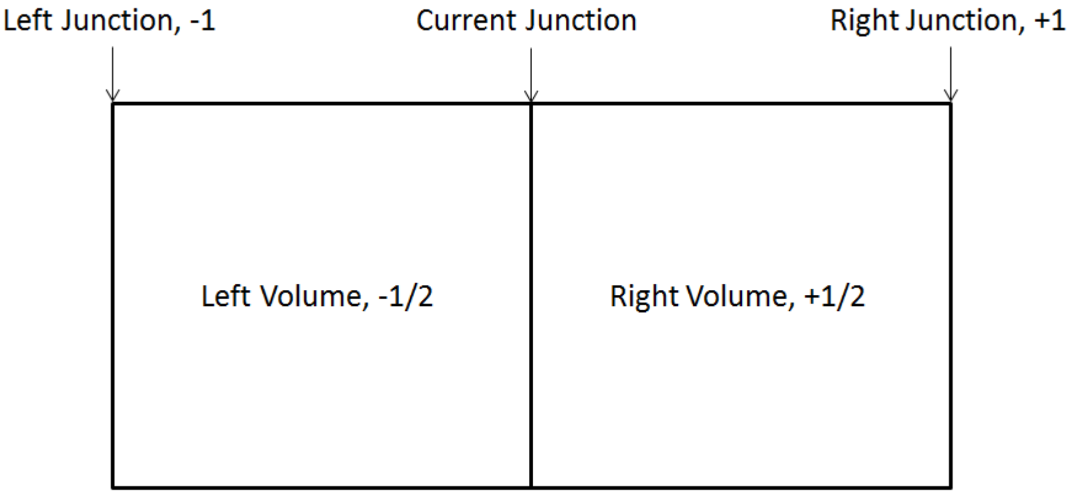

Figure 3. Diagram explaining junction subscript nomenclature. When making calculations of the properties of a junction, subscripts refer to the relative position of volumes or other junctions. Half-steps refer to the left (negative) or right (positive) adjacent volumes. Whole steps refer to the nearest junctions to the left (negative) or right (positive).

The simulation uses Equation (1) to find the temperature, density and velocity of the junction. With these values known, the simulation calculates pressure,

$$P = \rho T R \tag{2}$$

where ρ is density, T is temperature and R is the specific gas constant for the fluid.

Mass and Momentum Flow Rate

The junction block then calculates the mass, momentum and energy flows between its adjacent volumes. These three flow rates come from the flow properties within the junction—the length-weighted properties of the adjacent volumes. Mass flow,

$$\dot{m} = VA\rho \tag{3}$$

representing the mass that crosses the junction block to leave one control volume and enter another. Similarly, momentum flow,

$$\dot{M} = \dot{m}V \tag{4}$$

represents the momentum that the mass from Equation (3) carries from one control volume to another.

Energy Flow Rate

The mass flowing from one control volume to the next also carries energy, including enthalpy, kinetic energy, and potential energy. The total energy contained in a unit mass passing between the two volumes,

$$e = h + ke + pe \tag{5}$$

where kinetic energy,

$$ke = \frac{V^2}{2} \tag{6}$$

and potential energy,

$$pe = \rho g H \tag{7}$$

where H is the junction height, and enthalpy,

$$h = u + \frac{P}{\rho} \tag{8}$$

where internal thermal energy,

$$u = c_V T \tag{9}$$

where C_V is the constant-volume specific heat of the fluid and assumed constant, and the reference point for temperature is arbitrarily set at absolute zero. Thus, the total energy passing from one volume to another per unit mass,

$$e = \frac{V^2}{2} + c_V T + \frac{P}{\rho} + \rho g H \tag{10}$$

The total energy flow,

$$\dot{E} = \dot{m}e = \dot{m}(\frac{V^2}{2} + c_V T + \frac{P}{\rho} + \rho g H) \tag{11}$$

which is the total energy that the mass flow, from Equation (3), carries with it from one control volume to another. The energy flow equations simplifies further to

$$\dot{E} = \dot{m}(T[c_V + R] + \frac{V^2}{2} + \rho g H) \tag{12}$$

when the fluid is an ideal gas. The flows determined by equations (3), (4), and (12) are used by the adjacent volumes to determine how much mass, momentum and energy enters and leaves during the following time step.

Friction

The junction calculates frictional force as well. Three scenarios exist for friction calculations—no friction, constant friction factor, and smooth pipe friction. With a constant friction factor, including zero for the no friction case, calculations for frictional force begin at Equation (17).

For the smooth pipe friction calculation, friction factor is determined by Reynolds number,

$$Re_D = \frac{\rho V D_h}{\mu} \tag{13}$$

where V is the velocity of the fluid within the pipe, D_h is the hydraulic diameter, and μ is the dynamic viscosity. The simulation estimates dynamic viscosity as,

$$\mu = \mu_0 \sqrt{\frac{T}{T_0}} \tag{14}$$

where the subscript 0 refers to a reference point. In the simulation, this point,

$$(T_0, \mu_0) = (300\ [K], 1.983 \bullet 10^{-5}\ [Pa - s]) \tag{15}$$

With Reynolds number known, the simulation calculates friction factor,

$$f = \begin{cases} \frac{64}{Re_D} & , \quad Re_D < 1189.4 \\ 0.316 Re_D^{-\frac{1}{4}}, & 1189.4 < Re_D \leq 49{,}818.9 \\ 0.184 Re_D^{-\frac{1}{5}}, & Re_D \geq 49{,}818.9 \end{cases} \tag{16}$$

where the three equations come from (Incropera, DeWitt, Bergman, & Lavine, 2007). Typically, the transition points for the three equations occur at 2,300 and 20,000, but these points did not create a function that was continuous over the desired range of Reynolds numbers. The cut-off points in Equation (16) allow for a smoother transition between friction factor formulas.

Whether the friction factor was calculated or a constant, the simulation calculates the wall shear stress,

$$\tau_s = \frac{V^2 \rho f}{8} \tag{17}$$

and then frictional force,

$$F_f = \frac{(L_{+\frac{1}{2}} + L_{-\frac{1}{2}})\pi D_h \tau_s}{4} \tag{18}$$

The sign of F_f depends on the sign of V, such that the frictional force is always applied opposite fluid motion. Specifically, the code applies the opposite sign of V to F_f. The simulation divides the friction factor by four because of averaging explained in the volume block section.

The junction block sends the mass flow rate, Equation (3), momentum flow rate, Equation (4), energy flow rate, Equation (12), and friction force, Equation (18), to the adjacent volume blocks so that the total mass, momentum, and energy in that volume block may be calculated for the next time step. Please note that wall heat transfer is not yet included in the model. When included, it will operate in a similar manner to friction; the temperature difference between the fluid and the wall will drive heat transfer, much like the velocity difference between the fluid and the wall drives friction.

Volume Calculations

At the start of each time step, the volume blocks receive flow rates from the adjacent junction blocks. The flow data includes mass flow, momentum flow, and energy flow, as well as frictional force. The volume block uses the flow rates and forces to determine the new mass, momentum and energy of the fluid within the block for the current time step. Combined with the geometry of the block, the mass, momentum, and energy held within the control volume determine the state of the fluid: the temperature, density, pressure, and velocity. The state of the fluid, is passed to the neighboring junction blocks in order to calculate the flow rates (and friction) for the next step.

When calculating volume properties, the subscripts show the relative position of other blocks. The nomenclature for these subscripts parallels the nomenclature for junction calculations—shown in **Figure 3**. Junctions lay directly next to volumes, so the subscript decreases (left) or increases (right) by one-half when referring to an adjacent junction. Another step further—to the nearest volume—results in a subscript change of one. **Figure 4** below shows this relationship between the volume in question and its nearby blocks.

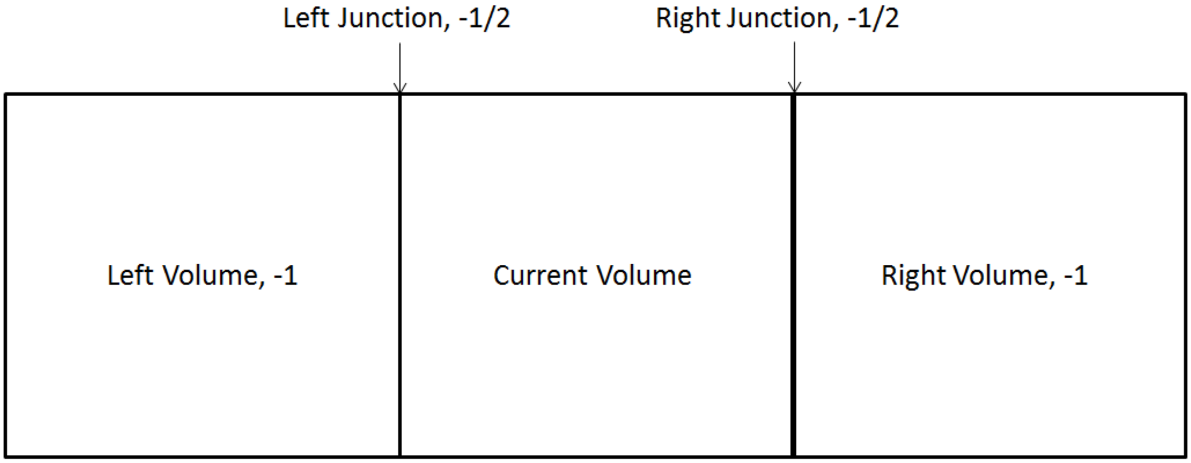

Figure 4. Diagram explaining volume subscript nomenclature. When making calculations of the properties of a volume, subscripts refer to the relative position of junctions or other volumes. Half-steps refer to the left (negative) or right (positive) adjacent junctions. Whole steps refer to the nearest volumes to the left (negative) or right (positive).

Mass and Energy

The volume first finds the rate of change of mass, momentum, and energy of the fluid within the volume block. The net rates of change of mass and energy are simply

$$\dot{m}_{net} = \dot{m}_{-\frac{1}{2}} - \dot{m}_{+\frac{1}{2}} \tag{19}$$

and

$$\dot{E}_{net} = \dot{E}_{-\frac{1}{2}} - \dot{E}_{+\frac{1}{2}} \tag{20}$$

where the subscripts refer to the flows of the adjacent junctions; $+\frac{1}{2}$ and $-\frac{1}{2}$ refer to the left and right adjacent junctions, respectively. Using Equation (25) below, the volume block integrates the rates of change to determine the total mass and energy held in the control volume at that time step.

Momentum

Because the change in momentum not only includes the fluid flow, but frictional and pressure forces as well, the net rate of change equation for momentum contains more terms than the corresponding mass and energy equations. The frictional force is already calculated by the adjacent junctions and passed to the volume block.

Pressure

Driving the flow of fluid through the pipe is the pressure differential from one end to the other. Likewise, each volume block has a pressure differential—the pressure calculated in its adjacent junction blocks. With a pressure differential, the net force applied on the block due to pressure,

$$F_P = (P_{-\frac{1}{2}} - P_{+\frac{1}{2}})A \tag{21}$$

However, the simulation allows for varying area so the right and left boundaries of the volume block may not have the same area. **Figure 5** shows the force balance (for pressure forces) acting on a volume block whose neighbors do not have equal cross-sectional areas; the double lines create the borders of the volume blocks. The upstream pressure is applied over the upstream volume's area, while the downstream pressure is applied over the downstream volume's area, depicted by arrows in the figure.

If the upstream and downstream cross-sectional areas differ, the (hypothetical) walls of the volume block will slant, as seen in the light dotted lines in **Figure 5**. The slanted walls apply a pressure force normal to their surface; considering the component of pressure force in the flow dimension, the resulting force is shown by triangles in **Figure 5**. The pressure force applied is the product of the volume's pressure and the difference between the upstream and downstream area.

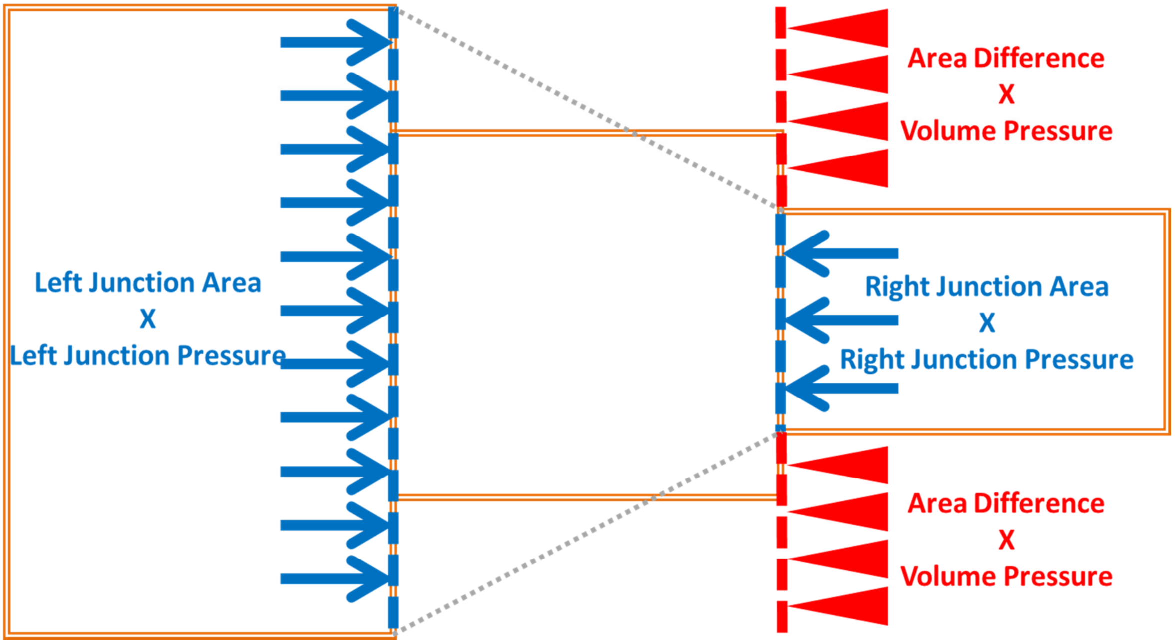

Figure 5. Illustration of the pressure forces acting on a volume block. The pressure differential between the left and right junctions provides the driving force behind fluid motion. The circumferential pipe wall does not contribute to fluid motion, as the uniform pressure along the circumference of the pipe cancels itself. The remaining surface area of the volume, the difference between the upstream and downstream area, applies force to the fluid equal and opposite to the pressure force the fluid applies on that same area, shown with arrows.

Therefore, the net force due to pressure acting on the volume,

$$F_P = P_{-\frac{1}{2}}A_{-1} - P_{+\frac{1}{2}}A_{+1} + \frac{1}{2}\left(P_{-\frac{1}{2}} + P_{+\frac{1}{2}}\right)(A_{+1} - A_{-1}) \tag{22}$$

The final term in Equation (22) is the average pressure within the volume applied over the area difference. If the flow is expanding from left to right, the area difference will be positive, which correctly results in an additional pressure force acting in the positive (right) direction.

Weight

Weight is the final force acting on the fluid. If the pipe is completely horizontal, then the momentum balance contains no weight term, as no component of the weight lies in the axis of flow. If, however, the pipe has any other angle, then weight,

$$\cancel{W} = \rho\cancel{V}g \bullet sin(\theta) \tag{23}$$

where θ is the angle above horizontal and $\cancel{V}$ is the volume of the cell.

Integration

With terms for pressure force, friction, and weight developed, the net change in momentum over time of the volume,

$$\dot{M}_{net} = \left(\dot{M} + F_f\right)_{-\frac{1}{2}} + \left(-\dot{M} + F_f\right)_{+\frac{1}{2}} + F_P + -\cancel{W} \tag{24}$$

with the $-\frac{1}{2}$ components from the left junction, and the $+\frac{1}{2}$ components from the right junction. Next, the volume block finds how much mass, momentum and energy is within its boundaries. The current amount of a property,

$$X(t_0 + \Delta t) = \int_{t_0}^{t_0+\Delta t}\left(\dot{X}\right)dt + X(t_0) \tag{25}$$

where t_0 is the time of the last simulation step, Δt is the time between the current and last simulation step, and $X(t_0)$ is the value of the property at time t_0. Equation (25) applies to mass, momentum and energy within the volume block.

Initial Conditions

Initial conditions are needed for the first time step; else equation (25) would be undefined. Because the user cannot directly measure initial quantities of mass, momentum, and energy, the user defines the state using temperature, density and velocity. The simulation then converts these values to mass, momentum, and energy so that equation (25) can be used. The initial mass,

$$m_0 = \cancel{V}\rho_0 \tag{26}$$

where the volume of the cell,

$$\cancel{V} = AL \tag{27}$$

the initial momentum,

$$M_0 = m_0V_0 \tag{28}$$

and the initial energy,

$$E_0 = m_0 \left(c_V T_0 + \frac{V_0^2}{2} + gH \right) \tag{29}$$

where the subscript 0 refers to the initial condition at the first time step.

MATLAB-Simulink Integration

Simulink provides several ordinary differential equation (ODE) solvers; when used with the one-dimensional, one- and two-phase models, Simulink treats the entire system as a system of ODEs. According to the documentation (The MathWorks, Inc, 2012), Simulink computes the states—variable values—at each time step using the user-selected solver. Time steps vary based on the rate of changes of the states; rapidly changing states require smaller time steps to improve accuracy.

The ODE solvers split into two categories, stiff and non-stiff. A stiff ODE involves variation on a short time scale relative to the overall simulation time. The one-dimensional, one- and two-phase models are stiff ODEs, as small fluctuations in a variable such as mass lead to fluctuations in other variables, perpetuating the problem. Stiff ODE models require stiff ODE solvers, like the “ode23tb” solver used for the validation cases starting on page 33, to overcome the instability associated with stiff ODEs.

The stiff ODE solver, ode23tb, is the solver used primarily during the development of this thesis. The documentation describes this solver as “An implementation of TR-BDF2, an implicit Runge-Kutta formula with a first stage that is a trapezoidal rule step and a second stage that is a backward differentiation formula of order 2.” (The MathWorks, Inc, 2012).” Ode23tb was selected through trial-and-error, selecting the most efficient solver that reliably finished simulations to steady state without encountering an error.

Ideal Gas State

Once the volume block has a defined mass, momentum, and energy within its boundaries, it calculates the fluid properties for use by the adjacent junction blocks. Because the fluid is an ideal gas, the definition of density,

$$\rho = \frac{m}{V\!\!\!-} \tag{30}$$

is used to find the density, as it is assumed the fluid consumes all available space within the cell. Also, the definition of momentum,

$$M = mV \tag{31}$$

is solved for velocity,

$$V = \frac{M}{m} \tag{32}$$

Velocity and density, along with the energy equation—equation (10) above—are used to find temperature,

$$T = \frac{1}{c_V} \left(\frac{E}{m} - \frac{V^2}{2} - Hg \right) \tag{33}$$

where the flow work term, $\frac{P}{\rho}$, has been removed, as the fluid is not performing net work within the block; flow work is only considered during mass transfer. Although the fluid has been completely defined, pressure is also calculated, using equation (2) above, so that the volume's pressure is available when finding the pressure force balance, using equation (22) above.

With the time derivative complete, and the state of the fluid found, the simulation sends the state of the fluid to the adjacent junction blocks to calculate the flow rates (space derivatives) and friction for the volume block's next time step.

Boundary Conditions

Solving a fluid flow problem requires boundary conditions. With three governing equations—mass continuity, momentum conservation, and energy conservation—the simulation needs three boundary conditions. More boundary conditions leads to an over-constrained model, while fewer boundary conditions leave the model undefined. The one-fluid simulation requires an inlet density, inlet temperature, and outlet pressure. This provides an overall pressure drop that drives fluid flow, as well as the state of the fluid entering the model. For the sake of symmetry—allowing reverse flow—the user provides a density and temperature for both ends of the simulation. For the boundary with exiting flow, the code only uses the defined density and pressure to calculate the boundary pressure. **Figure 6** illustrates the dynamic boundary conditions used by the simulation for forward and reverse flow.

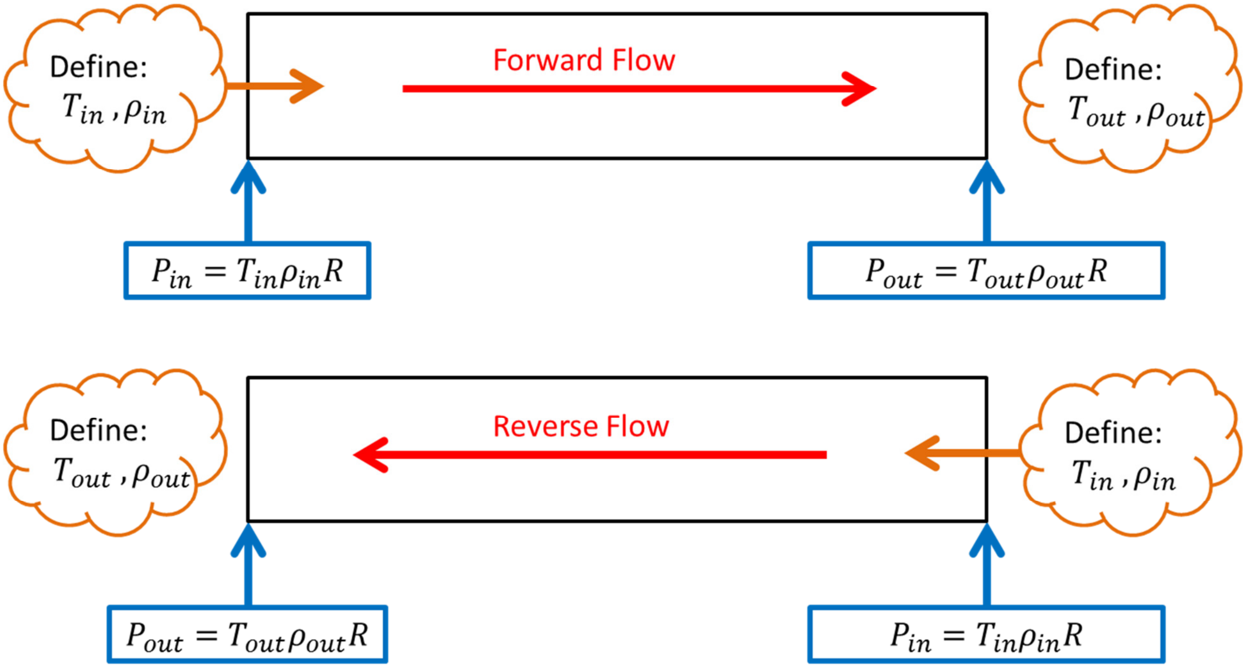

Figure 6. Boundary condition usage. For both forward and reverse flow conditions, density and temperature is defined for both boundaries. This definition of state leads to a pressure defined on both ends of the simulation. For forward flow, the left boundary supplies the state of the fluid entering the simulation—same for reverse flow and the right boundary. The temperature and density of the other boundary remain unused after pressure is defined. For both cases, this yields a complete state—temperature and density—inlet condition and a pressure exit condition; the simulation's three boundary conditions match the three governing mass, momentum, and energy equations.

The junction and volume blocks described in the previous sections do not account for boundary conditions. Each volume block functions as if it is adjacent to two junction blocks. Each junction block finds the length-weighted average of the adjacent volume blocks, using Equation (1), before calculating mass, momentum, and energy flow rates. A junction at the boundary of the simulation—with only one adjacent volume block—cannot calculate junction fluid properties in the same manner. If junctions represent the boundaries to the model, then a different method must be employed to find the fluid properties.

To find fluid properties for the junction blocks at the boundaries, extrapolation can be used. (Hirsch, 1990) provides several methods for extrapolation across time and space. A first-order space extrapolation involves three co-linear, equidistant points—A, B, C, shown in **Figure 7**. If a property is known at A and B, first-order space extrapolation estimates that property at C. The change in property between B and C is assumed to match the change in property between A and B.

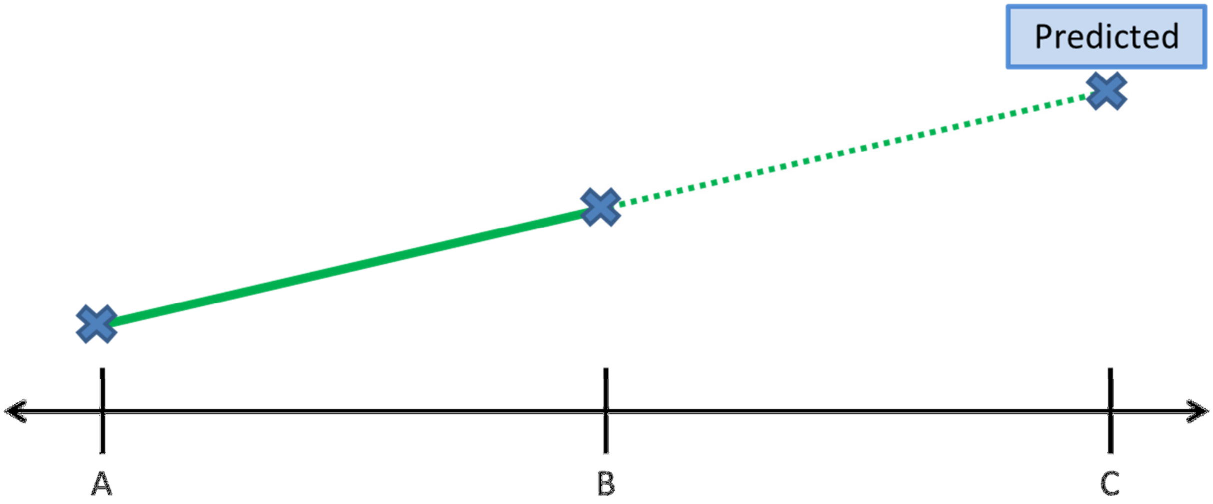

Figure 7. Visualization of first-order space extrapolation. The increasing (or decreasing) trend of some property from A to B continues on to predict C, such that C – B = B – A.

In the illustration of **Figure 7**, C would be the boundary junction—that needs extrapolation to determine some of its properties, B is the adjacent volume block and A is the nearest junction block. With the subscript system explained in **Figure 3**, the value of a property at the boundary,

$$X_B = 2X_{+\frac{1}{2}} - X_{+1} \tag{34}$$

where the subscripts are either positive or negative depending on if the boundary is a left or right boundary.

One caveat exists, preventing the simulation from solely using Equation (34) to estimate properties at the boundary. A unit time delay occurs in the output of every junction block, so that volume blocks use flow rate information from the previous time step. Without this delay, the simulation cannot work. Therefore, when estimating the properties at the boundary junction, the current property of the nearest junction, X_{+1}, is unknown, and Equation (34)—in its current form—cannot be used.

A first-order time extrapolation allows estimation of X_{+1}, using information from previous time steps. Similar to the first-order space extrapolation, the time extrapolation (Hirsch, 1990) takes the previous two values of X_{+1} to estimate its current value, assuming that the property continues on the same trend. Therefore, the estimated current property of the nearest junction,

$$X_{+1} = 2X_{+1,t-1} - X_{+1,t-2} \tag{35}$$

where the subscript $t - n$ indicates that the property occurred n times steps in the past. Combining Equation (34) and Equation (35) yields the final estimation for a boundary property,

$$X_B = 2X_{+\frac{1}{2}} - 2X_{+1,t-1} + X_{+1,t-2} \tag{36}$$

Figure 8 shows the two extrapolations combined to estimate the unknown value. The outlet, the right boundary for forward flow, utilizes Equation (36) to estimate the junction density, temperature, and velocity. With the inlet fluid state already defined, the inlet junction block only estimates velocity using Equation (36). The use of extrapolation prevents over constraining the model by allowing the undefined properties to be defined by the system, rather than a fixed constant.

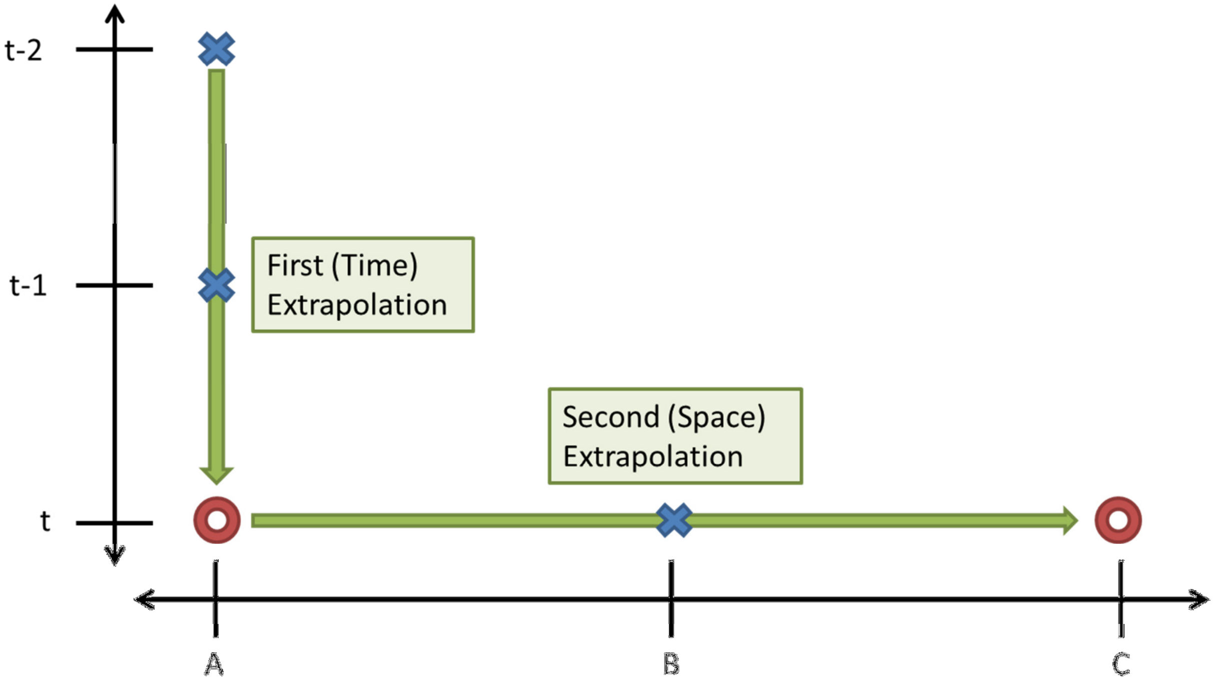

Figure 8. Visualization of two-step extrapolation. In this diagram, crosses represent properties with a known value, while circles represent properties with a value that must be estimated via extrapolation. The first extrapolation uses the previous two values at point A to estimate the current value at point A. The second extrapolation uses the estimated value at point A—along with the known value at point B—to estimate the value at point C.

Especially in transient situations, this extrapolation method can lead to instability; an extreme extrapolation result will affect the system, possible causing an even more extreme extrapolation result in the next time step. To place a limit on how far the extrapolated value can deviate from calculated values the adjacent volume, the simulation checks the extrapolation result against a "stability fraction," z. This forces the extrapolation result to fall within,

$$[X_{1,0}z, \frac{X_{1,0}}{z}] \tag{37}$$

where $0 < z \leq 1$. For the results shown in this thesis, $z = 0.8$.

Relation to Balance Equations

To ensure that the classical mass, momentum, and energy balance equations are obeyed, this section compares the simulation calculations to the integral forms of the mass, momentum, and energy equations found in (Potter & Foss, 1982).

Mass Continuity

The integral from of the conservation of mass from (Potter & Foss, 1982),

$$\frac{d}{dt}\int_{CV}\rho d\cancel{V} + \int_{CS}\rho V \bullet \hat{n} dA = 0 \tag{38}$$

where the integral subscripts CV and CS refer to integrals over a control volume and a control surface, respectively, and $\hat{n}$ is the vector normal to the cross-sectional area. The first term in Equation (38) refers to the mass rate of change of the control volume, while the second term refers to the flow of mass across the boundary of the control volume. The first term can be simplified to

$$\frac{d}{dt}\int_{CV}\rho d\cancel{V} = \dot{m}_{CV} \tag{39}$$

Restricting the flow to one-dimension—perpendicular to the cross-sectional area—and treating flow from left to right as positive,

$$\int_{CS}\rho\vec{V} \bullet \hat{n} dA = -(\rho VA)_{left} + (\rho VA)_{right} \tag{40}$$

where $left$ and $right$ refer to the side of the volume those values are taken from. The reduced continuity equation,

$$\dot{m}_{CV} = (\rho VA)_{left} - (\rho VA)_{right} \tag{41}$$

matches the combination of Equations (3) and (19) used in the simulation,

$$\dot{m}_{net} = (\rho VA)_{-\frac{1}{2}} - (\rho VA)_{+\frac{1}{2}} \tag{42}$$

verifying that the simulation satisfies mass continuity.

Momentum Balance

Furthermore, (Potter & Foss, 1982) gives the one-dimension integral form of the momentum equation as

$$\Sigma F = \frac{d}{dt}\int_{CV}\rho V d\cancel{V} + \int_{CS}\rho V\left(\vec{V} \bullet \hat{n}\right) dA \tag{43}$$

where ΣF is the total force acting on the fluid within the control volume. The first term on the left side of the equation simplifies to

$$\frac{d}{dt}\int_{CV}\rho V d\cancel{V} = \dot{M}_{CV} \tag{44}$$

The second term also reduces,

$$\int_{CS} \rho V\left(\vec{V} \bullet \hat{n}\right)dA = -(\rho AV|V|)_{left} + (\rho AV|V|)_{right} \tag{45}$$

with the same conventions as Equation (41) above. The absolute value velocity replaces the scalar velocity, while the velocity that retains its sign replaces the dot product between the unit vector and the velocity vector. With the substitutions, the momentum equation becomes,

$$\dot{M}_{CV} = \Sigma F + (\rho AV|V|)_{left} - (\rho AV|V|)_{right} \tag{46}$$

which matches Equation (24),

$$\dot{M}_{net} = \dot{M}_{-\frac{1}{2}} - \dot{M}_{+\frac{1}{2}} + F_P + F_{f,-\frac{1}{2}} + F_{f,+\frac{1}{2}} - \cancel{W}$$

as

$$\Sigma F = F_P + F_{f,-\frac{1}{2}} + F_{f,+\frac{1}{2}} - \cancel{W} \tag{47}$$

Therefore, as long as the external forces are applied correctly, the simulation holds true to momentum equilibrium.

Energy Balance

The final balance equation, (Potter & Foss, 1982) provides the integral form of the energy balance equation,

$$\dot{Q} - \dot{W} = \frac{d}{dt}\int_{CV}\left(\frac{V^2}{2} + gH + u\right)\rho d\cancel{V} + \int_{CS}\left(\frac{V^2}{2} + gH + u\right)\rho\,\vec{V} \bullet \hat{n}dA \tag{48}$$

where $\dot{Q}$ is the amount of heat transferred into the control volume from conduction, radiation, and other source terms. Assuming constant property values—velocity, height, internal energy, and density—over the entire control volume,

$$\frac{d}{dt}\int_{CV}\left(\frac{V^2}{2} + gH + u\right)\rho d\cancel{V} = \dot{E}_{CV} \tag{49}$$

Also, the energy flowing across the control surface, using the same conventions as above,

$$\int_{CS}\left(\frac{V^2}{2} + gH + u\right)\rho\,\vec{V} \bullet \hat{n}dA = -\left[\left(\frac{V^2}{2} + gH + u\right)\dot{m}\right]_{left} + \left[\left(\frac{V^2}{2} + gH + u\right)\dot{m}\right]_{right} \tag{50}$$

making the substitution for mass flow rate from Equation (39). The work done by the fluid, the flow work,

$$\frac{d}{dt}(PV) = \dot{m}(h - u) \tag{51}$$

where the fluid flowing into the control volume does work to the control volume, while the work flowing out of the control volume is work done by the control volume. Therefore, the net work done by the system,

$$\dot{W} = [\dot{m}(h - u)]_{right} - [\dot{m}(h - u)]_{left} \tag{52}$$

The current state of the simulation neglects heat transfer, so Equation (48) becomes,

$$\dot{E}_{CV} = \left[\left(\frac{V^2}{2} + gH + h\right)\dot{m}\right]_{left} - \left[\left(\frac{V^2}{2} + gH + h\right)\dot{m}\right]_{right} \tag{53}$$

which matches Equation (20),

$$\dot{E}_{net} = \dot{E}_{-\frac{1}{2}} - \dot{E}_{+\frac{1}{2}}$$

showing that the simulation matches the energy conservation equation as well.

The simulation obeying all three continuity equations supports the idea that it accurately models real fluid cases. Further support exists in the validation section found later in this thesis, where results of the simulation are compared to expected results from various flow models.

Two-Phase Model

Like the single phase model, the two phase simulation employs alternating junction and volume blocks which base their calculations on the mass, momentum, and energy held in the volume blocks, the independent variables of the system. Both blocks perform the same basic functions as their single phase counterparts; the junction block calculates the flow rates of mass, momentum, and energy, while the volume block integrates the flow rates over time to find the state of the fluids.

Because of the liquid and gas phases, each junction block is divided into two parts, one to calculate the flow rates for each phase. The gas section executes first, following a process similar to the single-phase junction block. The pressure is determined by the gas alone, so the liquid section must run after, using the average gas pressure in the momentum flow calculation. Instead of sending one set of flow rates to adjacent volume blocks, the junction block sends the mass, momentum, and energy flow rates separately for each phase.

The volume block also differs from the single phase model, incorporating the interactions between the two phases. Before the volume block integrates the energy flows, the energy rate of change adjusts for each flow based on the temperature difference between the phases. Likewise, because of interphase drag, the momentum flow for each phase changes based on the velocity difference. The energy and momentum transfers include adjustable coefficients: the interphase heat transfer coefficient and the interphase friction factor. Though the fluids exchange momentum and energy, they do not exchange mass; phase change is not yet incorporated into the simulation.

Also, because the gas phase does not occupy all of the space within the volume block, the state calculations following the flow integrations differ in the two phase model. First, the state of the liquid is found. The density of the liquid remains constant; in addition to the state of the liquid, the volume block calculates the space occupied by the liquid, using the constant density and the current mass of liquid. The remaining volume the gas phase occupies. The state of the gas is now able to be found, given the adjusted volume.

Junction Calculations

The previous section gave a brief overview on the differences between the single phase and two phase models. This junction calculations section, and the following volume calculations section, will explain the operation of the two phase simulation in detail.

As with the single phase simulation, the two phase junction block uses Equation (1) to find the average temperature, density, and velocity for both the liquid and gas phases. Junctions with only adjacent volume block use the extrapolating Equation (36) to find the same properties. The junction block also length averages (or extrapolates) void fraction, defined as

$$\alpha \equiv \frac{\cancel{V}_G}{\cancel{V}} \tag{54}$$

where the subscripts G and L refer to the gas and liquid phases, is the volume occupied by the gas phase. With the state of the gas phase known, Equation (2), the equation of state for an ideal gas, is used to find gas pressure. Assuming that the gas phase drives the pressure, the junction pressure,

$$P = P_G = P_L \tag{55}$$

so that the same pressure is used for both phases, and the overall junction pressure.

Because the perimeter of pipe is assumed to be wetted, wall friction affects the liquid phase only. Various models have been proposed that derive a smooth pipe friction factor, but none are used in this simulation. Equations (17) and (18) are used with the liquid phase properties to determine the force of friction on the liquid phase.

To calculate the mass, momentum and energy flows for each phase, Equations (3), (4), and (11) are used with one small adjustment; the cross-sectional area for each phase is not full cross-sectional area of the pipe and must be calculated using void fraction. The junction finds the length-weighted average of void fraction using Equation (1), as with the other state variables. Therefore, the mass flow of gas,

$$\dot{m}_G = \rho_G \alpha A V_G \tag{56}$$

and liquid,

$$\dot{m}_L = \rho_L (1 - \alpha) A V_L \tag{57}$$

Using the new values for mass flow, the simulation finds the momentum flow rates for gas,

$$\dot{M}_G \equiv \dot{m}_G V_G \tag{58}$$

and liquid,

$$\dot{M}_L \equiv \dot{m}_L V_L \tag{59}$$

as well as energy flow rates for gas,

$$\dot{E}_G = \dot{m}_G \left(\frac{V_G^2}{2} + c_{V,G} T_G + \frac{P}{\rho_G}\right) \tag{60}$$

and liquid,

$$\dot{E}_L = \dot{m}_L \left(\frac{V^2}{2} + c_{V,L} T_L + \frac{P}{\rho_L}\right) \tag{61}$$

For two-phase flow, Equations (56) through (61) provide the flow rates needed by the adjacent volume blocks, explained in the following section.

Volume Calculations

The volume block contains the interactions between the liquid and gas phases, the primary difference between the single phase and two phase model. The two phase volume block takes the flow rate (and friction) information from the adjacent junction blocks as inputs. The momentum and energy flow rates are adjusted based on the friction and heat transfer between the two phases. Pressure and wall friction alter the momentum flow rates as well. The adjusted flow rates are integrated to find the current values of mass, momentum and energy within the cell. Finally the amount of mass, momentum and energy (of each phase) determine the state of the fluids, including void fraction.

Weight

Like Equation (23), a weight is applied to the fluids in the pipe; however, the two phase simulation uses a separate equation for each phase. In each volume, the gas phase weighs,

$$\cancel{W}_G = \rho_G \alpha \cancel{V} g \bullet sin(\theta) \tag{62}$$

and the liquid phase weighs,

$$\cancel{W}_L = \rho_L (1-\alpha) \cancel{V} g \bullet sin(\theta) \tag{63}$$

The weights are applied in the momentum balance equations, where the gas momentum balance includes $\cancel{W}_G$, and the liquid balance equation includes $\cancel{W}_L$.

Pressure Balance

In the single phase model, pressure applies a force on the inlet and outlet of each volume block. Also, if the area changes from one end to the other, the pressure force normal to the wall of the pipe has a component in the flow dimension. The simulation calculates this pressure balance using Equation (22). Similarly, the two phase model balances inlet, outlet, and wall pressures; however, this balance occurs for each phase. The inlet and outlet areas change based on the void fractions in the neighboring junctions. The gas boundary area,

$$A_{G,} = \alpha A \tag{64}$$

and the liquid boundary area,

$$A_{L,} = (1-\alpha) A \tag{65}$$

where the properties are taken from adjacent volumes. Applying Equation (22) to the two phases yields the pressure forces,

$$F_{P,G} = (A_G P)_{-\frac{1}{2}} - (A_G P)_{+\frac{1}{2}} + \frac{1}{2}\left(P_{-\frac{1}{2}} + P_{+\frac{1}{2}}\right)\left(A_{G_{+\frac{1}{2}}} - A_{G_{-\frac{1}{2}}}\right) \tag{66}$$

for the gas phase, and

$$F_{P,L} = (A_L P)_{-\frac{1}{2}} - (A_L P)_{+\frac{1}{2}} + \frac{1}{2}\left(P_{-\frac{1}{2}} + P_{+\frac{1}{2}}\right)\left(A_{L_{+\frac{1}{2}}} - A_{L_{-\frac{1}{2}}}\right) \tag{67}$$

for the liquid phase. Equations (66) and (67) are included in the momentum balances to follow.

Interphase Drag Momentum Transfer

The interphase momentum transfer is driven by the velocity difference between the two phases. If the two fluids move at different velocities, a drag force appears, acting against the greater velocity fluid and with the lower velocity fluid. The interphase velocity difference,

$$\Delta V_{ip} = V_G - V_L \tag{68}$$

where the subscript ip refers to "interphase". The simulation uses the velocity difference to calculate the drag force included in the momentum balance equations,

$$D_{ip} = \frac{\not{V}}{D_h} f_{ip} \alpha(1-\alpha) \rho_L \Delta V_{ip}^2 \tag{69}$$

Please note that the sign of D_{ip} is the same as the sign of ΔV_{ip}, so that force is always applied to the lower velocity fluid in the positive direction. Equation (69) crudely represents interphase drag; more sophisticated models exist, but there is no consensus on the exact mechanisms of interphase drag. This model of interphase drag prevents one phase—namely the gas, wall friction does not affect the gas phase—from travelling at a velocity much higher than the other. The product $\alpha(1-\alpha)$ reduces drag for high and low void fractions, when there is less interphase area, increasing stability for those cases.

Interphase Drag Energy Dissipation

Interphase drag not only transfers momentum between phases, but involves the phases performing work on one another. The time-derivative work term is power,

$$\dot{W} = \frac{d}{dt}(W) = \frac{d}{dt}(Fd) = FV \tag{70}$$

where W is work. Since both phases are moving and applying a force to one another, Equation (70) shows the power each phase exerts on the other. The gas phase applies

$$\dot{W}_{G \to L} = D_{ip} V_G \tag{71}$$

to the liquid phase, while the liquid phase applies

$$\dot{W}_{L \to G} = -D_{ip} V_L \tag{72}$$

to the gas phase, where the subscripts $G \to L$ and $L \to G$ describe the source and sink of the power.

Notice that Equation (72) is negative. Drag force shares its sign with velocity difference, which is positive if the gas velocity is greater. By this convention, drag force is applied in the negative direction on the gas phase and in the positive direction on the liquid phase. Therefore the power applied on the gas phase, Equation (72), must be negative.

Because the fluid velocities are not necessarily the same,

$$\dot{W}_{L \to G} \neq -\dot{W}_{G \to L} \tag{73}$$

and some of the work due to interphase friction is dissipated. The dissipated power,

$$\dot{W}_{disp} = \dot{W}_{G \to L} + \dot{W}_{L \to G} \tag{74}$$

which represents the kinetic energy lost by the gas phase, but not gained by the liquid phase. This dissipated is assumed to split evenly between the two phases, such that,

$$\dot{W}_{net,G} = \frac{\dot{W}_{disp}}{2} - \dot{W}_{G\to L} \tag{75}$$

and

$$\dot{W}_{net,L} = \frac{\dot{W}_{disp}}{2} + \dot{W}_{G\to L} \tag{76}$$

No energy is destroyed, and using the Equations (71) through (76), the interphase power due to friction,

$$\dot{W}_{ip} = \dot{W}_{net,G} = -\dot{W}_{net,L} = \frac{1}{2}(V_L + V_G)D_{ip} \tag{77}$$

which is added to the liquid energy balance and subtracted from the gas energy balance. In reality, this dissipation may not be evenly distributed between the phases, but splitting the dissipation is a closer approximation that one phase taking all of the dissipated energy, which would occur without this correction term. Regardless, interphase heat transfer dominates the flow of energy from one phase to the other.

Expansion Work

An additional work term exists between the two phases. If the volumes of each phase change over time, then the expanding volume performs work on the contracting volume. The pressure of each phase is assumed to be equal, while the volumes are not necessarily equal. Therefore, the power done on the gas phase by the liquid phase,

$$\dot{W}_{expan,L} = P\frac{d\forall_L}{dt} \tag{78}$$

and the power done by the gas phase on the liquid phase,

$$\dot{W}_{expan,G} = P\frac{d\forall_G}{dt} \tag{79}$$

Because the liquid phase gains any volume lost by the gas phase,

$$\frac{d\forall_L}{dt} = -\frac{d\forall_G}{dt} \tag{80}$$

and, because the density of liquid is assumed constant, the liquid mass rate of change determines the liquid volume rate of change,

$$\frac{d\forall_L}{dt} = \frac{\dot{m}_{net,L}}{\rho_L} \tag{81}$$

So the net work due to expansion,

$$\dot{W}_{expan,net} = P\frac{\dot{m}_{net,L}}{\rho_L} \tag{82}$$

which is added to the gas phase energy balance, and subtracted from the liquid phase energy balance.

Interphase Heat Transfer

The final interphase transfer term is the heat transfer between the two phases. The temperature difference between the phases,

$$\Delta T_{ip} = T_G - T_L \tag{83}$$

drives the flow of heat from one phase to the other. The interphase heat transfer rate per unit volume,

$$\dot{Q}_{ip} = \hbar \Delta T_{ip} \alpha (1 - \alpha) \cancel{V} \tag{84}$$

where $\hbar_{ip}$ is the volumetric heat transfer coefficient, in $\left[\frac{W}{m^3-K}\right]$. Equation (84) is a simple formulation based on convective heat transfer. Again, similar to the interphase friction model, Equation (69), the term $\alpha(1-\alpha)$ represents the reduction in interphase area as void fraction approaches 1 or 0. Reducing heat transfer in these cases prevents too much heat being transferred to a phase with significantly less mass, improving stability in those cases.

Balance Equations

Like Equation (19), the mass balance for the two phase model only includes the inlet and outlet flows. For the two phase simulation, the difference is the separate balance for each phase. Equation (19) becomes

$$\dot{m}_{net,G} = \dot{m}_{-\frac{1}{2},G} - \dot{m}_{+\frac{1}{2},G} \tag{85}$$

for the ideal gas phase, and

$$\dot{m}_{net,L} = \dot{m}_{-\frac{1}{2},L} - \dot{m}_{+\frac{1}{2},L} \tag{86}$$

for the incompressible liquid phase, with the gas and liquid junction mass flow terms defined by Equations (56) and (57), respectively.

Compared to the one-phase energy balance equation, Equation (20), the two phase energy balance contains additional terms, the frictional work, expansion work, and interphase heat transfer. For the liquid phase, the rate of change of energy,

$$\dot{E}_{net,L} = \dot{E}_{-\frac{1}{2},L} - \dot{E}_{+\frac{1}{2},L} + \dot{Q}_{ip} + \dot{W}_{ip} + \dot{W}_{expan,net} \tag{87}$$

while for the gas phase,

$$\dot{E}_{net,G} = \dot{E}_{-\frac{1}{2},G} - \dot{E}_{+\frac{1}{2},G} - \dot{Q}_{ip} - \dot{W}_{ip} - \dot{W}_{expan,net} \tag{88}$$

The signs on the work and heat transfer terms change between Equations (87) and (88) because those terms transfer energy from one phase to the other.

The momentum balance also includes an additional term compared to the single phase counterpart, Equation (24). Interphase drag transfers momentum from one phase to the other. The resulting momentum rate of change for liquid,

$$\dot{M}_{net,L} = \dot{M}_{-\frac{1}{2},L} - \dot{M}_{+\frac{1}{2},L} + F_{P,L} + F_{f,-\frac{1}{2}} + F_{f,+\frac{1}{2}} - \cancel{W}_L + D_{ip} \tag{89}$$

and gas,

$$\dot{M}_{net,G} = \dot{M}_{-\frac{1}{2},G} - \dot{M}_{+\frac{1}{2},G} + F_{P,G} - \cancel{W}_G - D_{ip} \tag{90}$$

Like in the energy equations, the transfer term D_{ip} has a different sign in Equations (89) and (90), representing the transfer of momentum from one phase to the other due to interphase friction. Also, Equation (90) does not contain frictional terms, as the liquid phase is the only phase that contacts the wall of the pipe.

With all six rates of change known ($\dot{m}_{net,L}, \dot{m}_{net,G}, \dot{E}_{net,L}, \dot{E}_{net,G}, \dot{M}_{net,L}, \dot{M}_{net,G}$), the two phase model employs the same integration procedure as the single phase model, Equation (25). The integration results in knowing the total mass, momentum, and energy of each phase within the cell.

Equations of State

The volume begins calculating values to be used by adjacent junction blocks. First, void fraction must be found. Knowing that the mass of liquid,

$$m_L = \rho_L \cancel{V}_L = \rho_L (1 - \alpha) \cancel{V} \tag{91}$$

and that the density of the liquid does not change, the volume's void fraction,

$$\alpha = 1 - \frac{m_L}{\rho_L \cancel{V}} \tag{92}$$

As the gas density varies, the volume calculates it at each time step. The density of gas,

$$\rho_G = \frac{m_G}{\cancel{V}_G} = \frac{m_G}{\alpha \cancel{V}} \tag{93}$$

The remaining properties, velocity and temperature, are calculated using Equations (32) and (33), except that the volume block finds a different temperature and velocity for each phase.

As with the single phase model, the two phase model passes the flow rate information from the junction blocks to the volume blocks. The volume blocks use this information to determine the states of the fluids in the next time step. The gas and liquid states are given to the junction blocks, which use them to calculate the flow rate information, thus perpetuating the cycle.

Relation to Balance Equations

The equations presented in (Ishii & Takashi, 2011) provide a standard of comparison for the two-phase, one-dimensional flow simulation developed in this thesis. The following sections show that, using the assumptions employed by the model, each balance equation simplifies to the governing equation of the simulation.

Mass Continuity

The work of (Ishii & Takashi, 2011) provides the mass balance equation in rectangular coordinates,

$$\frac{\partial}{\partial t}(\alpha_k\bar{\bar{\rho}}_k) + \frac{\partial}{\partial x}(\alpha_k\bar{\bar{\rho}}_k\hat{v}_{xk}) + \frac{\partial}{\partial y}(\alpha_k\bar{\bar{\rho}}_k\hat{v}_{yk}) + \frac{\partial}{\partial z}(\alpha_k\bar{\bar{\rho}}_k\hat{v}_{zk}) = \Gamma_k \tag{94}$$

where Γ is the mass generation term, the subscript k specifies to which fluid the property belongs, α_k refers to the volume fraction of fluid- k, not necessarily the void fraction, the subscripts x, y, and z refer to the axis the vector component lies on, the hat, $\hat{}$, indicates the property is a mass-weighted mean, and the double-bar, $\bar{\bar{}}$, indicates the property is a mean value. As a one-dimensional model only considers one axis of fluid flow, Equation (94) reduces to

$$\frac{d}{dt}(\alpha_k\bar{\bar{\rho}}_k) + \frac{d}{dx}(\alpha_k\bar{\bar{\rho}}_k\hat{v}_k) = \Gamma_k \tag{95}$$

where all fluid velocity occurs in the x-direction. Also, the model cannot currently model phase change; Equation (95) further reduces to

$$\frac{d}{dt}(\alpha_k\bar{\bar{\rho}}_k) + \frac{d}{dx}(\alpha_k\bar{\bar{\rho}}_k\hat{v}_k) = 0 \tag{96}$$

which, after multiplying all terms by the volume of the volume block (the control volume), yields

$$\cancel{V}\left[\frac{d}{dt}(\alpha_k\bar{\bar{\rho}}_k)\right] + \cancel{V}\left[\frac{d}{dx}(\alpha_k\bar{\bar{\rho}}_k\hat{v}_k)\right] = \dot{m}_k + LA\frac{d}{dx}(\alpha_k\bar{\bar{\rho}}_k\hat{v}_k) = 0 \tag{97}$$

Setting the differential length equal to the length of the control volume,

$$\dot{m}_k + A\left[(\alpha_k\bar{\bar{\rho}}_k\hat{v}_k)_{right} - (\alpha_k\bar{\bar{\rho}}_k\hat{v}_k)_{left}\right] = 0 \tag{98}$$

where the distance between the left and right boundary is the length of the control volume. Now, to apply the reduced mass continuity equation to the two phase simulation, it must be represented in the gas form,

$$\dot{m}_G = A\left[(\alpha\bar{\bar{\rho}}_G\hat{v}_G)_{left} - (\alpha\bar{\bar{\rho}}_G\hat{v}_G)_{right}\right] \tag{99}$$

and liquid form,

$$\dot{m}_L = A\left[([1-\alpha]\bar{\bar{\rho}}_G\hat{v}_G)_{left} - ([1-\alpha]\bar{\bar{\rho}}_G\hat{v}_G)_{right}\right] \tag{100}$$

which matches the gas continuity, Equation (85), and liquid continuity, Equation (86), used by the simulation, except for two differences. First, Equation (100) does not evaluate the cross-sectional area at the control volume boundaries, but uses a constant cross-sectional area for the entire control volume. Second, the simulation employs length-weighted averaging of fluid properties like velocity, whereas Equation (100) utilizes mass weighted averaging. The subtle differences negligibly affect the result of the simulation, especially if the length resolution is large enough.

Momentum Balance

The x-component of the momentum balance, given by (Ishii & Takashi, 2011), is

$$\alpha_k \bar{\bar{\rho}}_k \left(\frac{\partial \hat{v}_{xk}}{\partial t} + \hat{v}_{xk} \frac{\partial \hat{v}_{xk}}{\partial x} + \hat{v}_{yk} \frac{\partial \hat{v}_{xk}}{\partial y} + \hat{v}_{zk} \frac{\partial \hat{v}_{xk}}{\partial z} \right) =$$

$$-\alpha_k \frac{\partial \bar{\bar{P}}_k}{\partial x} + \alpha_k \bar{\bar{\rho}}_k \hat{g}_{xk} + \left[\frac{\partial}{\partial x} \alpha_k \left(\bar{\bar{\tau}}_{xxk} + \tau_{xxk}^T \right) + \frac{\partial}{\partial y} \alpha_k \left(\bar{\bar{\tau}}_{yxk} + \tau_{yxk}^T \right) + \frac{\partial}{\partial z} \alpha_k \left(\bar{\bar{\tau}}_{zxk} + \tau_{zxk}^T \right) \right]$$

$$+\left(\bar{\bar{P}}_{ki} - \bar{\bar{P}}_k \right) \frac{\partial \alpha_k}{\partial x} + (\hat{v}_{xki} - \hat{v}_{xk}) \Gamma_k + M_{ixk} - \left(\frac{\partial \alpha_k}{\partial x} \bar{\bar{\tau}}_{xxki} + \frac{\partial \alpha_k}{\partial y} \bar{\bar{\tau}}_{yxki} + \frac{\partial \alpha_k}{\partial z} \bar{\bar{\tau}}_{zxki} \right) \tag{101}$$

where τ_{xx} represents the a shear stress on the fluid oriented by the axis used in the first two subscripts, $\hat{g}$ represents Gibbs free energy (acceleration due to gravity), M_{ik} represents generalized interfacial drag, and the subscript i indicated the property occurs at the interface. As all motion is assumed restricted to the x-direction, all other spatial partial derivatives are eliminated, yielding

$$\alpha_k \bar{\bar{\rho}}_k \left(\frac{d \hat{v}_{xk}}{dt} + \hat{v}_{xk} \frac{d \hat{v}_{xk}}{dx} \right) =$$

$$-\alpha_k \frac{d \bar{\bar{P}}_k}{dx} + \alpha_k \bar{\bar{\rho}}_k \hat{g}_{xk} + \left[\frac{d}{dx} \alpha_k \left(\bar{\bar{\tau}}_{xxk} + \tau_{xxk}^T \right) \right] + \left(\bar{\bar{P}}_{ki} - \bar{\bar{P}}_k \right) \frac{d\alpha_k}{dx} + (\hat{v}_{xki} - \hat{v}_{xk}) \Gamma_k + M_{ixk} - \frac{d\alpha_k}{dx} \bar{\bar{\tau}}_{xxki} \tag{102}$$

Some assumptions simplify Equation (102) further. Other than the pressure differential and gravity, no work enters or exits the system, allowing the Gibbs free energy term to be replaced with the weight of the fluid. At any given point in the system, all phases have the same pressure, so the interface pressure difference term also reduces to zero. As no phase change occurs, there is also no momentum transfer due to phase change. Removing these terms gives

$$\alpha_k \bar{\bar{\rho}}_k \left(\frac{d \hat{v}_{xk}}{dt} + \hat{v}_{xk} \frac{d \hat{v}_{xk}}{dx} \right) = -\alpha_k \frac{d \bar{\bar{P}}}{dx} + \alpha_k \bar{\bar{\rho}}_k g_{xk} + \left[\frac{d}{dx} \alpha_k \left(\bar{\bar{\tau}}_{xxk} + \tau_{xxk}^T \right) \right] + M_{ixk} - \frac{d\alpha_k}{dx} \bar{\bar{\tau}}_{xxki} \tag{103}$$

which, multiplied by the volume of the volume block (control volume), and then setting the differential length equal to the volume block's length, becomes

$$\not{V} \alpha_k \bar{\bar{\rho}}_k \frac{d \hat{v}_{xk}}{dt} + A \alpha_k \bar{\bar{\rho}}_k \hat{v}_{xk} \left(\hat{v}_{xk,right} - \hat{v}_{xk,left} \right) =$$

$$-\alpha_k A \left(\bar{\bar{P}}_{right} - \bar{\bar{P}}_{left} \right) + \not{V} \alpha_k \bar{\bar{\rho}}_k g_{xk} + A \left\{ \left[\alpha_k \left(\bar{\bar{\tau}}_{xxk} + \tau_{xxk}^T \right) \right]_{right} - \left[\alpha_k \left(\bar{\bar{\tau}}_{xxk} + \tau_{xxk}^T \right) \right]_{left} \right\}$$

$$+\not{V} M_{ixk} - A \bar{\bar{\tau}}_{xxki} (\alpha_{k,right} - \alpha_{k,left}) \tag{104}$$

and simplifies further to

$$\dot{M}_k = \dot{m}_k \left(\hat{v}_{xk,left} - \hat{v}_{xk,right} \right) + \alpha_k A \left(\bar{\bar{P}}_{left} - \bar{\bar{P}}_{right} \right)$$

$$-\not{W}_k + A \alpha_k F_f + \not{V} M_{ixk} + PA(\alpha_{k,left} - \alpha_{k,right}) \tag{105}$$

Equation (104) becomes

$$\dot{M}_G = \dot{m}_G\left(\hat{v}_{G,left} - \hat{v}_{G,right}\right) + \alpha A\left(\bar{\bar{P}}_{left} - \bar{\bar{P}}_{right}\right) - \cancel{W}_G + \cancel{V}M_{L\to G} + PA(\alpha_{left} - \alpha_{right}) \tag{106}$$

for the gas phase, and

$$\dot{M}_L = \dot{m}_L\left(\hat{v}_{L,left} - \hat{v}_{L,right}\right) + (1-\alpha)A\left(\bar{\bar{P}}_{left} - \bar{\bar{P}}_{right}\right) - \cancel{W}_G + \cancel{V}M_{G\to L} - PA(\alpha_{left} - \alpha_{right}) \tag{107}$$

for the liquid phase matching the gas and liquid momentum equations presented in Equations (89) and (90).

Energy Balance

(Ishii & Takashi, 2011) gives the total energy balance equation,

$$\alpha_k \bar{\bar{\rho}}_k \frac{D}{Dt}\left(\hat{e}_k + \frac{\hat{v}_k^2}{2}\right) =$$

$$-\boldsymbol{\nabla} \bullet \alpha_k\left(\bar{\bar{\boldsymbol{q}}}_{\boldsymbol{k}} + \boldsymbol{q}_{\boldsymbol{k}}^{\boldsymbol{T}}\right) + \boldsymbol{\nabla} \bullet \left(\alpha_k \bar{\bar{\mathbb{T}}}_{\mathbb{k}} \bullet \hat{\boldsymbol{v}}_{\boldsymbol{k}}\right) + \alpha_k \bar{\bar{\rho}}_k \hat{\boldsymbol{v}}_{\boldsymbol{k}} \bullet \hat{\boldsymbol{g}}_{\boldsymbol{k}} + \Gamma_k[(\hat{e}_{ki} - \hat{e}_k) + (\hat{\boldsymbol{v}}_{\boldsymbol{ki}} - \hat{\boldsymbol{v}}_{\boldsymbol{k}}) \bullet \hat{\boldsymbol{v}}_{\boldsymbol{k}}]$$

$$+\alpha_i \bar{\bar{q}}''_{ki} - \bar{\bar{P}}_{ki}\left(\frac{\partial \alpha_k}{\partial t} - \frac{\Gamma_k}{\bar{\bar{\rho}}_{ki}}\right) + \boldsymbol{M}_{\boldsymbol{ik}} \bullet \hat{\boldsymbol{v}}_{\boldsymbol{ki}} - (\boldsymbol{\nabla}\alpha_k \bullet \bar{\bar{\tau}}_{\mathbb{ki}}) \bullet \hat{\boldsymbol{v}}_{\boldsymbol{ki}} + W_{ki}^T \tag{108}$$

where **bold** variables are vectors, outlined variables are tensors,$\hat{e}_k$ is specific (non-kinetic) energy, $\bar{\bar{\boldsymbol{q}}}_{\boldsymbol{k}}$ is mean conduction heat flux, $\boldsymbol{q}_{\boldsymbol{k}}^{\boldsymbol{T}}$ is the turbulent heat flux, $\bar{\bar{\mathbb{T}}}_{\mathbb{k}}$ is the stress tensor, $\bar{\bar{\tau}}_{\mathbb{ki}}$ is the interfacial shear stress tensor, and W_{ki}^T is the work done by fluctuations in drag forces. Restricting Equation (108) to the x-direction yields

$$\alpha_k \bar{\bar{\rho}}_k \frac{d}{dt}\left(\hat{e}_k + \frac{\hat{v}_k^2}{2}\right) + \alpha_k \bar{\bar{\rho}}_k \hat{v}_k \frac{d}{dx}\left(\hat{e}_k + \frac{\hat{v}_k^2}{2}\right) =$$

$$\frac{d}{dx}\alpha_k\left(\bar{\bar{q}}_k + q_k^T\right) + \frac{d}{dx}\left(\alpha_k \bar{\bar{T}}_{xxk}\hat{v}_k\right) + \alpha_k \bar{\bar{\rho}}_k \hat{v}_k g_x + \Gamma_k[(\hat{e}_{ki} - \hat{e}_k) + (\hat{v}_{ki} - \hat{v}_k)\hat{v}_k]$$

$$+\alpha_i \bar{\bar{q}}''_{ki} - \bar{\bar{P}}_{ki}\left(\frac{d\alpha_k}{dt} - \frac{\Gamma_k}{\bar{\bar{\rho}}_{ki}}\right) + M_{ik}\hat{v}_{ki} - \frac{d}{dx}(\alpha_k \bar{\bar{\tau}}_{xxki})\hat{v}_{ki} + W_{ki}^T \tag{109}$$

where all vectors and tensors have been reduced to their x-direction scalar component. The simulation does not involve conductive heat transfer, phase change, or drag force fluctuations, simplifying the energy balance equation to

$$\alpha_k \bar{\bar{\rho}}_k \frac{d}{dt}\left(\hat{e}_k + \frac{\hat{v}_k^2}{2}\right) + \alpha_k \bar{\bar{\rho}}_k \hat{v}_k \frac{d}{dx}\left(\hat{e}_k + \frac{\hat{v}_k^2}{2}\right) =$$

$$\frac{d}{dx}\left(\alpha_k \bar{\bar{T}}_{xxk}\hat{v}_k\right) + \alpha_k \bar{\bar{\rho}}_k \hat{v}_k g_x + \alpha_i \bar{\bar{q}}''_{ki} - \bar{\bar{P}}_{ki}\frac{d\alpha_k}{dt} + M_{ik}\hat{v}_{ki} - \frac{d}{dx}(\alpha_k \bar{\bar{\tau}}_{xxki})\hat{v}_{ki} \tag{110}$$

Multiplying the balance by the volume of the volume block (control volume), with the assumption that the differential length equals the length of the control volume, gives

$$V\alpha_k\bar{\bar{\rho}}_k\frac{d}{dt}\left(\hat{e}_k+\frac{\hat{v}_k^2}{2}\right)+A\alpha_k\bar{\bar{\rho}}_k\hat{v}_k\left[\left(\hat{e}_k+\frac{\hat{v}_k^2}{2}\right)_{right}-\left(\hat{e}_k+\frac{\hat{v}_k^2}{2}\right)_{left}\right]=$$

$$A\left[\left(\alpha_k\bar{\bar{\bar{T}}}_{xxk}\hat{v}_k\right)_{right}-\left(\alpha_k\bar{\bar{\bar{T}}}_{xxk}\hat{v}_k\right)_{left}\right]+\cancel{V}\alpha_k\bar{\bar{\rho}}_k\hat{v}_k g_x+\cancel{V}\alpha_i\bar{\bar{\bar{q}}}_{ki}''-\cancel{V}\bar{\bar{\bar{P}}}_{ki}\frac{d\alpha_k}{dt}$$

$$+\cancel{V}M_{ik}\hat{v}_{ki}-A\left[(\alpha_k\bar{\bar{\bar{\tau}}}_{xxki}\hat{v}_{ki})_{right}-(\alpha_k\bar{\bar{\bar{\tau}}}_{xxki}\hat{v}_{ki})_{left}\right] \tag{111}$$

which further reduces to

$$\dot{E}_k=$$

$$\dot{m}_k\left[\left(\hat{e}_k+\frac{\hat{v}_k^2}{2}\right)_{left}-\left(\hat{e}_k+\frac{\hat{v}_k^2}{2}\right)_{right}\right]+AF_{fk}\hat{v}_k+\cancel{W}_k\hat{v}_k+\cancel{V}\alpha_i\bar{\bar{\bar{q}}}_{ki}''$$

$$-\dot{W}_{k,expan}-\dot{W}_{ik,drag}+A\left[(\alpha_k\bar{\bar{\bar{\tau}}}_{xxki}\hat{v}_{ki})_{left}-(\alpha_k\bar{\bar{\bar{\tau}}}_{xxki}\hat{v}_{ki})_{right}\right] \tag{112}$$

using nomenclature from the Volume Calculations of the Two-Phase Model section. The new reduced energy balance equation matches the form of Equations (87) and (88) the gas and liquid balances used in the simulation.

Simulation Validation

Although the simulation matches the mass, momentum, and energy balance equations, to completely trust the model, it must be compared against analytical flow models. Analytical models typically involve assumptions that simplify the governing equations of a model, enabling certain flow characteristics to be calculated without running the simulation. The simulation results are compared against the analytical calculations to verify that the simulation can accurately represent the analytic model.

Instead of an analytical model, experimental data could be used for validation; however, matching real data involves perfectly tuning correlations—such as friction factor, or heat transfer coefficient—to the experimental setup. An empirical validation would not confirm the accuracy of the simulation as much as it would confirm the accuracy of the correlations used. Because the goal of this thesis is to develop the fluid flow model, and not to develop specific correlations, validation only includes analytical models as standards of comparison.

The single-phase simulation is validated by three analytical models: an incompressible model with friction, an adiabatic model with friction (Fanno flow), and an isentropic model with area change. The incompressible model assumes that density remains constant over the length of the pipe. As the simulation uses the ideal gas law as its equation of state, the incompressible assumption only applies when the change of density is negligible. One measure of compressibility is the Mach number,

$$Ma = \frac{V}{c} \tag{113}$$

where c is the speed of sound in the fluid. The speed that sound travels through a fluid is calculated by

$$c = \sqrt{kRT} \tag{114}$$

where k is the ratio of specific heats. For Mach numbers less than 0.3, the density remains approximately constant and the incompressible assumption applies. The incompressible model calculates the pressure drop due to friction for a given velocity. To validate the simulation, a pressure drop across the system is selected, the corresponding incompressible velocity is calculated, and then the simulation velocity is compared to the expected result.

The Fanno flow analytical model also validates the simulation. Fanno flow requires the fluid to be steady, one-dimensional, adiabatic, and constant area (Munson, Young, & Okiishi, 1998), which the simulation satisfies. The Fanno flow assumption allows ratios to be found as functions of Mach number for each point along the pipe. These ratios relate a property—like velocity or pressure—to the value of that property at a choking condition, where the Mach number equals 1. For a given simulation run, the choking conditions should remain constant for each point along the pipe once steady state is achieved. To validate that the simulation, the simulation runs until steady state, and the analytical choking condition is found for several points along the pipe. If the choking condition remains constant, then the simulation is validated.

The isentropic model verifies the accuracy of the single-phase model in a similar manner to the Fanno flow model. Like Fanno flow, involves ratios of properties to a reference condition—either stagnation or choking—each ratio is a function of Mach number, and the simulation is validated if the reference conditions remain constant over the length of the pipe. The isentropic model employs two assumptions that differ from the Fanno model; area varies along the pipe and the fluid flows without friction.

Lastly, the two-phase simulation is validated as well. In two phase flow, a homogenous equilibrium model (HEM) refers to an assumption that two fluids may be treated as a single fluid whose properties represent the average of the two fluids. The HEM requires that there is no interphase velocity difference, and that the two phases exist in thermal equilibrium. To match this assumption in the simulation, the interphase friction coefficient must be large enough such that the difference between the liquid and gas velocity is negligible. Similarly, a higher heat transfer coefficient satisfies the thermal equilibrium requirement. Using these assumptions, an equation was developed in this thesis that expresses mass flow rate as a function of the input parameters of the simulation. This formulation enables the resulting liquid mass flow rate to be predicted before the simulation runs. If the HEM assumption applies, then the simulation's liquid mass flow rate should match the predicted value, validating the simulation.

Incompressible Flow Model

The purpose of the incompressible validation is to verify that the model appropriately applies friction, and that a fluid's velocity is correctly limited by the pressure gradient it travels down. The pressure and frictional forces will balance—at steady state—for a particular flow velocity. If the simulation's steady state matches the velocity predicted by the incompressible flow model, then the incompressible model validates the simulation.

Now, consider the pressure drop for an incompressible fluid in a pipe with friction,

$$\Delta P = \frac{f \rho V^2 L}{2 D_h} \tag{115}$$

As the simulation defines all other variables, velocity is the only dependent variable in the incompressible flow equation. Therefore, solving equation (115) for incompressible velocity,

$$V = \sqrt{\frac{2 \Delta P D_h}{f \rho L}} \tag{116}$$

gives a target velocity for the simulation to achieve. To quantify the difference between the simulation and the incompressible model, percent error,

$$Err = \frac{|X_{sim} - X_{model}|}{X_{model}} \tag{117}$$

is used, where the subscript "sim." refers to the simulation result and the subscript "model" refers to the expected result according to the analytical model. For the incompressible validation, velocity is the variable in question; the model velocity is the result of equation (116), while the simulation velocity is defined as the velocity at the median junction.

Test Procedure

To initialize an incompressible validation run, values for inlet density, area (hydraulic diameter), pipe length, and friction factor are selected. Inlet temperature--though it does not appear in Equation

(116)—must be chosen along with exit properties to establish a pressure drop. With these independent variables selected, Equation (116) predicts the steady state velocity of the system. To get an idea of how well the simulation should match this value, Mach number can be predicted as well and compared to the 0.3 rule-of-thumb.

The simulation takes the independent variables as inputs and begins simulating the system. Once the velocity settles, the average velocity is recorded and compared to the predicted value using Equation (117). The lower the Mach number, the lower the percent difference between predicted and simulated should be.

To complete the validation, each independent variable should be varied in new runs. Varying the independent variables between runs reveals any effects certain variable may have on the application of the incompressible model. Also, analyzing more runs improves confidence in the validation result. **Table 1**, in Appendix B: Simulation Data, contains the raw data used to validate the simulation's ability to model incompressible flow. For cases that met the incompressible assumption, inlet temperature varied from 300 to 315 K, inlet density varied between 1.2 and 1.3 kg/m^3, friction ranged from 0.05 to 0.10, area ranged from 0.01 to 0.03 m^2, length remained constant at 1.66 m, and the total pressure drop was as high as 8,600 Pa. A larger variable range for test cases was employed, but those cases did not meet the 0.3 Mach number restriction.

Results

As expected, the error increases with increasing Mach number. For results with a Mach number less than 0.3, the percent error does not exceed 5%, validating the simulation for low Mach numbers. Most of the "error" present is not, in fact, a fault of the simulation, but the inability of the incompressible model to predict velocity for an ideal gas—especially for higher Mach numbers.

To compare the agreement between the incompressible model and the simulation, the velocity results of both are plotted against one another, as a function of Mach number. Each simulation run yields an expected velocity (from the incompressible model) and the simulation velocity (taken from the length midpoint of the pipe). Plotting the pair of results against Mach number shows agreement where Mach number is less than 0.3—the incompressible region—and divergence for higher Mach numbers. **Figure 9** shows the trend of increased disagreement with higher Mach numbers while **Figure 10** examines the data with less than 5% error.

As the simulation produces results that match the incompressible model's prediction (for low Mach numbers), the incompressible model validates the simulation. This confirms that the simulation appropriately manages the balance between pressure drop and friction, finding the appropriate balance between the two once steady state has been reached.

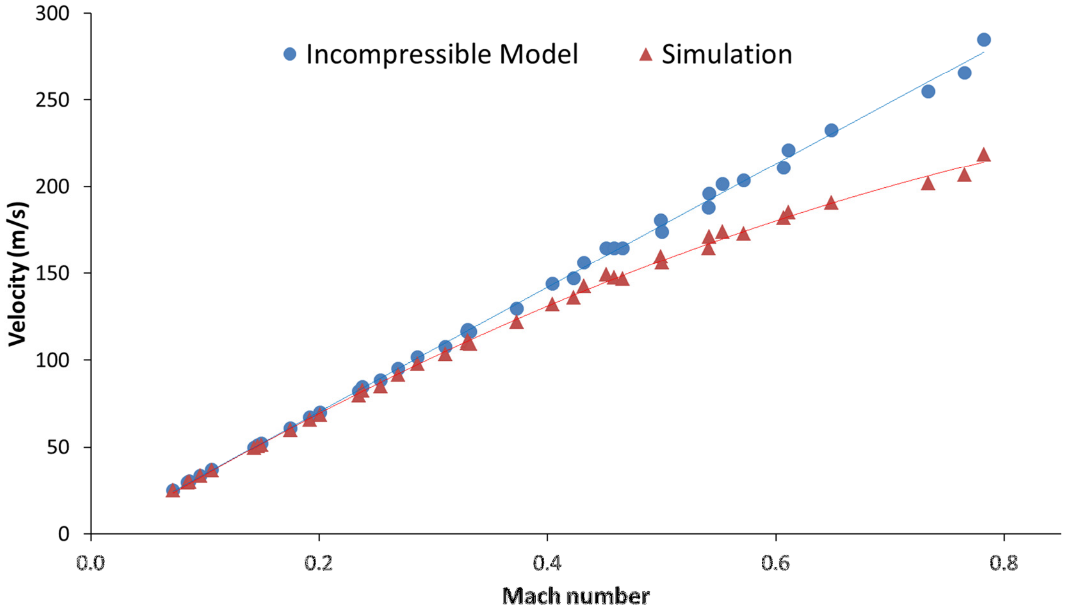

Figure 9. Plot of incompressible validation results. Each run includes an expected result (circle) and a simulation result (triangle). Both plot velocity against the expected Mach number—calculated from the incompressible velocity result and the inlet temperature. The solid lines show the polynomial best fit for both sets of data. As expected, the simulation does not match the incompressible model for higher Mach numbers, where the compressibility of air becomes more of a factor. **Figure 10** below shows the agreement in the low Mach number range of this chart.

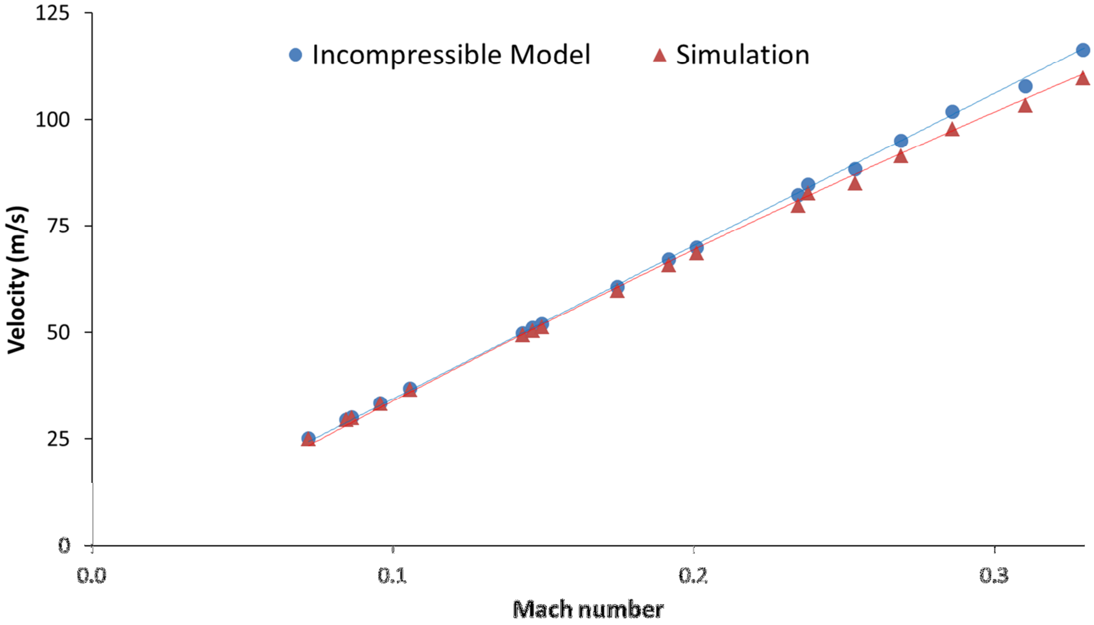

Figure 10. Plot of incompressible validation for low Mach numbers. This plot shows the low Mach number results from **Figure 9**, above, in more detail. Again, circles signify that the expected velocity if the fluid were incompressible, and the triangles show the simulation velocity result. The solid lines depict the polynomial best fit over the entire Mach number range (0 – 0.8). The trend of higher Mach numbers showing deviation from the incompressible model continues, but for results with a Mach number less than 0.3, that deviation remains below 5%.

Fanno Flow Model

The purpose of the Fanno flow validation is to confirm that the simulation properly captures the compressibility effects of an ideal gas moving through a pipe. An incompressible fluid does not accelerate over the length of a pipe with friction, as density remains constant and mass flow rate is constant (at steady state). For compressible fluids, with a velocity less than the speed of sound, the velocity will increase over the length of the pipe. Fanno flow requires the flow to be steady, one-dimensional, adiabatic, and constant area. If the simulation results match Fanno flow conditions, then the validation confirms that the simulation models the compressible effects of an ideal gas correctly.

If Fanno flow exists, then the state at the choke point of the flow may be determined from the state at any given point along the pipe. The ratio of a property at this arbitrary point to that property at the choke point can be found. This includes a pressure ratio,

$$r_P = \frac{P}{P^*} \tag{118}$$

a temperature ratio,

$$r_T = \frac{T}{T^*} \tag{119}$$

and a velocity ratio,

$$r_V = \frac{V}{V^*} \tag{120}$$

where the superscript $*$ refers to the property at choking conditions. To determine the values of the ratios without information from the choking point, the pressure, temperature, and velocity ratios can be found as functions of Mach number. According to (Munson, Young, & Okiishi, 1998), the pressure ratio,

$$r_P = \frac{1}{Ma}\left(\frac{\frac{k+1}{2}}{1+\frac{k+1}{2}Ma^2}\right)^{\frac{1}{2}} \tag{121}$$

the temperature ratio,

$$r_T = \frac{\frac{k+1}{2}}{1+\frac{k-1}{2}Ma^2} \tag{122}$$

and the velocity ratio,

$$r_V = \left(\frac{\frac{k+1}{2}Ma^2}{1+\frac{k-1}{2}Ma^2}\right)^{\frac{1}{2}} \tag{123}$$

So, even if the simulation does not encompass the choking point, the choking properties may be found from the state at any one simulation point.

Each simulation only has one set of choking point conditions; the choking values should not vary based on which point was used to determine them. Therefore, to verify that the simulation can model Fanno flow, the choking pressure, temperature, and velocity is found using each point of the simulation. If these conditions remain constant, then the Fanno flow model validates the simulation.

Test Procedure

This validation of Fanno does not involve a prediction like the incompressible validation. To validate Fanno flow, the simulation runs using any set of conditions that meet the requirements of Fanno flow. Most notably, friction factor must be set to a non-zero constant—not using the smooth pipe correlation of Equation (16)—and the cross-sectional area must be the same at all points along the system. All other conditions are inherently met by the simulation.

Once the simulation reaches steady state, density, temperature, and velocity are recorded at each junction block. Then, for each set of properties, Mach number is found, and Equations (121) through (123) calculate the choking condition property ratios. Using the recorded state and the calculated ratios, an estimated choking condition is found for each point. If the simulation matches Fanno flow, the choking state should not vary between junction blocks.

A normalized standard deviation measures the consistency of these choking properties and, if low enough, validates the simulation's ability to model Fanno flow. The normalized standard deviation,

$$\sigma_{norm} = \frac{\sigma(X_{ref})}{\overline{X_{ref}}} \tag{124}$$

where X_{ref} is the calculated reference (choking) property, $^{-}$ refers to the mean of the ten points, and σ refers to the standard deviation of the points in the simulation. The normalized standard deviation quantifies how much the choking properties vary between the simulation points from which they were calculated.

A variety of different cases were simulated to validate the simulations ability to represent the Fanno flow model. The recorded densities varied between 0.62 to 1.40 kg/m^3; temperatures varied from 284 to 330 K; velocities ranged from 105 to 348 m/s; pressures ranged from 51 to 112 kPa. Without the low Mach number restriction, a greater range of acceptable properties becomes available. The Fanno flow validation data is available for all runs tested, available in **Table 2** of Appendix B: Simulation Data.

Results

For all runs, the simulation had a normalized standard deviation around 0.01%, indicating good agreement with the Fanno flow model. To visualize the agreement between the Fanno flow model and the simulation results, **Figure 11**, **Figure 12**, and **Figure 13** plot both against Mach number (calculated from simulation velocity and temperature). In these figures, the hollow squares show the simulated property ratios,

$$r_X = \frac{X}{\overline{X_{ref}}} \tag{125}$$

for each point of each simulation run. Equation (121) through Equation (123) are plotted on **Figure 11** through **Figure 13** respectively, to show the expected Fanno flow property ratio as a function of Mach number. Deviation from the expected value is not discernible on a scale that accounts for the properties' fluctuation along the pipe.

The agreement between the Fanno flow model and the simulation indicate that the simulation properly accounts for the effects of a compressible gas.

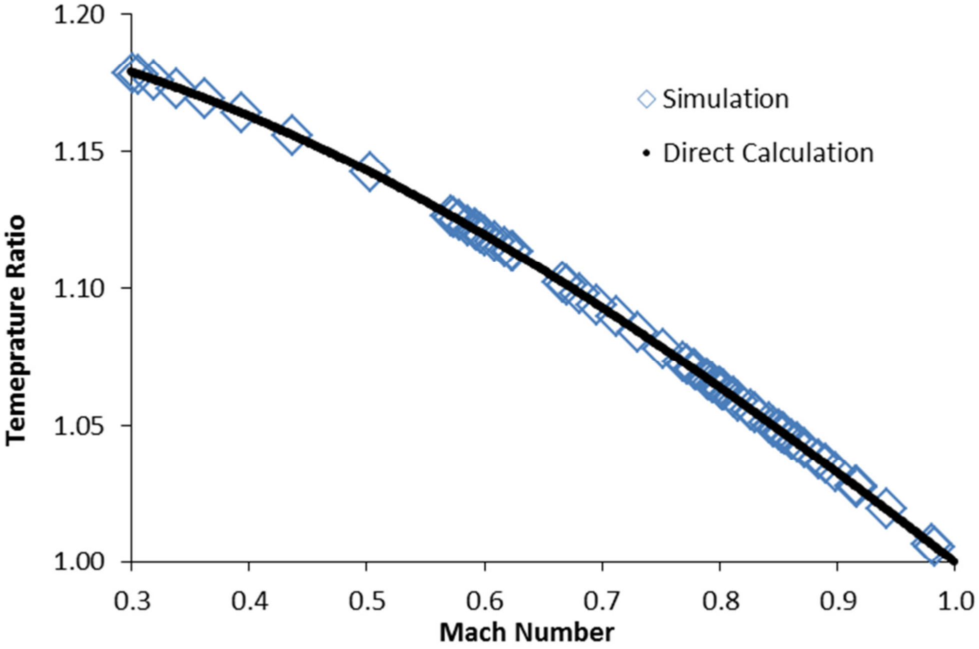

Figure 11. Plot of Fanno flow validation, showing temperature property ratios against Mach number. The empty squares plot the temperature at each point of each simulation, divided by the average estimated choking temperature of that simulation run. The solid black line represents the calculated temperature ratio based on Mach number. No deviation can be seen at this scale, and more zoomed scales yield the same conclusion. The simulation accurately models Fanno flow.

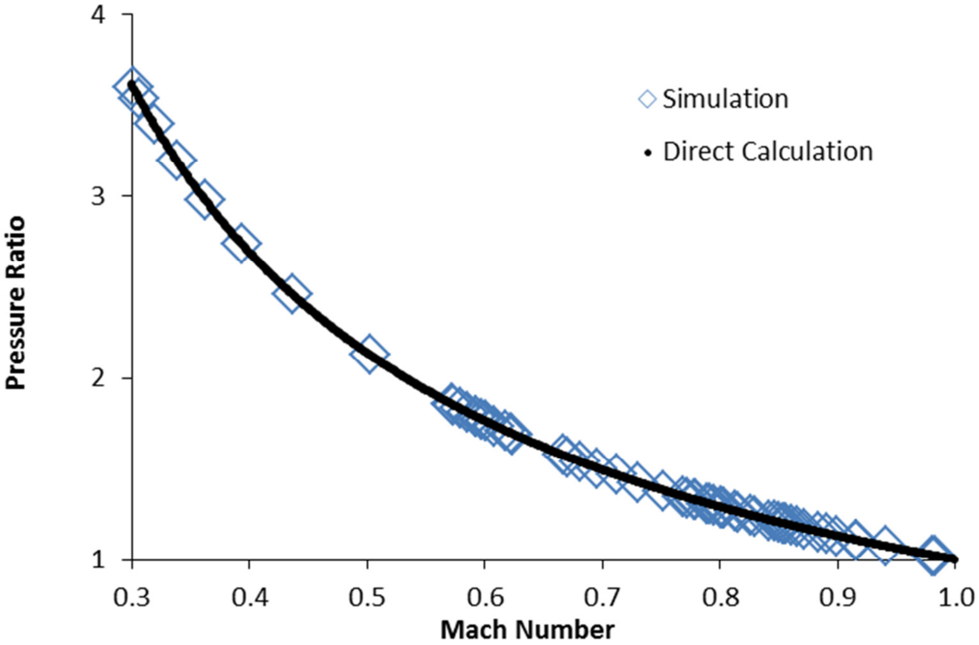

Figure 12. Plot of Fanno flow validation, showing pressure property ratios against Mach number. The empty squares plot the pressure at each point of each simulation, divided by the average estimated choking pressure of that simulation run. The solid black line represents the calculated pressure ratio based on Mach number. No deviation can be seen at this scale, and more zoomed scales yield the same conclusion. The simulation accurately models Fanno flow.

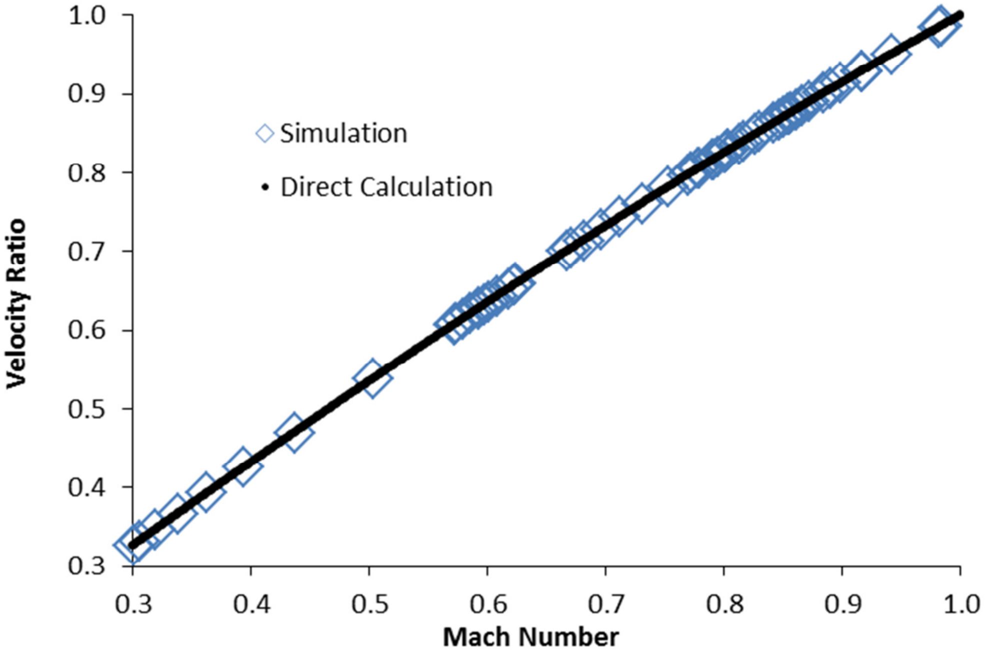

Figure 13. Plot of Fanno flow validation, showing velocity property ratios against Mach number. The empty squares plot the velocity at each point of each simulation, divided by the average estimated choking velocity of that simulation run. The solid black line represents the calculated velocity ratio based on Mach number. No deviation can be seen at this scale, and more zoomed scales yield the same conclusion. The simulation accurately models Fanno flow.

Isentropic Flow Model

The isentropic flow validation checks the simulation to see if the effects of expansion and contraction are properly modelled. Also, as with Fanno flow, the isentropic flow model validates that the compressibility of the ideal gas is modelled properly. To achieve isentropic flow, any losses must be reversible, so friction cannot exist in the simulation. Also, area may change when modeling isentropic flow, allowing fluid to flow in expanding and contracting pipes.

Like the Fanno flow model, various properties can be expressed as ratios to those properties at a specific condition—for isentropic flow, this condition was either stagnation or choking. Each ratio can be calculated as a function of Mach number. The three ratios used to validate the simulations ability to model an isentropic case were the cross-sectional area ratio,

$$r_A = \frac{A}{A^*} = \frac{1}{Ma}\left(\frac{1+\frac{k-1}{2}Ma^2}{1+\frac{k-1}{2}}\right)^{\frac{k+1}{2(k-1)}} \tag{126}$$

the pressure ratio,

$$r_P = \frac{P}{P_0} = \left(\frac{1}{1+\frac{k-1}{2}Ma^2}\right)^{\frac{k}{k-1}} \tag{127}$$

and the temperature ratio,

$$r_T = \frac{T}{T_0} = \frac{1}{1+\frac{k-1}{2}Ma^2} \tag{128}$$

according to (Munson, Young, & Okiishi, 1998). So, like the Fanno flow model, the reference properties may be estimated from the values at any point of the simulation.

Each simulation only has one set of reference conditions; the reference values should not vary based on which point was used to determine them. Therefore, to verify that the simulation can model isentropic flow, the area, pressure, and temperature is found using each point of the simulation. If these conditions remain constant, then the Fanno flow model validates the simulation.

Test Procedure

The isentropic validation procedure involves a process similar to the Fanno flow validation procedure. Any combination of inlet and outlet conditions may be used for a validation run, and, once the simulation reaches steady-state, the properties of interest—cross-sectional area, pressure, and temperature—are recorded at each junction block. Then, in a manner similar to the Fanno flow validation, Equations (126) through (128) use the recorded values and a calculated Mach number to determine the choking cross sectional area, and the stagnation pressure and temperature. If these reference values remain constant for all points along the pipe, the simulation accurately models isentropic flow.

Two differences exist between Fanno flow and isentropic flow setup. The first is that no friction exists when validating isentropic flow, as friction is an irreversible process; friction factor is set to 0 for these runs. The second involves the cross sectional area of the pipe. Fanno flow requires that cross-sectional area remain constant at all points for a given simulation. Isentropic allows the cross-sectional area to change; flow expansion and contraction is a reversible process that the isentropic validation models.

The isentropic validation involves testing both contraction and expansion. Each volume block accepts an input for cross-sectional area; for isentropic validation, these inputs must each be specified. For each contraction case, the cross-sectional area decreases for each successive downstream volume block. Likewise, expanding sections require the cross-sectional area to increase for each successive block.

The contracting sections provide resistance to flow, as the flow area decreases. The area difference term in Equation (22) shows that a decreasing area creates a force opposite the direction of flow. This flow-resisting force enables the simulation to reach steady-state, a substitute for the flow-resisting friction force not allowed in an isentropic model. The expanding sections, however, cannot run stably on its own because of the opposite effect; the area change yields a force in the direction of flow, perpetuating instability. To counteract the instability, a contraction was added to the expansion cases. Thus, the simulation included a net area reduction—net force against flow—while still having expansion to validate the simulation's ability to model expanding flow.

In Appendix B: Simulation Data, **Table 3** shows the isentropic validation results for a contracting pipe section. The results for an expanding-contracting pipe section are contained in **Table 4** through **Table 7**. Again, like the Fanno flow validation, a large range of flow properties were tested to ensure the validity of the simulation's ability to model isentropic flow. Cross-sectional areas ranged from 0.02 to 0.04 m^2; temperatures varied from 300 to 400 K; densities ranged from 0.95 to 1.25 kg/m^3; pressures fluctuated between 82 and 145 kPa; Mach numbers covered the range from 0.12 to 0.97.

Results

The results demonstrate that the simulation matched the isentropic model as the normalized deviation—using Equation (124)—remaining below 2% for the contraction validation cases. In **Figure 14** through **Figure 17**, the property ratios—area over choking area, pressure over stagnation pressure, and temperature over stagnation temperature—are plotted against Mach number. The solid line in these figures show the result of Equations (126) through (128), the analytical ratios based on Mach number. The empty squares show the ratios derived from the simulation, using Equation (125).

Compared to the Fanno flow validation, some visible deviation from the analytical model exists. However, this deviation is small; as seen in **Figure 14** through **Figure 17**, the difference between the simulation and analytical results is not significant, when compared to the entire range of data. Please note that **Figure 15** shows the same data as **Figure 14**, except on a smaller scale so the deviation may be visible.

The expansion-contraction validation surprisingly resulted in a slightly better match between the simulation and analytical results, with normalized deviation less than 1% for all points. As seen in **Figure 18** through **Figure 20**, when the expansion-contraction results are compared to the analytical expected values, little deviation can be seen. These plots were made using the same method as the contraction validation plots.

With good agreement between the analytical and simulation results, the isentropic model validates the accuracy of the simulation. This confirms the simulation's ability to model the effect of expansion and contraction on an ideal gas. The mismatches do require future study; the deviation may originate from the extrapolation of boundary junction volumes or the resolution of the model.

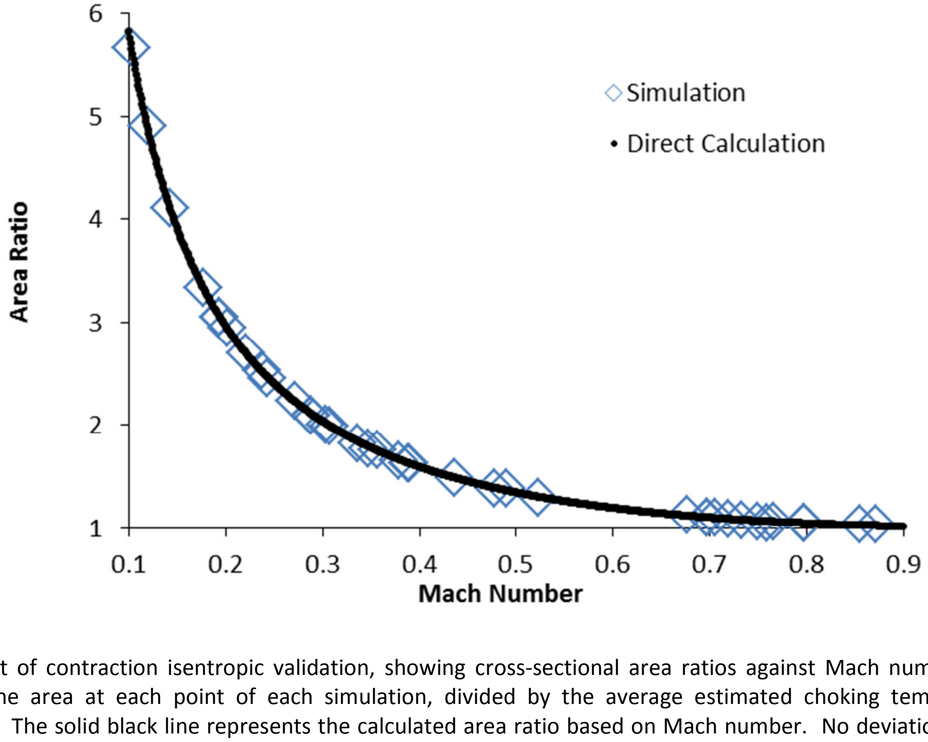

Figure 14. Plot of contraction isentropic validation, showing cross-sectional area ratios against Mach number. The empty squares plot the area at each point of each simulation, divided by the average estimated choking temperature of that simulation run. The solid black line represents the calculated area ratio based on Mach number. No deviation can be seen at this scale, but zooming reveals variation on a smaller scale, as seen in **Figure 15**. This variation is minimal, so the simulation accurately models isentropic flow.

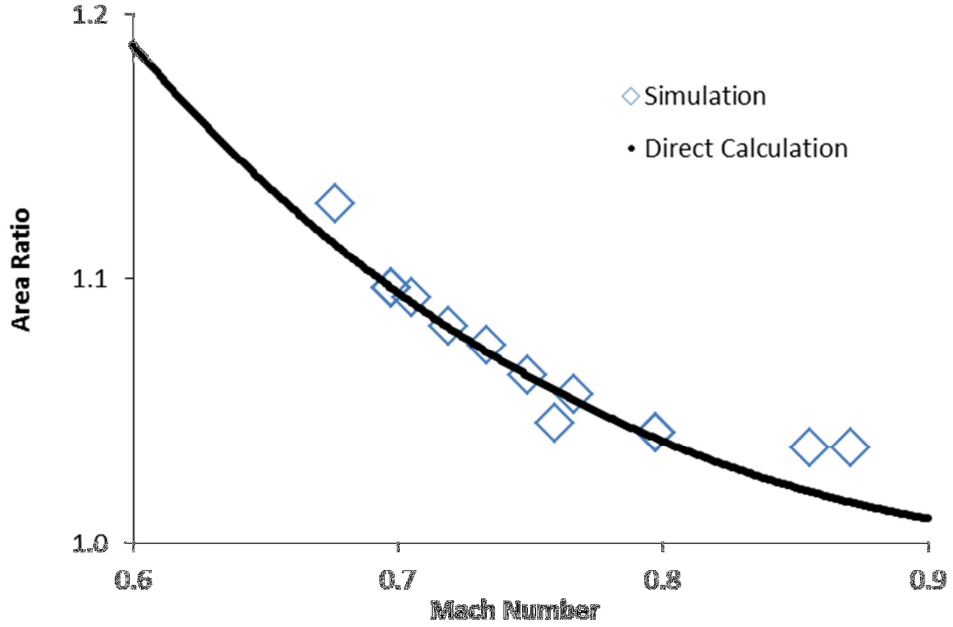

Figure 15. Plot of contraction isentropic validation, showing cross-sectional area ratios on a smaller Mach number range. The empty squares plot the area at each point of each simulation, divided by the average estimated choking area of that simulation run. The solid black line represents the calculated area ratio based on Mach number. This scale reveals variation, as it is a subset of the data shown in **Figure 14**. This variation is minimal—considering the range—so the simulation accurately models isentropic flow.

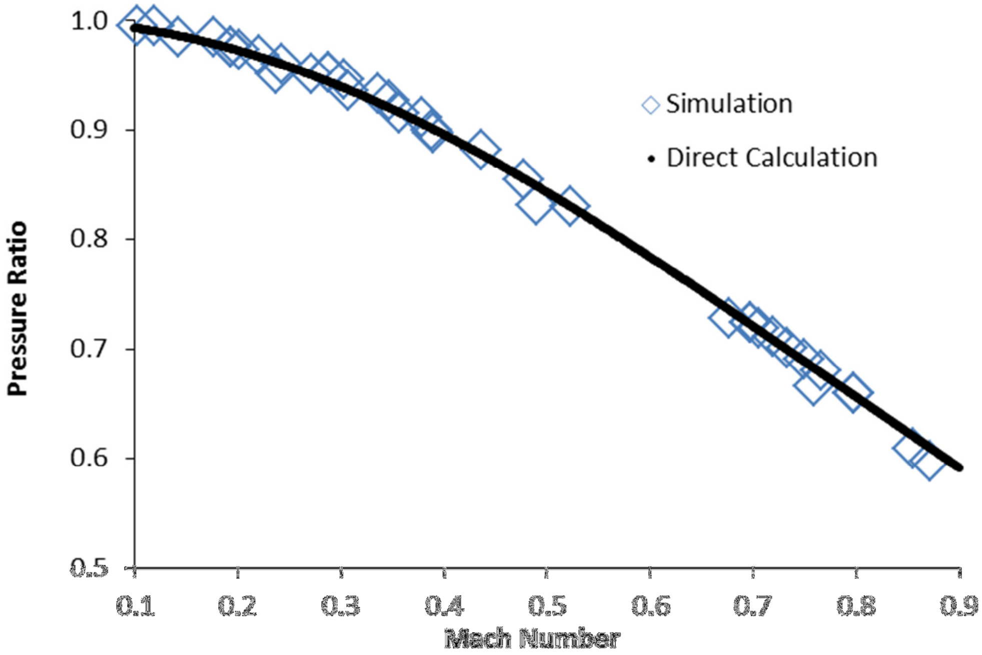

Figure 16. Plot of contraction isentropic validation, showing pressure ratios against Mach number. The empty squares plot the pressure at each point of each simulation, divided by the average estimated stagnation pressure of that simulation run. The solid black line represents the calculated pressure ratio based on Mach number. Some deviation can be seen at this scale; however, this variation is minimal, so the simulation accurately models isentropic flow.

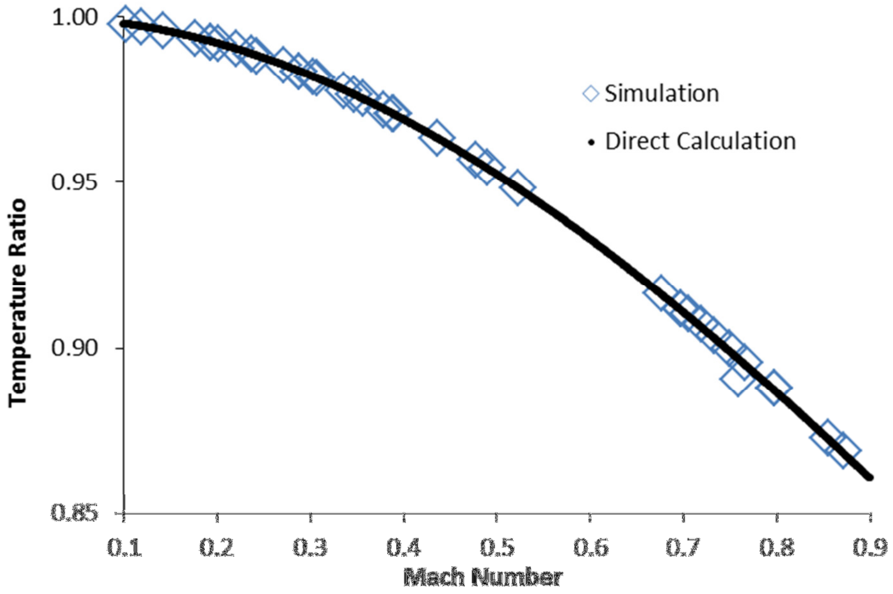

Figure 17. Plot of contraction isentropic validation, showing temperature ratios against Mach number. The empty squares plot the temperature at each point of each simulation, divided by the average estimated stagnation temperature of that simulation run. The solid black line represents the calculated temperature ratio based on Mach number. Some deviation can be seen at this scale; however, this variation is minimal, so the simulation accurately models isentropic flow.

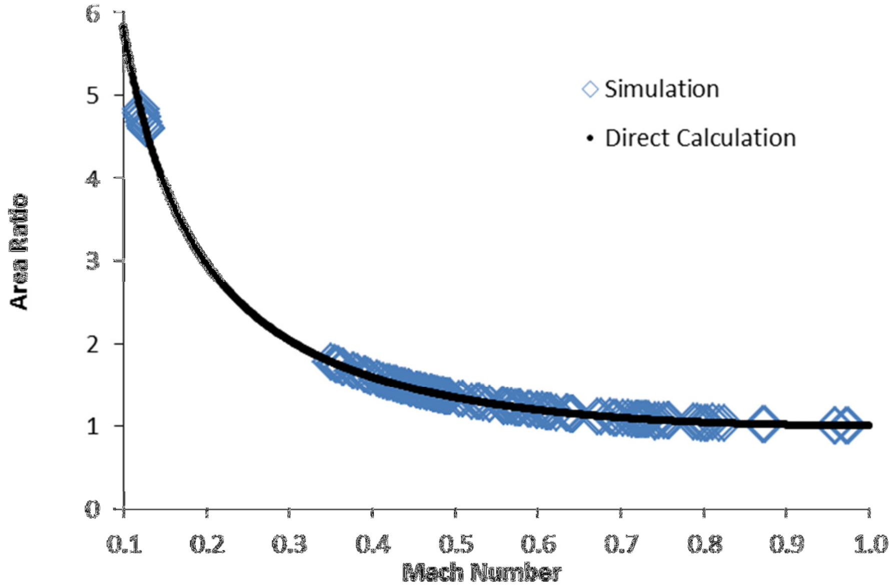

Figure 18. Plot of expansion-contraction isentropic validation, showing cross-sectional area ratios against Mach number. The empty squares plot the area at each point of each simulation, divided by the average estimated choking area of that simulation run. The solid black line represents the calculated area ratio based on Mach number. Deviation is even less in the expansion-contraction cases, so the simulation still accurately models isentropic flow.

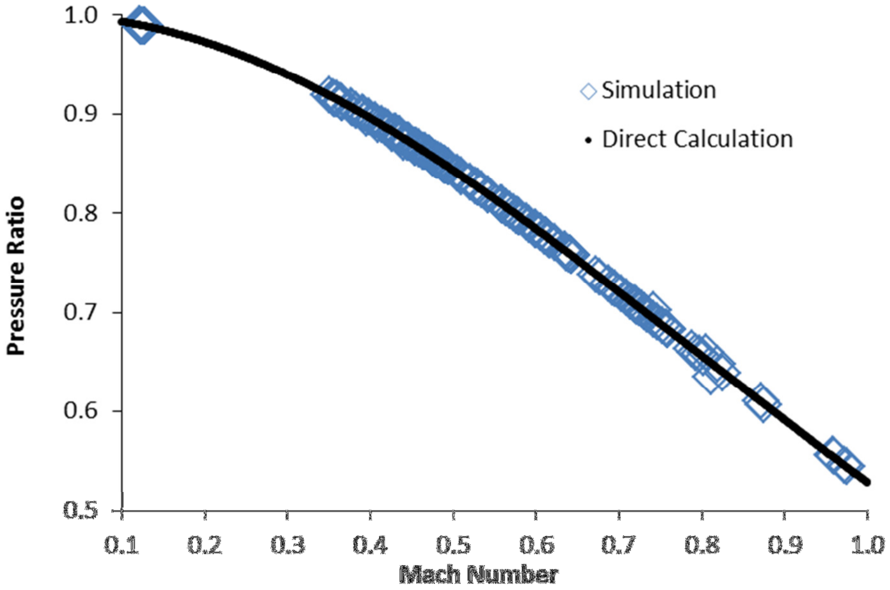

Figure 19. Plot of expansion-contraction isentropic validation, showing pressure ratios against Mach number. The empty squares plot the pressure at each point of each simulation, divided by the average estimated stagnation pressure of that simulation run. The solid black line represents the calculated pressure ratio based on Mach number. Deviation is even less in the expansion-contraction cases, so the simulation still accurately models isentropic flow.

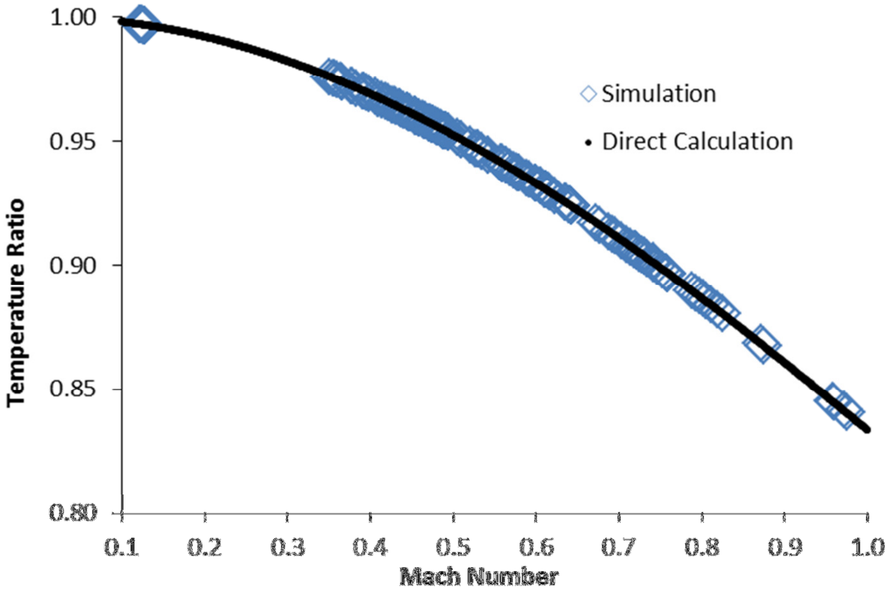

Figure 20. Plot of expansion-contraction isentropic validation, showing temperature ratios against Mach number. The empty squares plot the temperature at each point of each simulation, divided by the average estimated stagnation temperature of that simulation run. The solid black line represents the calculated temperature ratio based on Mach number. Deviation is even less in the expansion-contraction cases, so the simulation still accurately models isentropic flow.

Two-Phase Validation

Homogeneous Equilibrium Model

To validate the two phase simulation, a model must be developed—a homogeneous equilibrium model (HEM) simplifies calculations. The HEM assumes that there is no interphase velocity difference, and that the two phases exist in thermal equilibrium. To match this assumption in the simulation, the interphase friction coefficient must be large enough such that the difference between the liquid and gas velocity is negligible. Similarly, a higher heat transfer coefficient satisfies the thermal equilibrium requirement.

Successfully validating the simulation against the HEM demonstrates that the two phases correctly interact with one another when their temperatures and velocities are nearly equal. One interaction validated is the liquid phase occupying space that was, in the single phase model, only occupied by the gas phase, reducing the available volume for the gas phase's equation of state calculations. The transfer mechanisms—interphase drag and heat transfer—are not addressed in this validation, their only function is to balance the fluids to reach the HEM assumptions. Future work (with more sophisticated interphase drag and heat transfer models) will require additional two-phase validations.

Developing the Validation Criterion

The pressure drop across the pipe drives the flow of liquid and gas from a high pressure to low pressure. Working against this pressure drop is the force of friction, which only applies to the liquid phase. Steady state occurs when these opposing force balance one another out. Modifying Equation (115), the differential pressure change per unit length of pipe,

$$\frac{dP}{dy} = -\frac{f\rho_L V_L^2}{2D_h} \tag{129}$$

where all properties are based on the liquid phase. To solve Equation (129), all variables must either be a constant or a function of pressure. Solving Equation (57) for velocity yields,

$$V_L = \frac{\dot{m}_L}{A(1-\alpha)\rho_L} \tag{130}$$

and Equation (129) becomes,

$$\frac{dP}{dy} = \frac{-C_1}{(1-\alpha)^2} \tag{131}$$

where,

$$C_1 = \frac{f\dot{m}_L^2}{2A^2 D_h \rho_L} \tag{132}$$

which is a constant for a given simulation run. C_1 represents a pressure over length and its components do not vary with pressure, so it may be joined together as a constant to ease the integration that follows. Void fraction, however, varies with pressure, and must be substituted. Related to void fraction is flow quality,

$$x = \frac{\dot{m}_G}{\dot{m}_L + \dot{m}_G} \tag{133}$$

or, using Equations (56) and (57),

$$x = \frac{[\rho_G A \alpha V_G]}{[\rho_L A(1-\alpha)V_L]+[\rho_G A \alpha V_G]} \tag{134}$$

which may be simplified using the HEM assumption,

$$V_L = V_G \tag{135}$$

to

$$x = \frac{\rho_G \alpha}{\rho_L(1-\alpha)+\rho_G \alpha} \tag{136}$$

or

$$1-\alpha = \frac{\rho_V}{\rho_V+\rho_L\frac{x}{1-x}} \tag{137}$$

Substituting Equation (137) into Equation (131) yields,

$$\frac{dP}{dy} = -C_1 \frac{\left(\rho_V+\rho_L\frac{x}{1-x}\right)^2}{\rho_V^2} \tag{138}$$

Vapor density is a function of pressure. Applying the ideal gas law,

$$\rho_V = \frac{P}{RT} \tag{139}$$

yields,

$$\frac{dP}{dy} = -C_1 \frac{(P+C_2)^2}{P^2} \tag{140}$$

where,

$$C_2 = \rho_L RT \frac{x}{1-x} \tag{141}$$

which is a constant with units of pressure. Note that temperature remains approximately constant throughout the simulation because: (1) the HEM assumes that the liquid and gas phases have the same temperature; and (2) the high heat capacity of the liquid phase prevents much temperature change over the length of the pipe. Therefore, C_2 remains essentially constant with respect to pressure, and simplifies the following integration.

Now, with Equation (140) in terms of pressure, it may be integrated,

$$\int dy = -\frac{1}{C_1}\int \frac{P^2}{(P+C_2)^2}dP \tag{142}$$

over the length of the pipe, such that,

$$y_2 - y_1 = -\frac{1}{C_1}\left[P + C_2 - 2C_2\ln(P+C_2) - \frac{C_2^2}{P+C_2}\right]_{P(y_1)}^{P(y_2)} \tag{143}$$

where y_1 and y_2 refer to the inlet and exit positions of the pipe. Defining the inlet and exit pressures as P_1 and P_2, the integration result yields,

$$L = -\frac{1}{C_1}\left[(P_1 - P_2) - 2C_2 \ln\left(\frac{P_1+C_2}{P_2+C_2}\right) + C_2^2\left(\frac{1}{P_2+C_2} - \frac{1}{P_1+C_2}\right)\right] \tag{144}$$

Returning the constant values to the result allows the equation to be solved for mass flow rate of liquid,

$$\dot{m}_L = A\sqrt{\frac{2D_h\rho_L}{fL}\left[(P_1 - P_2) - 2RT\rho_L\frac{x}{1-x}\ln\left(\frac{P_1+RT\rho_L\frac{x}{1-x}}{P_2+RT\rho_L\frac{x}{1-x}}\right) + \left(RT\rho_L\frac{x}{1-x}\right)^2\left(\frac{1}{P_2+RT\rho_L\frac{x}{1-x}} - \frac{1}{P_1+RT\rho_L\frac{x}{1-x}}\right)\right]} \tag{145}$$

Equation (145) exists in a form that predicts the result of a simulation run before it completes. The two phase simulation defines all of the independent variables prior to beginning a run, while producing the dependent variable, liquid mass flow rate, as an output of the simulation. The simulation matching the predicted liquid mass flow rate would validates the simulation's agility to model the HEM.

Test Procedure

To validate the simulation's ability to model homogeneous equilibrium, multiple simulation runs execute following the assumptions of the HEM. Interphase friction factor (and interphase heat transfer coefficient) must be large enough to ensure the velocity (and temperature) of the gas phase approximately equal the velocity (and temperature) of the liquid phase. Also, temperature must remain constant for all points along the system, which the high heat capacity of the fluid enables.

If the HEM assumption remains valid, the independent variables found in Equation (145) are selected, and the predicted liquid mass flow rate is found. The simulation uses the same values and begins simulation. Once steady-state is reached, the simulation liquid mass flow rate is recorded and compared to the expected value. Equation (117) calculates the percent difference between the predicted and simulation result.

The validation varied many of the independent variables found in Equation (145). The cross-sectional area varied between 0.03 and 0.08 m^2; the length of the simulation ranged from 25 to 39 m; the wall friction factor varied between 0.02 and 0.07; temperature ranged from 250 to 320 K; density varied between 1.30 and 1.44 kg/m^3; inlet void fraction ranged from 0.3 to 0.7; finally, the overall pressure drop varied between 2 and 31 kPa. **Table 8** in Appendix B: Simulation Data contains the data from the HEM validation.

Results

The results show that the simulation matches the analytical model from Equation (145). For all runs attempted, the simulation liquid mass flow rate remained within 2% of the prediction. As expected, the interphase velocity difference contributes to how well the model from Equation (145) applies; if the velocity difference is too great, the HEM assumption is no longer valid.

As **Figure 21** shows, a lower velocity difference improves the agreement between the model from Equation (145) and the simulation. For the series of runs shown in **Figure 21**, the predicted liquid mass flow rate remained 61.34 kg/s. Each point represents a different interphase friction factor; higher friction factors lead to more similar liquid and gas velocities. As the difference between the two velocities decreases, the simulation approaches a closer match to the HEM result.

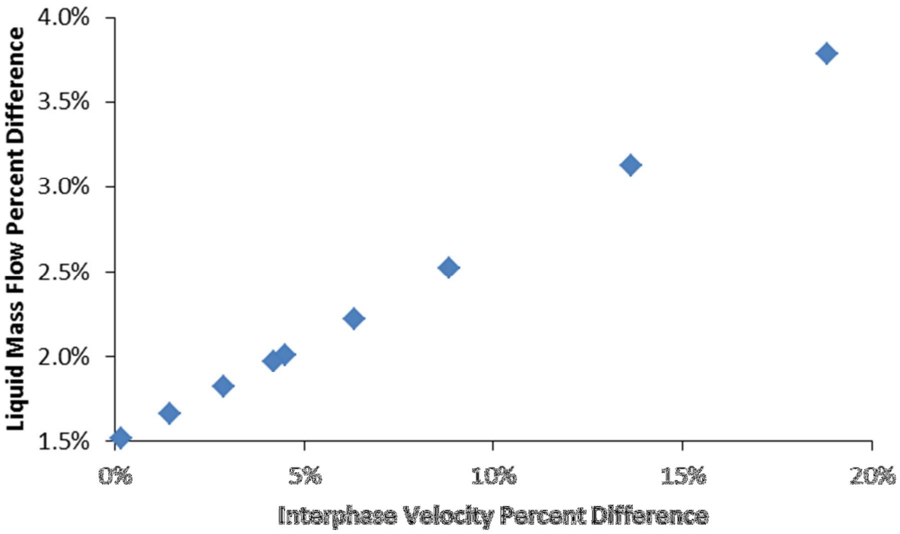

Figure 21. Increasing liquid mass flow rate error with increasing velocity difference. The simulation data was produced by varying the interphase drag coefficient while keeping all other flow parameters constant for two phase flow. A higher velocity difference between the two phases decreases how well the HEM approximation matches the simulation. For these flow parameters, the simulation, at best, can reach a liquid mass flow rate that is 1.5% of the expected liquid mass flow rate. The inability to reach a 0% prediction difference may be the result of poor resolution or too much temperature variation along the length of the pipe. Runs 13-21 from **Table 8** were used to create this plot. Please note that worst match is presented here to demonstrate the effect of interphase velocity difference; runs 1-12 show closer simulation-prediction matching.

Conclusions

Comparison to Previous Work

This section examines the work done by others related to one-dimensional flow modeling and highlights the differences between other literature and this thesis project.

Others have used Simulink to model one-dimensional fluid flow. (Alamian, Behbahani-Nejad, & Ghanbarzadeh, 2012) developed Simulink functions to model the transportation of natural gas through pipelines. Their model does not include an energy conservation term, assuming that the flow is isothermal. Also, Alamian's simulation uses transfer functions in s-space to solve flow conditions. Alamian references (Herrán-González, De La Cruz, De Andrés-Toro, & Risco-Martín, 2009), who also built a Simulink library for analyzing gas distribution pipelines. Herrán-González also assumes isothermal conditions, but makes no menthion of s-space or Laplace transforms.

Similar to the simulation described in this thesis, (Davis & Campbell, 2007) employs a one-dimensional fluid flow model using mass, momentum, and energy continuity equations in their simulation. Rather than utilizing the ideal-gas law, Davis utilizes the REFPROP database (from the National Institute for Standards and Testing) to find the values of state variables for real fluids (as well as two-phase mixtures). Davis's two-phase simulation appears limited to homogeneous equilibrium (modeled as a single fluid with a single equation of state), while the simulation featured in this thesis incorporates two-phase flow by using the mass, momentum, and energy continuity equations separately on each phase. Also, at the time of the journal article, Davis had not yet incorporated area change in their simulation, which the simulation featured in this thesis includes.

The simulation from (Scheuerer & Scheuerer, 1992) employs a similar structure to the simulation developed for this thesis. Scheuerer utilizes separate mass and momentum conservation equations for each phase, where upstream and downstream flux terms originate from the average properties of the adjacent control volumes; the simulation in this thesis performs the same process for conserving mass, momentum and energy. Scheuerer did not include an energy conservation equation in their simulation, the major difference from the simulation described by this thesis.

RELAP Comparison

RELAP5-3D is a one-dimensional, two-phase simulation tool and the primary standard of comparison for this thesis's simulation. This section will explore the similarities and differences between RELAP and the new simulation, using the RELAP5-3D user's manual, (Idaho National Laboratory, 2005).

Mass Continuity

Like the new simulation, RELAP employs mass, momentum, and energy equations to simulate fluid flow. The manual states the mass continuity equations,

$$\frac{d}{dt}(\alpha\rho_G)+\frac{1}{A}\frac{d}{dx}(\alpha\rho_G V_G A)=\Gamma_G \tag{146}$$

and

$$\frac{d}{dt}([1-\alpha]\rho_L)+\frac{1}{A}\frac{d}{dx}([1-\alpha]\rho_L V_L A)=\Gamma_L \tag{147}$$

where Γ is the mass generation of each phase, and the other variables have been adjusted to match the conventions of this thesis. RELAP does not typically employ mass sources or sinks, but does include phase change, so that

$$\Gamma_L=-\Gamma_G \tag{148}$$

The primary mass continuity difference between the new simulation and RELAP is that RELAP includes a mechanism for phase change, while the new simulation cannot accurately model scenarios where phase change occurs.

Momentum Conservation

The REALAP manual gives the momentum conservation equations as well. With variable substitutions to account for the nomenclature in this thesis, the gas phase momentum balance is

$$\alpha\rho_G A\frac{dV_G}{dt}+\frac{1}{2}\alpha\rho_G A\frac{dV_G^2}{dx}=-\alpha A\frac{dP}{dx}+\alpha\rho_G B_X A-(\alpha\rho_G A)f_{R,G}V_G+\Gamma_G A\big(V_{G,ip}-V_G\big)$$

$$-(\alpha_G\rho_G A)f_{ip}(V_G-V_L)-C\alpha(1-\alpha)\rho_{GL}A\left[\frac{d(V_G-V_L)}{dt}+V_L\frac{dV_G}{dx}-V_G\frac{dV_L}{dx}\right] \tag{149}$$

and the liquid phase momentum balance is

$$(1-\alpha)\rho_L A\frac{dV_L}{dt}+\frac{1}{2}(1-\alpha)\rho_L A\frac{dV_L^2}{dx}=$$

$$-(1-\alpha)A\frac{dP}{dx}+(1-\alpha)\rho_L B_X A-\big((1-\alpha)\rho_L A\big)f_{R,L}V_L+\Gamma_G A\big(V_{L,ip}-V_L\big)$$

$$-((1-\alpha)\rho_L A)f_{ip}(V_L-V_G)-C\alpha(1-\alpha)\rho_{GL}A\left[\frac{d(V_L-V_G)}{dt}+V_G\frac{dV_L}{dx}-V_L\frac{dV_G}{dx}\right] \tag{150}$$

where f_R is RELAP's wall friction factor, $V_{if}$is the velocity at the interface between the fluids, ρ_{GL} is the average density of both fluids, B_X is the sum of the body forces acting in the flow direction, and C is the coefficient of virtual mass.

The new simulation does not include the 4th term on the right side of Equations (149) and (150), as the momentum transfer do to mass transfer does not apply when there is no phase change. Furthermore, the 6th term on the right side is excluded, as the new simulation neglects the effect of force due to virtual mass. Also, the 5th term on the right side of Equation (149) is omitted—the new simulation assumes a wetted pipe perimeter and only applies wall friction to the liquid phase.

The wall friction term exists in a different form in the new simulation. Instead of being proportional to velocity, the new simulation's frictional force terms are proportional to velocity-squared. Furthermore, while RELAP includes many factors in its body force term, the new simulation only includes the force due to gravity. The remaining terms in Equations (149) and (150)—the momentum flow across boundaries (2nd term on left), and the pressure differential (1st term on the right)—exist in both RELAP and the thesis simulation.

Energy Conservation

The RELAP manual also gives the energy balance equations used in the RELAP simulation. The gas energy equation is

$$\frac{d}{dt}(\alpha\rho_G u_G) + \frac{1}{A}\frac{d}{dx}(\alpha\rho_G u_G V_G A) = -P\frac{d\alpha}{dt} - \frac{P}{A}\frac{d}{dx}(\alpha V_G A) + \dot{Q}_{W,G} + \dot{Q}_{ip,G} + \Gamma_{ip,G}h_G^{\#} + \Gamma_{w,G}h'_G + DISS_G \tag{151}$$

and the liquid energy equation is

$$\frac{d}{dt}([1-\alpha]\rho_L u_L) + \frac{1}{A}\frac{d}{dx}([1-\alpha]\rho_L u_L V_L A) = P\frac{d\alpha}{dt} - \frac{P}{A}\frac{d}{dx}([1-\alpha]V_L A) + \dot{Q}_{W,L} + \dot{Q}_{ip,L} + \Gamma_{ip,G}h_L^{\#} + \Gamma_{w,G}h'_L + DISS_L \tag{152}$$

where $\dot{Q}_W$ is the heat transfer rate from the pipe wall to the fluid, $h^{\#}$ is the specific enthalpy associated with bulk interface mass transfer, h' is the specific enthalpy associated with mass transfer at the wall, and $DISS$ is the energy dissipation term.

Again, the simulation of this thesis does not include phase change, so terms that involve energy transfer due to phase change—the 5th and 6th terms on the right side of Equations (151) and (152)—are not included in the new simulation. Also, the new simulation does not incorporate wall heat transfer, so the 3rd right side term is excluded as well.

The new simulation employs a different convention for energy balance management. Rather than include a dissipation term, which adds thermal energy as kinetic energy is lost due to friction, the new simulation incorporates kinetic energy—and gravitational potential energy—into the energy conservation equation. Therefore, when the velocity decreases due to friction—or the height of the fluid increases—there is no net change in total energy. The simulation does not track thermal energy as a separate entity; at each time step, the simulation subtracts the kinetic and potential energy—based in the velocity and height—and the remaining energy is the thermal energy used to calculate temperature.

The new simulation includes the remaining terms, total energy rate of change (1st term on the left), energy flow across boundaries (2nd term on the left), flow work due to void fraction change (1st term on the right), flow work due to velocity (2nd term on the right), and interphase heat transfer (4th term on the right).

Next Steps

This section contains potential ways to improve the simulation code. The basis of the two-phase, one-dimensional simulation code already exists; any of the following features can be added without changing the underlying structure of the code.

Accurate Interphase Models

Currently, the simulation allows for transfer of heat and momentum between the two phases. The temperature difference between the two phases drives the flow of energy from the higher temperature phase to the lower temperature phase. The heat transfer from Equation (84) is proportional to a heat transfer coefficient. The coefficient, in the current simulation, is represented by a constant with no empirical or theoretical backing; the HEM validation only required this constant to be large enough to ensure that the gas and liquid temperatures would be approximately equal.

Also, the transfer of momentum due to friction—the interphase drag force—involves the placeholder model shown in Equation (69). Not only is the frictional coefficient not known, but there is little consensus on methods to determine interphase drag. The literature review of this thesis examines several potential models that this simulation could incorporate. The placeholder interphase friction model enables the simulation to run stably, as the gas phase velocity would increase with little bound without friction from the liquid phase. Also, like the interphase heat transfer, the friction coefficient is large enough so that the gas and liquid velocities are similar enough for the HEM validation.

To improve the interphase heat transfer and friction in the simulation, the placeholder models must be replaced with theoretically—or empirically—backed models.

Validate Transients

The four validation cases performed on the simulation—incompressible, Fanno, isentropic, HEM—all required steady state to be achieved. Though the steady state scenario has been validated, no validation of the transient state of the system has been performed. The transient functions; the system proceeds from an initial state to the steady state. It is not known if this transition occurs over the proper amount of time. Also, the system's response to an oscillating input should be examined.

Phase Change

While the current simulation allows for a two-phase mixture, it does not allow for phase change. To incorporate phase change, a rate of vaporization would be needed. The rate of vaporization would be incorporated into the gas mass balance,

$$\dot{m}_{G,net} = (\rho_G V_G A \alpha)_{-\frac{1}{2}} - (\rho_G V_G A \alpha)_{+\frac{1}{2}} + \Gamma \tag{153}$$

and the liquid mass balance,

$$\dot{m}_{L,net} = (\rho_L V_L A [1-\alpha])_{-\frac{1}{2}} - (\rho_L V_L A [1-\alpha])_{+\frac{1}{2}} - \Gamma \tag{154}$$

where the rate of vaporization,

$$\Gamma = f(T_G, T_L, P, \alpha, A, L) \tag{155}$$

With a correct mass transfer model in place of Equation (155), the current simulation allows easy implementation of phase change, simply adding the equation's result to the mass balance equation for each phase. The correct mass transfer model will likely involve the heat transfer across the temperature difference between each phase and the interface. If the two heat transfers do not balance, the difference would yield phase change.

Wall Heat Transfer

Another desired feature is the generation of heat in the system. The heat would originate from the wall, so the heat generation term would appear in the liquid energy balance,

$$\dot{E}_{net,L} = \dot{E}_{-\frac{1}{2},L} - \dot{E}_{+\frac{1}{2},L} + \dot{Q}_{ip} + \dot{W}_{ip} + \dot{W}_{expan,net} + \dot{G}_{W} \tag{156}$$

The heat generation term could either be a constant, or the term could be based on the temperature difference between the wall and the liquid phase. Then, wall heat transfer,

$$\dot{G}_{W} = f(T_L, T_W, \hbar_W, A, L) \tag{157}$$

To validate the heat transfer model, Rayleigh flow would be used. Rayleigh flow requires heat transfer into the fluid so that temperature remains constant. To run this validation, a wall temperature would be selected, then Rayleigh flow requires the heat transfer coefficient be large enough so that the fluid temperature matches the wall temperature at all points, making the Rayleigh flow assumption valid. The resulting heat transfer rate would be recorded and compared to the Rayleigh flow predicted values.

Special Components

Currently, the only component the simulation can model is a straight pipe section, with the option to vary the cross-sectional area. Adding different types of components would improve the code. A pump would behave the same as a junction component, except that the pressure sent to the downstream volume would be higher than the pressure sent to the upstream volume. A tee pipe section would replace a junction, except that the tee would exchange information with three adjacent sections, rather than two. A separator would act similar to tee, with the flow output in each branch restricted to a certain void fraction. A valve would also replace a junction, behaving the same when open, but preventing flow when closed. For curved pipe sections, a constant could be added to the friction in a volume component, representing the losses associated with those components.

Bibliography

Alamian, R., Behbahani-Nejad, M., & Ghanbarzadeh, A. (2012, May 29). A state space model for transient flow simulation in natural gas pipelines. *Journal of Natural Gas Science and Engineering*(9), 51-59.

Anderson, D. A., Tannehill, J. C., & Pletcher, R. H. (1984). *Coputational Fluid Mechanics and Heat Transfer.* New York: Hemisphere Publishing Corporation.

Collier, J. G., & Thome, J. R. (1994). *Convective Boiling and Condensation* (3rd ed.). New York: Oxford University Press.

Davis, R. L., & Campbell, B. T. (2007, October). Quasi-One-Dimensional Unsteady-Flow Procedure for Real Fluids. (C. Kaplan, Ed.) *AIAA Journal, 45*(10), 2422-2428.

Herrán-González, A., De La Cruz, J. M., De Andrés-Toro, B., & Risco-Martín, J. L. (2009, March). Modeling and simulation of a gas distribution pipeline network. *Applied Mathematical Modelling, 33*(3), 1584-1600.

Hirsch, C. (1990). *Numerical Computation of Internal and External Flows* (Vol. 2: Computational Methods for Inviscid and Viscous Flows). Chichester, West Sussex, England: John Wiley & Sons.

Idaho National Laboratory. (2005). *RELAP5-3D (C) Code Manual* (2.4 ed., Vols. 1: Code Structure, System Models, and Solution Methods). Idaho Falls, Idaho.

Incropera, F. P., DeWitt, D. P., Bergman, T. L., & Lavine, A. S. (2007). *Fundamentals of Heat and Mass Transfer* (6th ed.). Hoboken, NJ: John Wiley & Sons.

Ishii, M., & Takashi, H. (2011). *Thermo-Fluid Dynamics of Two-Phase Flow* (2nd ed.). New York: Springer Science + Business Media.

Kays, W., Crawford, M., & Wiegand, B. (2005). *Convective Heat and Mass Transfer* (4th ed.). New York, New York: McGraw-Hill.

Keenan, J. H., & Kaye, J. (1948). *Gas Tables.* New York: John Wiley & Sons.

Liles, D. e. (1988). *TRAC-PF1/MOD1 correlations and models.* Washington, D.C.: Nuclear Regulatory Commission, Washington, DC (USA). Div. of Reactor Accident Analysis; Los Alamos National Lab., NM (USA).

Martinelli, R. C., & Nelson, D. B. (1948, August). Prediction of Pressure Drop During Forced-Circulation Boiling of Water. *Transactions of the American Society of Mechanical Engineers*, 695-702.

Munson, B. R., Young, D. F., & Okiishi, T. H. (1998). *Fundamentals of Fluid Mechanics* (3rd ed.). New York: John Wiley & Sons.

Potter, M. C., & Foss, J. M. (1982). *Fluid Mechanics.* Okemos, MI: Great Lakes Press, Inc.

Scheuerer, G., & Scheuerer, M. (1992). Two-fluid model simulation of two-phase flow problems using a conservative finite-volume method. *Forschung und Ingenieurwesen, 58*(5), 128-134.

The MathWorks, Inc. (2012, September). *MATLAB Mathematics*. Retrieved December 6, 2013, from MathWorks - MATLAB and Simulink for Technical Computing: http://www.mathworks.com/help/releases/R2012b/pdf_doc/allpdf.html#matlab

Todreas, N. E., & Kazimi, M. S. (2012). *Nuclear Systems* (2nd ed., Vol. 1: Thermal Hydraulic Fundamentals). Boca Raton: CRC Press.

United States Nuclear Regulatory Commission. (2012, March 29). *NRC: Computer Codes*. Retrieved December 19, 2013, from NRC: Home Page: http://www.nrc.gov/about-nrc/regulatory/research/comp-codes.html

Appendix A: Nomenclature

Variable Names

A	Cross-sectional area
α	Void Fraction
B_X	Net Body Force Acting in X-Direction
c	Speed of Sound
C	Coefficient of Virtual Mass
C_1	Constant for simplification. Units of pressure over distance.
C_2	Constant for simplification. Units of pressure.
C_f	(Fanning) Friction factor
c_p	Constant-pressure specific heat
c_V	Constant-volume specific heat
D	Drag (Force)
D_h	Hydraulic diameter
$DISS$	Energy Dissipation Rate
e	Specific total energy
E	Energy
Err	Percent Error Between Simulink Simulation and Flow Model
f	(Darcy) Friction factor
F_f	Frictional force
F_P	Force Due to Pressure
f_R	Friction Factor Used by RELAP
F_w	Wall forces
g	Acceleration of Gravity
Γ	Mass Generation Rate
h	Specific enthalpy
~~h~~	Heat Transfer Coefficient
H	Height

k	Ratio of Specific Heats
ke	Specific kinetic energy
L	Length of a volume block
M	Momentum
m	Mass
Ma	Mach Number
μ	Dynamic viscosity
$\hat{n}$	Vector Perpendicular to Cross-sectional Area
P	Pressure
ΔP_{exp}	Pressure drop due to expansion
ΔP_f	Pressure drop due to friction
pe	Specific Potential Energy
$Q\ (\dot{Q})$	Heat (Heat Transfer Rate)
R	Specific gas constant
Re_D	Reynolds number, for internal flows
ρ	Density
r_X	Ratio of a Generic Property
T	Temperature
τ_s	Wall shear stress
ΔT	Temperature Difference
Δt	Time Step
θ	Angle Above Horizontal
u	Specific internal energy
V	Velocity
$\cancel{V}$	Volume
ΔV	Velocity Difference
$\cancel{W}$	Weight (Force Due to Gravity)
$W\ (\dot{W})$	Work (Power)
X	General reference to a fluid property

x	Flow Quality
y	Position
z	Stability percentage

Subscripts

$-\frac{1}{2}$	Upstream Block of Opposite Type
$+\frac{1}{2}$	Downstream Block of Opposite Type
$+1$	Downstream Block of Same Type
-1	Upstream Block of Same Type
$x, 0$	Used in Extrapolation. x is the Number of Space Steps Away (Junctions and Volumes).
$0, y$	Used in Extrapolation. y is the Number of Time Steps Away.
0	Reference, Stagnation, or Initial Condition
B	Estimated Boundary Property
CS	Refers to Control Surface
CV	Refers to Control Volume
F	Ratio Pertains to Fanno Flow
G	Quantity Applies to Gas Phase
$G \rightarrow L$	Quantity Transfers from Gas Phase to Liquid Phase
GL	Quantity Applies to the Mass Average of both Pahses
I	Ratio Pertains to Isentropic Flow
L	Quantity Applies to Liquid Phase
$L \rightarrow G$	Quantity Transfers from Liquid Phase to Gas Phase
ND	Non-Dimensional
W	At Pipe Wall
a	Property at Point “a” Along the Length of the Pipe
ab	Between Points “a” and “b”
b	Property at Point “b” Along the Length of the Pipe
$disp$	Dissipated Energy

if	Quantity at Interface Between the Phases
inc	Incompresible
ip	Inter-phase
$isentropic$	Isentropic Model Validation
$left$	Property at Left Boundary of Control Volume
$model$	Quantity is the Theoretical Expected Value from a Flow Model
net	The Net Total of a Quantity
ref	Reference Property Value. Refers to Sonic or Stagnation
$right$	Property at Right Boundary of Control Volume
sim	Quantity is a Result from the Simulink Simulation
t	Value from Table (Expected Value)

Superscripts and Symbols

$\dot{X}, \frac{dX}{dt}$	Time Derivative of X
$\bar{X}$	Mean of X
$\frac{dX}{dy}$	Length Derivative of X
X^*	Property at Sonic Conditions
$h^{\#}$	Property Associated with Bulk Interface Mass Transfer
h'	Property Associated with Bulk Wall Mass Transfer

Appendix B: Simulation Data

Incompressible Simulation

The data contained in this section was used to validate that the single-phase simulation yields accurate results while an incompressible assumption is valid. The analysis is found on page 34.

Pre-set Conditions					Predictions		Result	
Inlet Temperature	Inlet Density	Friction Factor	Area	Total Pressure Drop	Velocity	Average Mach Number	Average Velocity	Velocity Percent Error
(K)	(kg/m^3)		(m^2)	(Pa)	(m/s)		(m/s)	
300	1.205	0.095	0.015	431	25.0	0.07	25.0	0.2%
302	1.200	0.090	0.010	689	29.4	0.08	29.4	0.3%
301	1.200	0.075	0.030	344	30.0	0.09	29.9	0.4%
302	1.200	0.070	0.010	689	33.4	0.10	33.2	0.4%
301	1.200	0.050	0.030	344	36.8	0.11	36.5	0.7%
300	1.220	0.095	0.015	1,722	49.7	0.14	49.3	0.9%
302	1.200	0.030	0.010	689	51.0	0.15	50.4	1.2%
301	1.200	0.025	0.030	344	52.0	0.15	51.2	1.5%
300	1.230	0.095	0.015	2,583	60.7	0.17	59.8	1.4%
305	1.200	0.075	0.030	1,722	67.1	0.19	65.8	2.0%
300	1.240	0.095	0.015	3,444	69.8	0.20	68.5	1.8%
305	1.200	0.050	0.030	1,722	82.2	0.23	79.7	3.1%
315	1.200	0.100	0.015	5,167	84.7	0.24	82.6	2.5%
302	1.200	0.010	0.010	689	88.3	0.25	85.0	3.8%
310	1.200	0.075	0.030	3,444	94.9	0.27	91.4	3.7%
315	1.200	0.080	0.020	5,167	101.7	0.29	97.7	3.9%
300	1.300	0.095	0.015	8,611	107.7	0.31	103.3	4.2%
310	1.200	0.050	0.030	3,444	116.3	0.33	109.6	5.7%
315	1.200	0.060	0.020	5,167	117.5	0.33	111.1	5.4%
305	1.200	0.025	0.030	1,722	116.3	0.33	109.2	6.1%
300	1.350	0.095	0.015	12,917	129.5	0.37	121.9	5.9%
315	1.200	0.040	0.020	5,167	143.9	0.40	132.1	8.2%
325	1.200	0.080	0.040	8,611	156.2	0.43	142.4	8.8%
300	1.400	0.095	0.015	17,222	146.8	0.42	135.9	7.4%
330	1.200	0.075	0.030	10,333	164.4	0.45	149.0	9.4%
320	1.200	0.050	0.030	6,889	164.4	0.46	147.3	10.4%
310	1.200	0.025	0.030	3,444	164.4	0.47	146.6	10.9%
325	1.200	0.060	0.040	8,611	180.3	0.50	159.5	11.6%
300	1.500	0.095	0.015	25,834	173.7	0.50	156.0	10.2%
325	1.300	0.060	0.015	17,940	195.7	0.54	171.1	12.6%
330	1.200	0.050	0.030	10,333	201.4	0.55	173.9	13.7%
300	1.408	0.060	0.015	17,911	187.9	0.54	164.4	12.5%
315	1.200	0.020	0.020	5,167	203.4	0.57	173.0	15.0%
325	1.200	0.040	0.040	8,611	220.9	0.61	184.9	16.3%
320	1.200	0.025	0.030	6,889	232.5	0.65	190.7	18.0%
300	1.700	0.095	0.015	43,056	210.7	0.61	181.8	13.7%
330	1.200	0.025	0.030	10,333	284.8	0.78	218.6	23.2%
300	1.700	0.065	0.015	43,056	254.7	0.73	201.6	20.9%
300	1.408	0.030	0.015	17,911	265.7	0.77	206.6	22.3%
325	1.200	0.020	0.040	8,611	312.3	0.86	229.4	26.6%

Table 1. Incompressible Validation Data. For all runs with a predicted Mach number less than 0.33, the percent difference between the predicted velocity (from incompressible model) and the simulation average velocity remained below 5%. As the Mach number increases, the incompressible model no longer applies. This data was created with an overall pipe length of 1.66 meters and an outlet pressure of 103,334 Pa.

Fanno Flow Validation

The data contained in this section was used to validate that the single-phase simulation yields accurate results while a Fanno flow assumption is valid. The analysis is found on page 37.

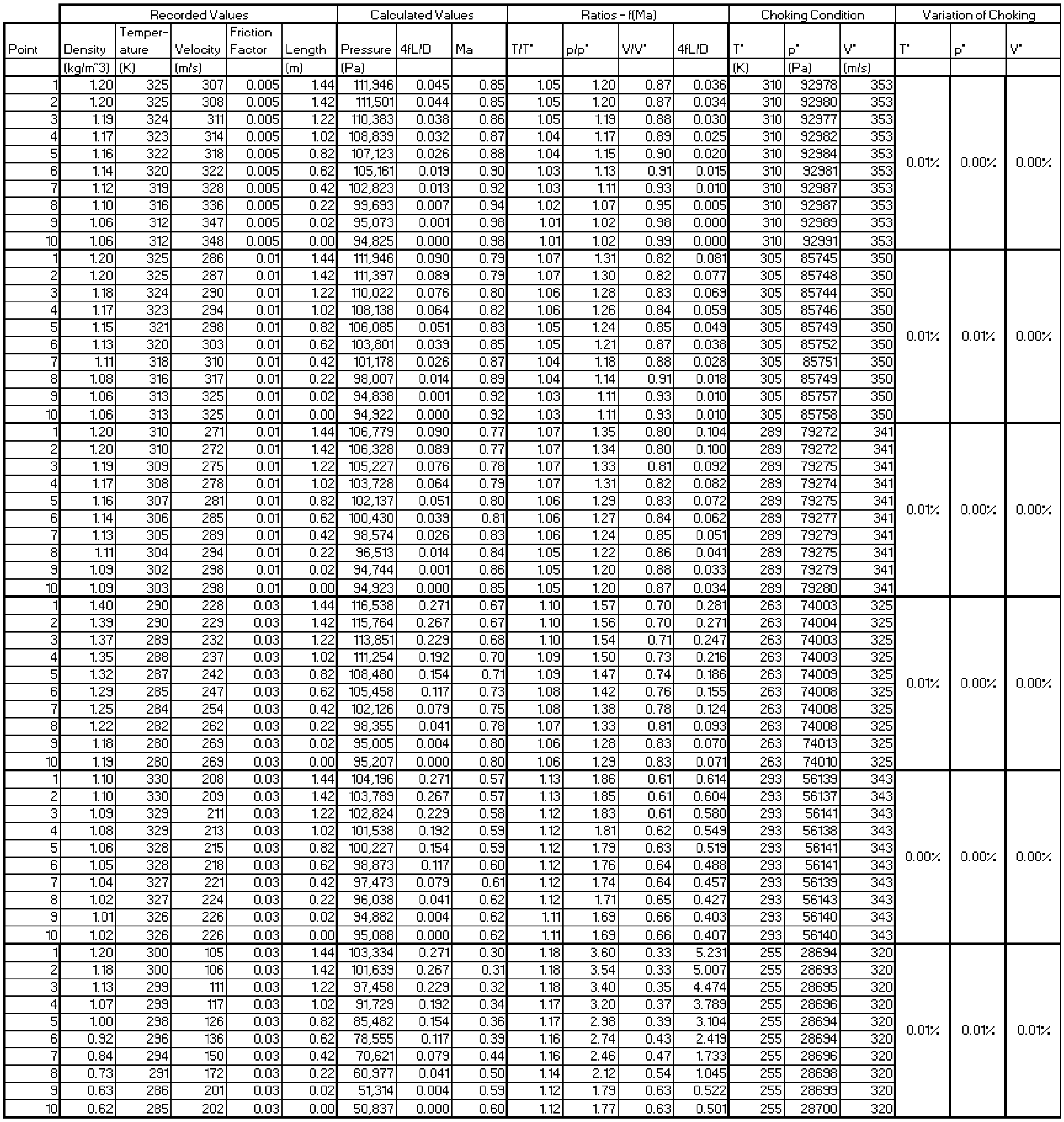

	Recorded Values					Calculated Values			Ratios - f(Ma)				Choking Condition			Variation of Choking		
Point	Density	Temperature	Velocity	Friction Factor	Length	Pressure	4fL/D	Ma	T/T*	p/p*	V/V*	4fL/D	T*	p*	V*	T*	p*	V*
	(kg/m^3)	(K)	(m/s)		(m)	(Pa)							(K)	(Pa)	(m/s)			
1	1.20	325	307	0.005	1.44	111,946	0.045	0.85	1.05	1.20	0.87	0.036	310	92978	353	0.01%	0.00%	0.00%
2	1.20	325	308	0.005	1.42	111,501	0.044	0.85	1.05	1.20	0.87	0.034	310	92980	353			
3	1.19	324	311	0.005	1.22	110,383	0.038	0.86	1.05	1.19	0.88	0.030	310	92977	353			
4	1.17	323	314	0.005	1.02	108,839	0.032	0.87	1.04	1.17	0.89	0.025	310	92982	353			
5	1.16	322	318	0.005	0.82	107,123	0.026	0.88	1.04	1.15	0.90	0.020	310	92984	353			
6	1.14	320	322	0.005	0.62	105,161	0.019	0.90	1.03	1.13	0.91	0.015	310	92981	353			
7	1.12	319	328	0.005	0.42	102,823	0.013	0.92	1.03	1.11	0.93	0.010	310	92987	353			
8	1.10	316	336	0.005	0.22	99,693	0.007	0.94	1.02	1.07	0.95	0.005	310	92987	353			
9	1.06	312	347	0.005	0.02	95,073	0.001	0.98	1.01	1.02	0.98	0.000	310	92989	353			
10	1.06	312	348	0.005	0.00	94,825	0.000	0.98	1.01	1.02	0.99	0.000	310	92991	353			
1	1.20	325	286	0.01	1.44	111,946	0.090	0.79	1.07	1.31	0.82	0.081	305	85745	350	0.01%	0.01%	0.00%
2	1.20	325	287	0.01	1.42	111,397	0.089	0.79	1.07	1.30	0.82	0.077	305	85748	350			
3	1.18	324	290	0.01	1.22	110,022	0.076	0.80	1.06	1.28	0.83	0.069	305	85744	350			
4	1.17	323	294	0.01	1.02	108,138	0.064	0.82	1.06	1.26	0.84	0.059	305	85746	350			
5	1.15	321	298	0.01	0.82	106,085	0.051	0.83	1.05	1.24	0.85	0.049	305	85749	350			
6	1.13	320	303	0.01	0.62	103,801	0.039	0.85	1.05	1.21	0.87	0.038	305	85752	350			
7	1.11	318	310	0.01	0.42	101,178	0.026	0.87	1.04	1.18	0.88	0.028	305	85751	350			
8	1.08	316	317	0.01	0.22	98,007	0.014	0.89	1.04	1.14	0.91	0.018	305	85749	350			
9	1.06	313	325	0.01	0.02	94,838	0.001	0.92	1.03	1.11	0.93	0.010	305	85757	350			
10	1.06	313	325	0.01	0.00	94,922	0.000	0.92	1.03	1.11	0.93	0.010	305	85758	350			
1	1.20	310	271	0.01	1.44	106,779	0.090	0.77	1.07	1.35	0.80	0.104	289	79272	341	0.01%	0.00%	0.00%
2	1.20	310	272	0.01	1.42	106,328	0.089	0.77	1.07	1.34	0.80	0.100	289	79272	341			
3	1.19	309	275	0.01	1.22	105,227	0.076	0.78	1.07	1.33	0.81	0.092	289	79275	341			
4	1.17	308	278	0.01	1.02	103,728	0.064	0.79	1.07	1.31	0.82	0.082	289	79274	341			
5	1.16	307	281	0.01	0.82	102,137	0.051	0.80	1.06	1.29	0.83	0.072	289	79275	341			
6	1.14	306	285	0.01	0.62	100,430	0.039	0.81	1.06	1.27	0.84	0.062	289	79277	341			
7	1.13	305	289	0.01	0.42	98,574	0.026	0.83	1.06	1.24	0.85	0.051	289	79279	341			
8	1.11	304	294	0.01	0.22	96,513	0.014	0.84	1.05	1.22	0.86	0.041	289	79275	341			
9	1.09	302	298	0.01	0.02	94,744	0.001	0.86	1.05	1.20	0.88	0.033	289	79279	341			
10	1.09	303	298	0.01	0.00	94,923	0.000	0.85	1.05	1.20	0.87	0.034	289	79280	341			
1	1.40	290	228	0.03	1.44	116,538	0.271	0.67	1.10	1.57	0.70	0.281	263	74003	325	0.01%	0.00%	0.00%
2	1.39	290	229	0.03	1.42	115,764	0.267	0.67	1.10	1.56	0.70	0.271	263	74004	325			
3	1.37	289	232	0.03	1.22	113,851	0.229	0.68	1.10	1.54	0.71	0.247	263	74003	325			
4	1.35	288	237	0.03	1.02	111,254	0.192	0.70	1.09	1.50	0.73	0.216	263	74003	325			
5	1.32	287	242	0.03	0.82	108,480	0.154	0.71	1.09	1.47	0.74	0.186	263	74009	325			
6	1.29	285	247	0.03	0.62	105,458	0.117	0.73	1.08	1.42	0.76	0.155	263	74008	325			
7	1.25	284	254	0.03	0.42	102,126	0.079	0.75	1.08	1.38	0.78	0.124	263	74008	325			
8	1.22	282	262	0.03	0.22	98,355	0.041	0.78	1.07	1.33	0.81	0.093	263	74008	325			
9	1.18	280	269	0.03	0.02	95,005	0.004	0.80	1.06	1.28	0.83	0.070	263	74013	325			
10	1.19	280	269	0.03	0.00	95,207	0.000	0.80	1.06	1.29	0.83	0.071	263	74010	325			
1	1.10	330	208	0.03	1.44	104,196	0.271	0.57	1.13	1.86	0.61	0.614	293	56139	343	0.00%	0.00%	0.00%
2	1.10	330	209	0.03	1.42	103,789	0.267	0.57	1.13	1.85	0.61	0.604	293	56137	343			
3	1.09	329	211	0.03	1.22	102,824	0.229	0.58	1.12	1.83	0.61	0.580	293	56141	343			
4	1.08	329	213	0.03	1.02	101,538	0.192	0.59	1.12	1.81	0.62	0.549	293	56138	343			
5	1.06	328	215	0.03	0.82	100,227	0.154	0.59	1.12	1.79	0.63	0.519	293	56141	343			
6	1.05	328	218	0.03	0.62	98,873	0.117	0.60	1.12	1.76	0.64	0.488	293	56141	343			
7	1.04	327	221	0.03	0.42	97,473	0.079	0.61	1.12	1.74	0.64	0.457	293	56139	343			
8	1.02	327	224	0.03	0.22	96,038	0.041	0.62	1.12	1.71	0.65	0.427	293	56143	343			
9	1.01	326	226	0.03	0.02	94,882	0.004	0.62	1.11	1.69	0.66	0.403	293	56140	343			
10	1.02	326	226	0.03	0.00	95,088	0.000	0.62	1.11	1.69	0.66	0.407	293	56140	343			
1	1.20	300	105	0.03	1.44	103,334	0.271	0.30	1.18	3.60	0.33	5.231	255	28694	320	0.01%	0.01%	0.01%
2	1.18	300	106	0.03	1.42	101,639	0.267	0.31	1.18	3.54	0.33	5.007	255	28693	320			
3	1.13	299	111	0.03	1.22	97,458	0.229	0.32	1.18	3.40	0.35	4.474	255	28695	320			
4	1.07	299	117	0.03	1.02	91,729	0.192	0.34	1.17	3.20	0.37	3.789	255	28696	320			
5	1.00	298	126	0.03	0.82	85,482	0.154	0.36	1.17	2.98	0.39	3.104	255	28694	320			
6	0.92	296	136	0.03	0.62	78,555	0.117	0.39	1.16	2.74	0.43	2.419	255	28694	320			
7	0.84	294	150	0.03	0.42	70,621	0.079	0.44	1.16	2.46	0.47	1.733	255	28696	320			
8	0.73	291	172	0.03	0.22	60,977	0.041	0.50	1.14	2.12	0.54	1.045	255	28698	320			
9	0.63	286	201	0.03	0.02	51,314	0.004	0.59	1.12	1.79	0.63	0.522	255	28699	320			
10	0.62	285	202	0.03	0.00	50,837	0.000	0.60	1.12	1.77	0.63	0.501	255	28700	320			

Table 2. Fanno Flow Validation Data. Each group of ten rows represents a single Fanno Flow validation run. Density, temperature and velocity were recorded at ten points along the pipe for each run. Mach number was calculated, which was then used to determine the choking condition ratios, per Equations (121) - (123). Based on these ratios, the choking conditions were found for each point in the run. The last three columns present the variation for each of the three choking variables in the form standard deviation divided by average of the ten points. The non-dimensional length, fL/D, did not match as closely to the expected values.

Isentropic Flow Validation

The data contained in this section was used to validate that the single-phase simulation yields accurate results while an Isentropic flow assumption is valid. The analysis is found on page 40. Two sets of data are present, the contraction case and the expansion-contraction case.

	Recorded Values				Calculated Values		Ratios - f(Ma)			Choking / Stagnation			Variation		
Point	Area	Velocity	Temper-ature	Density	Pressure	Ma	A/A*	P/P0	T/T0	A*	P0	T0	A*	P0	T0
	(m^2)	(m/s)	(K)	(kg/m^3)	(Pa)					(m^2)	(Pa)	(K)			
1	0.0150	37	363	1.20	125,000	0.10	6.07	0.99	1.00	0.0025	125,807	364	0.8%	0.9%	0.0%
2	0.0150	37	363	1.20	125,000	0.10	6.07	0.99	1.00	0.0025	125,807	364			
3	0.0141	39	363	1.20	124,518	0.10	5.66	0.99	1.00	0.0025	125,442	364			
4	0.0122	45	363	1.20	124,650	0.12	4.92	0.99	1.00	0.0025	125,884	364			
5	0.0102	54	362	1.19	123,341	0.14	4.10	0.99	1.00	0.0025	125,111	364			
6	0.0083	67	361	1.19	123,318	0.18	3.34	0.98	0.99	0.0025	126,026	364			
7	0.0063	90	360	1.15	119,018	0.24	2.53	0.96	0.99	0.0025	123,760	364			
8	0.0044	131	355	1.14	116,034	0.35	1.79	0.92	0.98	0.0025	126,081	364			
9	0.0035	178	348	1.07	106,977	0.48	1.39	0.86	0.96	0.0025	125,000	364			
10	0.0035	183	347	1.05	104,111	0.49	1.36	0.85	0.95	0.0025	122,642	364			
1	0.0200	72	348	1.20	120,000	0.19	3.06	0.97	0.99	0.0065	123,175	351	0.2%	0.2%	0.0%
2	0.0200	72	348	1.20	120,000	0.19	3.06	0.97	0.99	0.0065	123,175	351			
3	0.0193	75	348	1.20	119,675	0.20	2.94	0.97	0.99	0.0066	123,112	351			
4	0.0177	82	348	1.19	119,052	0.22	2.71	0.97	0.99	0.0065	123,140	351			
5	0.0161	91	347	1.19	118,067	0.24	2.47	0.96	0.99	0.0065	123,021	351			
6	0.0146	101	346	1.18	116,909	0.27	2.23	0.95	0.99	0.0065	123,036	351			
7	0.0130	114	344	1.16	115,003	0.31	1.99	0.94	0.98	0.0065	122,807	351			
8	0.0115	132	342	1.14	112,461	0.36	1.75	0.92	0.98	0.0066	122,757	351			
9	0.0107	144	341	1.13	110,572	0.39	1.63	0.90	0.97	0.0066	122,684	351			
10	0.0107	144	341	1.13	110,292	0.39	1.63	0.90	0.97	0.0066	122,434	351			
1	0.0100	91	250	1.81	130,000	0.29	2.11	0.94	0.98	0.0047	137,705	254	1.2%	1.1%	0.0%
2	0.0100	91	250	1.81	130,000	0.29	2.11	0.94	0.98	0.0047	137,705	254			
3	0.0096	96	250	1.80	129,118	0.30	2.02	0.94	0.98	0.0048	137,575	254			
4	0.0087	106	249	1.78	127,237	0.34	1.84	0.92	0.98	0.0047	137,560	254			
5	0.0079	119	247	1.75	124,314	0.38	1.66	0.91	0.97	0.0048	137,268	254			
6	0.0071	137	245	1.71	120,324	0.44	1.48	0.88	0.96	0.0048	137,125	254			
7	0.0062	163	241	1.64	113,167	0.52	1.30	0.83	0.95	0.0048	136,289	254			
8	0.0054	207	233	1.49	99,354	0.68	1.11	0.74	0.92	0.0049	134,971	254			
9	0.0050	255	222	1.31	83,152	0.86	1.02	0.62	0.87	0.0049	134,150	254			
10	0.0050	259	221	1.29	81,490	0.87	1.02	0.61	0.87	0.0049	133,616	254			
1	0.0300	252	325	1.29	119,996	0.70	1.10	0.72	0.91	0.0274	166,078	357	0.4%	0.8%	0.2%
2	0.0300	252	325	1.29	119,996	0.70	1.10	0.72	0.91	0.0274	166,078	357			
3	0.0299	255	324	1.28	119,167	0.71	1.09	0.72	0.91	0.0274	166,067	357			
4	0.0296	259	323	1.27	117,716	0.72	1.08	0.71	0.91	0.0274	166,058	357			
5	0.0294	264	322	1.26	116,142	0.73	1.07	0.70	0.90	0.0274	166,044	357			
6	0.0291	269	321	1.24	114,442	0.75	1.06	0.69	0.90	0.0274	166,042	357			
7	0.0289	274	319	1.23	112,552	0.77	1.05	0.68	0.89	0.0274	166,014	357			
8	0.0286	271	317	1.21	110,285	0.76	1.06	0.68	0.90	0.0270	161,566	354			
9	0.0285	284	316	1.20	109,183	0.80	1.04	0.66	0.89	0.0274	165,989	357			
10	0.0285	284	316	1.20	109,204	0.80	1.04	0.66	0.89	0.0274	166,007	357			

Table 3. Isentropic Flow Validation Data, Contraction. Each group of ten rows represents a single Isentropic Flow validation run. Density, temperature, velocity, and cross-sectional area were recorded at ten points along the pipe for each run. Mach number was calculated, which was then used to determine the choking and stagnation condition ratios, per Equations (126) - (128). Based on these ratios, the choking conditions were found for each point in the run. The last three columns present the variation for each of the three choking and stagnation variables in the form standard deviation divided by average of the ten points.

	Recorded Values				Calculated Values		Ratios - f(Ma)			Choking / Stagnation			Variation		
Point	Area	Velocity	Temperature	Density	Pressure	Ma	A/A*	P/P0	T/T0	A*	P0	T0	A*	P0	T0
	(m^2)	(m/s)	(K)	(kg/m^3)	(Pa)					(m^2)	(Pa)	(K)			
1	0.0180	294	375	1.20	129,168	0.76	1.06	0.68	0.90	0.0170	189,128	418	0.1%	0.1%	0.0%
2	0.0180	294	375	1.20	129,182	0.76	1.06	0.68	0.90	0.0170	189,137	418			
3	0.0181	292	376	1.21	129,979	0.75	1.06	0.69	0.90	0.0170	189,205	418			
4	0.0182	289	377	1.21	131,258	0.74	1.07	0.69	0.90	0.0170	189,243	418			
5	0.0183	286	378	1.22	132,258	0.73	1.07	0.70	0.90	0.0170	189,195	418			
6	0.0184	283	378	1.23	133,422	0.72	1.08	0.71	0.90	0.0170	189,227	418			
7	0.0185	279	380	1.24	134,763	0.71	1.08	0.71	0.91	0.0170	189,336	418			
8	0.0178	306	372	1.17	124,979	0.79	1.04	0.66	0.89	0.0170	189,069	418			
9	0.0170	361	354	1.04	105,271	0.96	1.00	0.55	0.84	0.0170	189,892	418			
10	0.0170	366	352	1.02	103,234	0.97	1.00	0.54	0.84	0.0170	189,709	418			
1	0.0180	294	375	1.20	129,168	0.76	1.06	0.68	0.90	0.0170	188,883	418	0.1%	0.1%	0.0%
2	0.0180	294	375	1.20	129,168	0.76	1.06	0.68	0.90	0.0170	188,883	418			
3	0.0181	290	376	1.21	130,477	0.75	1.06	0.69	0.90	0.0170	188,886	418			
4	0.0183	283	378	1.22	132,882	0.73	1.08	0.70	0.90	0.0170	188,877	418			
5	0.0185	277	380	1.24	135,065	0.71	1.09	0.72	0.91	0.0170	188,890	418			
6	0.0187	271	381	1.25	137,048	0.69	1.10	0.73	0.91	0.0170	188,890	418			
7	0.0184	280	379	1.23	133,898	0.72	1.08	0.71	0.91	0.0170	188,826	418			
8	0.0175	317	368	1.14	120,746	0.83	1.03	0.64	0.88	0.0170	188,805	418			
9	0.0170	361	353	1.03	104,741	0.96	1.00	0.55	0.84	0.0170	189,250	418			
10	0.0170	365	352	1.02	103,269	0.97	1.00	0.55	0.84	0.0170	189,129	418			
1	0.0180	283	375	1.20	129,168	0.73	1.07	0.70	0.90	0.0168	184,167	415	0.0%	0.0%	0.0%
2	0.0180	283	375	1.20	129,168	0.73	1.07	0.70	0.90	0.0168	184,167	415			
3	0.0181	280	376	1.21	130,282	0.72	1.08	0.71	0.91	0.0168	184,164	415			
4	0.0183	274	378	1.22	132,366	0.70	1.09	0.72	0.91	0.0168	184,164	415			
5	0.0185	268	379	1.23	134,275	0.69	1.10	0.73	0.91	0.0168	184,171	415			
6	0.0187	263	381	1.25	136,026	0.67	1.12	0.74	0.92	0.0168	184,171	415			
7	0.0184	271	378	1.23	133,257	0.70	1.10	0.72	0.91	0.0168	184,119	415			
8	0.0175	303	369	1.15	122,296	0.79	1.04	0.66	0.89	0.0168	184,096	415			
9	0.0170	331	360	1.09	112,440	0.87	1.02	0.61	0.87	0.0167	184,321	415			
10	0.0170	333	360	1.08	111,834	0.88	1.01	0.61	0.87	0.0168	184,140	415			
1	0.0180	249	375	1.20	129,168	0.64	1.14	0.76	0.92	0.0157	170,307	406	0.0%	0.0%	0.0%
2	0.0180	249	375	1.20	129,168	0.64	1.14	0.76	0.92	0.0157	170,307	406			
3	0.0181	247	376	1.20	129,860	0.63	1.15	0.76	0.93	0.0157	170,306	406			
4	0.0183	242	377	1.21	131,188	0.62	1.16	0.77	0.93	0.0157	170,310	406			
5	0.0185	238	378	1.22	132,413	0.61	1.18	0.78	0.93	0.0157	170,305	406			
6	0.0187	234	379	1.23	133,548	0.60	1.19	0.78	0.93	0.0157	170,295	406			
7	0.0184	240	377	1.22	131,741	0.62	1.17	0.77	0.93	0.0157	170,260	406			
8	0.0175	262	372	1.17	125,248	0.68	1.11	0.74	0.92	0.0157	170,244	406			
9	0.0170	277	368	1.14	120,643	0.72	1.08	0.71	0.91	0.0157	170,326	406			
10	0.0170	277	368	1.14	120,501	0.72	1.08	0.71	0.91	0.0157	170,251	406			

Table 4. Isentropic Flow Validation Data, Expansion-Contraction Part 1 / 4. Each group of ten rows represents a single Isentropic Flow validation run. Density, temperature, velocity, and cross-sectional area were recorded at ten points along the pipe for each run. Mach number was calculated, which was then used to determine the choking and stagnation condition ratios, per Equations (126) - (128). Based on these ratios, the choking conditions were found for each point in the run. The last three columns present the variation for each of the three choking and stagnation variables in the form standard deviation divided by average of the ten points. Note that the last run contains 14 points, to examine the effect of resolution on validation results.

	Recorded Values				Calculated Values		Ratios - f(Ma)			Choking / Stagnation			Variation		
Point	Area	Velocity	Temper-ature	Density	Pressure	Ma	A/A*	P/P0	T/T0	A*	P0	T0	A*	P0	T0
	(m^2)	(m/s)	(K)	(kg/m^3)	(Pa)					(m^2)	(Pa)	(K)			
1	0.0180	142	375	1.20	129,168	0.37	1.71	0.91	0.97	0.0105	141,688	385	0.0%	0.0%	0.0%
2	0.0180	142	375	1.20	129,168	0.37	1.71	0.91	0.97	0.0105	141,688	385			
3	0.0181	141	375	1.20	129,320	0.36	1.72	0.91	0.97	0.0105	141,685	385			
4	0.0183	139	375	1.20	129,620	0.36	1.74	0.91	0.97	0.0105	141,687	385			
5	0.0185	138	376	1.20	129,906	0.35	1.76	0.92	0.98	0.0105	141,686	385			
6	0.0187	136	376	1.21	130,189	0.35	1.78	0.92	0.98	0.0105	141,693	385			
7	0.0184	139	375	1.20	129,758	0.36	1.75	0.92	0.98	0.0105	141,680	385			
8	0.0175	147	374	1.19	128,345	0.38	1.66	0.91	0.97	0.0105	141,683	385			
9	0.0170	152	374	1.19	127,455	0.39	1.62	0.90	0.97	0.0105	141,697	385			
10	0.0170	152	374	1.19	127,422	0.39	1.62	0.90	0.97	0.0105	141,665	385			
1	0.0180	190	375	1.20	129,168	0.49	1.36	0.85	0.95	0.0132	152,181	393	0.0%	0.0%	0.0%
2	0.0180	190	375	1.20	129,168	0.49	1.36	0.85	0.95	0.0132	152,181	393			
3	0.0181	189	375	1.20	129,482	0.49	1.37	0.85	0.95	0.0132	152,183	393			
4	0.0183	186	376	1.21	130,085	0.48	1.38	0.85	0.96	0.0132	152,179	393			
5	0.0185	183	376	1.21	130,671	0.47	1.40	0.86	0.96	0.0132	152,185	393			
6	0.0187	181	377	1.21	131,217	0.46	1.41	0.86	0.96	0.0132	152,175	393			
7	0.0189	178	377	1.22	131,745	0.46	1.43	0.87	0.96	0.0132	152,174	393			
8	0.0183	187	376	1.20	129,876	0.48	1.38	0.85	0.96	0.0132	152,130	393			
9	0.0175	197	374	1.19	127,499	0.51	1.32	0.84	0.95	0.0132	152,192	393			
10	0.0175	198	374	1.19	127,345	0.51	1.32	0.84	0.95	0.0132	152,069	393			
1	0.0180	242	400	1.20	137,779	0.60	1.18	0.78	0.93	0.0152	176,398	429	0.0%	0.0%	0.0%
2	0.0180	242	400	1.20	137,779	0.60	1.18	0.78	0.93	0.0152	176,398	429			
3	0.0181	240	401	1.20	138,388	0.60	1.19	0.78	0.93	0.0152	176,399	429			
4	0.0183	236	401	1.21	139,548	0.59	1.20	0.79	0.94	0.0152	176,391	429			
5	0.0185	232	402	1.22	140,656	0.58	1.22	0.80	0.94	0.0152	176,401	429			
6	0.0187	229	403	1.22	141,691	0.57	1.23	0.80	0.94	0.0152	176,394	429			
7	0.0189	225	404	1.23	142,678	0.56	1.24	0.81	0.94	0.0152	176,394	429			
8	0.0183	238	401	1.21	139,127	0.59	1.20	0.79	0.93	0.0152	176,295	429			
9	0.0175	254	397	1.18	134,464	0.64	1.15	0.76	0.93	0.0152	176,423	429			
10	0.0175	254	397	1.18	134,199	0.64	1.15	0.76	0.93	0.0152	176,246	429			
1	0.0180	51	400	1.20	137,779	0.13	4.60	0.99	1.00	0.0039	139,340	401	0.0%	0.0%	0.0%
2	0.0180	51	400	1.20	137,779	0.13	4.60	0.99	1.00	0.0039	139,340	401			
3	0.0181	51	400	1.20	137,795	0.13	4.63	0.99	1.00	0.0039	139,338	401			
4	0.0183	50	400	1.20	137,827	0.12	4.68	0.99	1.00	0.0039	139,336	401			
5	0.0185	50	400	1.20	137,859	0.12	4.73	0.99	1.00	0.0039	139,336	401			
6	0.0187	49	400	1.20	137,891	0.12	4.78	0.99	1.00	0.0039	139,337	401			
7	0.0189	48	400	1.20	137,923	0.12	4.83	0.99	1.00	0.0039	139,338	401			
8	0.0185	50	400	1.20	137,860	0.12	4.73	0.99	1.00	0.0039	139,337	401			
9	0.0180	51	400	1.20	137,780	0.13	4.60	0.99	1.00	0.0039	139,342	401			
10	0.0180	51	400	1.20	137,745	0.13	4.60	0.99	1.00	0.0039	139,307	401			

Table 5. Isentropic Flow Validation Data, Expansion-Contraction, Part 2 / 4. Each group of ten rows represents a single Isentropic Flow validation run. Density, temperature, velocity, and cross-sectional area were recorded at ten points along the pipe for each run. Mach number was calculated, which was then used to determine the choking and stagnation condition ratios, per Equations (126) - (128). Based on these ratios, the choking conditions were found for each point in the run. The last three columns present the variation for each of the three choking and stagnation variables in the form standard deviation divided by average of the ten points. Note that the last run contains 14 points, to examine the effect of resolution on validation results.

	Recorded Values				Calculated Values		Ratios - f(Ma)			Choking / Stagnation			Variation		
Point	Area	Velocity	Temper-ature	Density	Pressure	Ma	A/A*	P/P0	T/T0	A*	P0	T0	A*	P0	T0
	(m^2)	(m/s)	(K)	(kg/m^3)	(Pa)					(m^2)	(Pa)	(K)			
1	0.0180	197	400	1.20	137,779	0.49	1.36	0.85	0.95	0.0132	162,391	419	0.0%	0.0%	0.0%
2	0.0180	197	400	1.20	137,779	0.49	1.36	0.85	0.95	0.0132	162,391	419			
3	0.0182	194	400	1.20	138,277	0.48	1.37	0.85	0.96	0.0132	162,389	419			
4	0.0185	190	401	1.21	139,226	0.47	1.39	0.86	0.96	0.0132	162,387	419			
5	0.0188	186	402	1.21	140,112	0.46	1.42	0.86	0.96	0.0132	162,383	419			
6	0.0191	183	403	1.22	140,949	0.45	1.44	0.87	0.96	0.0132	162,386	419			
7	0.0189	185	402	1.22	140,531	0.46	1.43	0.87	0.96	0.0132	162,379	419			
8	0.0183	193	401	1.21	138,587	0.48	1.38	0.85	0.96	0.0132	162,376	419			
9	0.0179	198	400	1.20	137,441	0.49	1.35	0.85	0.95	0.0132	162,396	419			
10	0.0179	198	400	1.20	137,428	0.49	1.35	0.85	0.95	0.0132	162,386	419			
1	0.0180	189	400	1.20	137,779	0.47	1.40	0.86	0.96	0.0129	160,371	418	0.0%	0.0%	0.0%
2	0.0180	189	400	1.20	137,779	0.47	1.40	0.86	0.96	0.0129	160,371	418			
3	0.0182	187	400	1.20	138,229	0.47	1.41	0.86	0.96	0.0129	160,370	418			
4	0.0185	183	401	1.21	139,081	0.46	1.43	0.87	0.96	0.0129	160,365	418			
5	0.0188	179	402	1.21	139,885	0.45	1.46	0.87	0.96	0.0129	160,365	418			
6	0.0191	176	402	1.22	140,642	0.44	1.48	0.88	0.96	0.0129	160,367	418			
7	0.0194	172	403	1.22	141,353	0.43	1.50	0.88	0.96	0.0129	160,366	418			
8	0.0187	180	402	1.21	139,706	0.45	1.45	0.87	0.96	0.0129	160,326	418			
9	0.0179	190	400	1.20	137,486	0.47	1.39	0.86	0.96	0.0129	160,386	418			
10	0.0179	190	400	1.20	137,324	0.47	1.39	0.86	0.96	0.0129	160,250	418			
1	0.0180	245	400	1.20	137,779	0.61	1.18	0.78	0.93	0.0153	177,312	430	0.0%	0.0%	0.0%
2	0.0180	245	400	1.20	137,779	0.61	1.18	0.78	0.93	0.0153	177,312	430			
3	0.0182	241	401	1.21	139,016	0.60	1.19	0.78	0.93	0.0153	177,310	430			
4	0.0186	233	403	1.22	141,291	0.58	1.21	0.80	0.94	0.0153	177,304	430			
5	0.0190	226	405	1.23	143,327	0.56	1.24	0.81	0.94	0.0153	177,306	430			
6	0.0194	219	406	1.25	145,146	0.54	1.27	0.82	0.94	0.0153	177,295	430			
7	0.0191	225	405	1.24	143,501	0.56	1.24	0.81	0.94	0.0153	177,258	430			
8	0.0180	245	400	1.20	137,740	0.61	1.18	0.78	0.93	0.0153	177,272	430			
9	0.0175	257	397	1.18	134,352	0.64	1.14	0.76	0.92	0.0153	177,329	430			
10	0.0175	257	397	1.18	134,312	0.64	1.14	0.76	0.92	0.0153	177,300	430			
1	0.0360	245	400	1.20	137,779	0.61	1.18	0.78	0.93	0.0306	177,297	430	0.0%	0.0%	0.0%
2	0.0360	245	400	1.20	137,779	0.61	1.18	0.78	0.93	0.0306	177,297	430			
3	0.0364	241	401	1.21	139,002	0.60	1.19	0.78	0.93	0.0306	177,285	430			
4	0.0372	233	403	1.22	141,271	0.58	1.21	0.80	0.94	0.0306	177,286	430			
5	0.0380	226	404	1.23	143,311	0.56	1.24	0.81	0.94	0.0306	177,286	430			
6	0.0388	219	406	1.25	145,160	0.54	1.27	0.82	0.94	0.0306	177,298	430			
7	0.0381	225	405	1.24	143,501	0.56	1.24	0.81	0.94	0.0306	177,251	430			
8	0.0360	245	400	1.20	137,725	0.61	1.18	0.78	0.93	0.0306	177,261	430			
9	0.0350	257	397	1.18	134,351	0.64	1.14	0.76	0.92	0.0306	177,332	430			
10	0.0350	257	397	1.18	134,312	0.64	1.14	0.76	0.92	0.0306	177,303	430			

Table 6. Isentropic Flow Validation Data, Expansion-Contraction, Part 3 / 4. Each group of ten rows represents a single Isentropic Flow validation run. Density, temperature, velocity, and cross-sectional area were recorded at ten points along the pipe for each run. Mach number was calculated, which was then used to determine the choking and stagnation condition ratios, per Equations (126) - (128). Based on these ratios, the choking conditions were found for each point in the run. The last three columns present the variation for each of the three choking and stagnation variables in the form standard deviation divided by average of the ten points. Note that the last run contains 14 points, to examine the effect of resolution on validation results.

	Recorded Values				Calculated Values		Ratios - f(Ma)			Choking / Stagnation			Variation		
Point	Area	Velocity	Temperature	Density	Pressure	Ma	A/A*	P/P0	T/T0	A*	P0	T0	A*	P0	T0
	(m^2)	(m/s)	(K)	(kg/m^3)	(Pa)					(m^2)	(Pa)	(K)			
1	0.0360	212	400	1.20	137,779	0.53	1.29	0.83	0.95	0.0279	166,706	422	0.0%	0.0%	0.0%
2	0.0360	212	400	1.20	137,779	0.53	1.29	0.83	0.95	0.0279	166,706	422			
3	0.0364	209	401	1.21	138,584	0.52	1.30	0.83	0.95	0.0279	166,699	422			
4	0.0372	203	402	1.21	140,095	0.50	1.33	0.84	0.95	0.0279	166,698	422			
5	0.0380	197	403	1.22	141,480	0.49	1.36	0.85	0.95	0.0279	166,706	422			
6	0.0388	192	404	1.23	142,741	0.48	1.39	0.86	0.96	0.0279	166,706	422			
7	0.0381	197	403	1.22	141,605	0.49	1.36	0.85	0.95	0.0280	166,671	422			
8	0.0358	214	400	1.20	137,200	0.53	1.28	0.82	0.95	0.0280	166,664	422			
9	0.0345	225	397	1.18	134,367	0.56	1.23	0.81	0.94	0.0279	166,738	422			
10	0.0345	225	397	1.18	134,290	0.56	1.23	0.81	0.94	0.0280	166,678	422			
1	0.0360	212	400	1.20	137,779	0.53	1.29	0.83	0.95	0.0279	166,706	422	0.0%	0.0%	0.0%
2	0.0360	212	400	1.20	137,779	0.53	1.29	0.83	0.95	0.0279	166,706	422			
3	0.0364	209	401	1.21	138,584	0.52	1.30	0.83	0.95	0.0279	166,699	422			
4	0.0372	203	402	1.21	140,095	0.50	1.33	0.84	0.95	0.0279	166,698	422			
5	0.0380	197	403	1.22	141,480	0.49	1.36	0.85	0.95	0.0279	166,706	422			
6	0.0388	192	404	1.23	142,741	0.48	1.39	0.86	0.96	0.0279	166,706	422			
7	0.0381	197	403	1.22	141,605	0.49	1.36	0.85	0.95	0.0280	166,671	422			
8	0.0358	214	400	1.20	137,200	0.53	1.28	0.82	0.95	0.0280	166,664	422			
9	0.0345	225	397	1.18	134,367	0.56	1.23	0.81	0.94	0.0279	166,738	422			
10	0.0345	225	397	1.18	134,290	0.56	1.23	0.81	0.94	0.0280	166,678	422			
1	0.0300	162	330	1.20	113,668	0.44	1.46	0.87	0.96	0.0205	130,199	343	0.0%	0.0%	0.0%
2	0.0300	162	330	1.20	113,668	0.44	1.46	0.87	0.96	0.0205	130,199	343			
3	0.0295	165	329	1.19	112,983	0.45	1.44	0.87	0.96	0.0205	130,191	343			
4	0.0280	177	327	1.18	110,623	0.49	1.36	0.85	0.95	0.0205	130,165	343			
5	0.0265	190	325	1.15	107,748	0.53	1.29	0.83	0.95	0.0205	130,199	343			
6	0.0250	207	322	1.13	103,923	0.58	1.22	0.80	0.94	0.0205	130,164	343			
7	0.0235	228	317	1.09	98,881	0.64	1.15	0.76	0.92	0.0205	130,239	343			
8	0.0222	255	311	1.03	92,003	0.72	1.08	0.71	0.91	0.0205	130,177	343			
9	0.0213	279	305	0.98	85,798	0.80	1.04	0.66	0.89	0.0205	130,367	343			
10	0.0213	280	304	0.98	85,272	0.80	1.04	0.66	0.89	0.0205	130,134	343			
1	0.0300	165	330	1.20	113,668	0.45	1.44	0.87	0.96	0.0209	130,937	344	0.5%	0.5%	0.0%
2	0.0300	165	330	1.20	113,667	0.45	1.44	0.87	0.96	0.0209	130,937	344			
3	0.0305	162	331	1.20	114,304	0.44	1.46	0.87	0.96	0.0209	130,910	344			
4	0.0315	156	332	1.21	115,513	0.43	1.51	0.88	0.96	0.0209	130,899	344			
5	0.0325	150	332	1.22	116,618	0.41	1.56	0.89	0.97	0.0208	130,913	344			
6	0.0335	144	333	1.23	117,578	0.39	1.61	0.90	0.97	0.0208	130,912	344			
7	0.0308	161	331	1.20	114,387	0.44	1.47	0.88	0.96	0.0209	130,697	344			
8	0.0244	220	320	1.11	101,566	0.61	1.17	0.78	0.93	0.0208	131,045	344			
9	0.0213	282	304	0.99	86,570	0.81	1.04	0.65	0.89	0.0206	132,712	344			
10	0.0213	286	303	0.98	84,998	0.82	1.03	0.64	0.88	0.0207	132,057	344			
1	0.0300	159	330	1.20	113,668	0.44	1.49	0.88	0.96	0.0202	129,479	343	0.6%	0.6%	0.0%
2	0.0300	159	330	1.20	113,765	0.44	1.49	0.88	0.96	0.0202	129,586	343			
3	0.0303	157	330	1.20	113,998	0.43	1.50	0.88	0.96	0.0202	129,498	343			
4	0.0308	154	331	1.21	114,583	0.42	1.52	0.88	0.97	0.0202	129,494	343			
5	0.0313	151	331	1.21	115,100	0.41	1.55	0.89	0.97	0.0202	129,471	342			
6	0.0318	148	332	1.21	115,590	0.41	1.57	0.89	0.97	0.0202	129,452	342			
7	0.0323	145	332	1.22	116,108	0.40	1.60	0.90	0.97	0.0202	129,468	342			
8	0.0328	142	332	1.22	116,589	0.39	1.62	0.90	0.97	0.0202	129,475	342			
9	0.0333	140	333	1.23	116,987	0.38	1.65	0.90	0.97	0.0202	129,448	342			
10	0.0338	138	333	1.23	117,376	0.38	1.67	0.91	0.97	0.0202	129,429	342			
11	0.0310	152	331	1.21	114,659	0.42	1.53	0.89	0.97	0.0202	129,307	342			
12	0.0247	206	321	1.12	103,600	0.57	1.22	0.80	0.94	0.0202	129,459	343			
13	0.0213	261	309	1.03	90,870	0.74	1.07	0.69	0.90	0.0200	130,873	343			
14	0.0213	283	303	0.95	82,224	0.81	1.03	0.65	0.88	0.0206	126,755	343			

Table 7. Isentropic Flow Validation Data, Expansion-Contraction, Part 4 / 4. Each group of ten rows represents a single Isentropic Flow validation run. Density, temperature, velocity, and cross-sectional area were recorded at ten points along the pipe for each run. Mach number was calculated, which was then used to determine the choking and stagnation condition ratios, per Equations (126) - (128). Based on these ratios, the choking conditions were found for each point in the run. The last three columns present the variation for each of the three choking and stagnation variables in the form standard deviation divided by average of the ten points. Note that the last run contains 14 points, to examine the effect of resolution on validation results.

HEM Simulation Validation

The data contained in this section was used to validate that the two-phase simulation yields accurate results while an HEM assumption is valid. The analysis is found on page 46.

	Pre-Set Conditions							Calculated Values		Prediction	Actual	Percent Difference	Velocity Difference			
Run	Cross-sectional Area	Length	Wall Friction Factor	Temper-ature	Inlet Gas Density	Inlet Void Fraction	Interphase Drag Coefficient	Inlet Pressure	Quality	Liquid Mass Flow Rate	Liquid Mass Flow Rate	Liquid Mass Flow Rate	Liquid Velocity	Gas Velocity	Velocity Difference	Percent Velocity Difference
	(m^2)	(m)		(K)	(kg/m^3)			(Pa)		(kg/s)	(kg/s)		(m/s)	(m/s)	(m/s)	
1	0.05	25	0.05	250	1.4353	0.7	10	103,000	0.00334	13.39	13.30	0.6%	0.90	0.98	0.08	9.0%
2	0.05	25	0.05	250	1.4353	0.3	10	103,000	0.00061	31.36	31.28	0.2%	0.90	0.95	0.05	5.9%
3	0.03	25	0.05	250	1.4353	0.3	10	103,000	0.00061	16.56	16.52	0.2%	0.79	0.84	0.05	5.9%
4	0.03	25	0.05	290	1.4353	0.3	10	119,480	0.00061	49.22	48.89	0.7%	2.39	2.54	0.15	6.0%
5	0.03	25	0.05	290	1.3000	0.3	10	108,214	0.00056	31.22	31.10	0.4%	1.50	1.59	0.09	6.0%
6	0.03	25	0.07	290	1.3000	0.3	10	108,214	0.00056	26.38	26.29	0.3%	1.27	1.36	0.09	7.0%
7	0.03	25	0.07	290	1.3000	0.5	10	108,214	0.00130	18.72	18.62	0.5%	1.27	1.38	0.11	8.3%
8	0.03	39	0.07	290	1.3000	0.5	10	108,214	0.00130	14.99	14.84	1.0%	1.01	1.10	0.09	8.6%
9	0.08	39	0.07	320	1.3000	0.5	10	119,409	0.00130	79.64	78.63	1.3%	2.06	2.25	0.19	8.7%
10	0.03	39	0.07	320	1.3000	0.5	10	119,409	0.00130	23.37	23.12	1.1%	2.06	2.25	0.19	8.7%
11	0.05	39	0.05	250	1.4353	0.7	10	103,000	0.00334	10.72	10.57	1.4%	0.72	0.79	0.07	9.3%
12	0.05	39	0.02	250	1.4353	0.7	10	103,000	0.00334	16.95	16.78	1.0%	1.13	1.20	0.07	6.0%
13	0.05	39	0.02	320	1.4353	0.7	10	131,840	0.00334	61.34	59.98	2.2%	4.39	4.68	0.29	6.3%
14	0.05	39	0.02	320	1.4353	0.7	20	131,840	0.00334	61.34	60.11	2.0%	4.39	4.60	0.20	4.5%
15	0.05	39	0.02	320	1.4353	0.7	23	131,840	0.00334	61.34	60.13	2.0%	4.39	4.58	0.19	4.2%
16	0.05	39	0.02	320	1.4353	0.7	50	131,840	0.00334	61.34	60.22	1.8%	4.40	4.52	0.13	2.9%
17	0.05	39	0.02	320	1.4353	0.7	200	131,840	0.00334	61.34	60.32	1.7%	4.40	4.46	0.06	1.4%
18	0.05	39	0.02	320	1.4353	0.7	16000	131,840	0.00334	61.34	60.41	1.5%	4.40	4.41	0.01	0.2%
19	0.05	39	0.02	320	1.4353	0.7	5	131,840	0.00334	61.34	59.79	2.5%	4.39	4.80	0.41	8.8%
20	0.05	39	0.02	320	1.4353	0.7	2	131,840	0.00334	61.34	59.42	3.1%	4.39	5.03	0.64	13.7%
21	0.05	39	0.02	320	1.4353	0.7	1	131,840	0.00334	61.34	59.02	3.8%	4.38	5.29	0.91	18.8%

Table 8. HEM Validation Data. Each row represents an HEM validation run. The first group of columns show the parameters used to set up the run. For all runs the liquid density was 1000 kg/m^3 and the outlet pressure was 101,000 Pa. The predicted mass flow rate was calculated, before the model ran, using Equation (145). The simulation produced a liquid mass flow rate result, once steady-state was achieved. To measure the validity of the HEM assumption, the differences in phase velocity were also recorded. Note that runs 13-21 have the same input parameters except for interphase drag coefficient. This was to isolate the effects of velocity difference on the variation from the expected mass flow rate value. These runs were used to create **Figure 21**.

Appendix C: Single Phase Simulation Code

Junction Block Code

Junction_OLD

```
function
[MassFlow,MomentumFlow,EnergyFlow,Friction,P_Ave,Ave_Vel,Ave_Rho,Ave_Temp] =
Junction_OLD(US_Temperature,US_Density,US_Velocity,US_Area,US_Length,US_Junc,
DS_Temperature,DS_Density,DS_Velocity,DS_Area,DS_Length,DS_Junc,Start,End_Pre
ssure,Last_Step,Last_2Step,US_Junc_OLD,DS_Junc_OLD,Height)
%JUNCTION This is the main function to calculate the flows and state
%between two adjacent volumes (or on a boundary condition).
%   This function finds the average temperature, pressure and velocity
%   between two volumes (or on a boundary condition), then calculates the
%   mass, momentum and energy flows between the two volumes.

%% Constants

Cv = 724.96;   % [J/kg-K]
R = 287.04;   % [J/kg-K]
expercent = 0.8;
f = 0.05;
% f = 0.00682613;
    %This constant can be adjusted to change how friction is calculated.
    %See the help for the function "FrictionCalc" for details.


%% Junction Type Determination

if End_Pressure > 0
    %% Right Boundary Condition

    A = US_Area;
    Total_L = 2*US_Length;

    if DS_Junc.PressureForce == 9999
        [Ave_Temp,Ave_Rho,Ave_Vel,P_Ave] =
Outlet_OLD(US_Temperature,US_Density,US_Velocity,DS_Temperature,DS_Density,DS
_Velocity,US_Junc,Last_Step,Last_2Step,US_Junc_OLD,expercent,R);
    else
        [Ave_Temp,Ave_Rho,Ave_Vel,P_Ave] =
Intlet_OLD(DS_Temperature,DS_Density,DS_Velocity,US_Temperature,US_Density,US
_Velocity,US_Junc,Last_Step,Last_2Step,US_Junc_OLD,expercent,R);
    end


elseif Start
    %% Left Boundary Condition

    Total_L = 2*DS_Length;
    A = DS_Area;

    if US_Junc.PressureForce == 9999
```

```
        [Ave_Temp,Ave_Rho,Ave_Vel,P_Ave] = 
Intlet_OLD(US_Temperature,US_Density,US_Velocity,DS_Temperature,DS_Density,DS
_Velocity,DS_Junc,Last_Step,Last_2Step,DS_Junc_OLD,expercent,R);
    else
        [Ave_Temp,Ave_Rho,Ave_Vel,P_Ave] = 
Outlet_OLD(DS_Temperature,DS_Density,DS_Velocity,US_Temperature,US_Density,US
_Velocity,DS_Junc,Last_Step,Last_2Step,DS_Junc_OLD,expercent,R);
    end


else
    %% Interior Cells

    [Ave_Temp,Ave_Rho,Ave_Vel,P_Ave,A,Total_L] = 
Inner_OLD(US_Temperature,US_Density,US_Velocity,US_Area,US_Length,DS_Temperat
ure,DS_Density,DS_Velocity,DS_Area,DS_Length,R);
end


%% Other Losses
    % These losses are added to the friction factor.

% f_adj = RapidExpansion(Ave_Vel,Ave_Rho,US_Area,DS_Area,A,Total_L,0);
f_adj = 0;
% P_Ave = P_Ave + 2*P_loss;

%% Flow Calculations
    % To be used by adjacent volumes.

[MassFlow,MomentumFlow,EnergyFlow,Friction] = 
FlowPropsOLD(Ave_Temp,Ave_Rho,Ave_Vel,A,Total_L,f,f_adj,Cv,R,Height);


end
```

Outlet_OLD

```
function [Ave_Temp,Ave_Rho,Ave_Vel,Ave_P] = 
Outlet_OLD(IN_Temp,IN_Rho,IN_Vel,OUT_Temp,OUT_Rho,OUT_Vel,IN_Junc,Last_Step,L
ast_2Step,Adj_Junc,expercent,R)
%OUTLET This function calculates the properties of a boundary condition that
%is letting fluid out of the model.
%   This function calculates junction properties with a real volume inlet
%   and a constant outlet.


%Property extrapolation:

Ave_Temp = 
extrapolate(IN_Temp,IN_Junc.Ave_Temp,Last_Step.Ave_Temp,Last_2Step.Ave_Temp,A
dj_Junc.Ave_Temp,IN_Temp,expercent);
```

```
Ave_Rho =
extrapolate(IN_Rho,IN_Junc.Ave_Rho,Last_Step.Ave_Rho,Last_2Step.Ave_Rho,Adj_J
unc.Ave_Rho,IN_Rho,expercent);
Ave_Vel =
extrapolate(IN_Vel,IN_Junc.Ave_Vel,Last_Step.Ave_Vel,Last_2Step.Ave_Vel,Adj_J
unc.Ave_Vel,IN_Vel,expercent);


%Calculate pressure based on type of boundary condition:

if OUT_Vel == 0
    Ave_P = OUT_Rho*OUT_Temp*R;
else
    Ave_P = Ave_Rho*Ave_Temp*R;
end

end
```

Inlet_OLD

```
function [Ave_Temp,Ave_Rho,Ave_Vel,Ave_P] =
Intlet(IN_Temp,IN_Rho,IN_Vel,OUT_Temp,OUT_Rho,OUT_Vel,OUT_Junc,Last_Step,Last
_2Step,Adj_Junc,expercent,R)
%INLET This function performs calculations for the boundary condition that
%fluid is flowing into.
%   This calculates junction properties from upstream constants and
%   properties from a real downstream cell.


%Pass Constants:

Ave_Temp = IN_Temp;
Ave_Rho = IN_Rho;
Ave_P = IN_Temp*IN_Rho*R;


%Calculate Velocity based on BC method:

if IN_Vel == 0
    Ave_Vel =
extrapolate(OUT_Vel,OUT_Junc.Ave_Vel,Last_Step.Ave_Vel,Last_2Step.Ave_Vel,Adj
_Junc.Ave_Vel,OUT_Vel,expercent);
else
    Ave_Vel = IN_Vel;
    Ave_P = 0;
end

end
```

Inner_OLD

```
function [Ave_Temp,Ave_Rho,Ave_Vel,P_Ave,A,L,Void] =
Inner_OLD(IN_Temp,IN_Rho,IN_Vel,IN_Area,IN_Length,OUT_Temp,OUT_Rho,OUT_Vel,OU
T_Area,OUT_Length,R)
%INNER This function calculates the average properties for a junction with
%two real adjacent volumes.
%   All properties are length-averaged, or calculated from length-averaged
%   properties.

[Ave_Temp,L] = LengthAve(IN_Temp,IN_Length,OUT_Temp,OUT_Length);
[Ave_Rho,~] = LengthAve(IN_Rho,IN_Length,OUT_Rho,OUT_Length);
[Ave_Vel,~] = LengthAve(IN_Vel,IN_Length,OUT_Vel,OUT_Length);
[A,~] = LengthAve(IN_Area,IN_Length,OUT_Area,OUT_Length);
% IN_Temp
% OUT_Temp
% Ave_Temp


%Pressure is calculated from the length-averaged density and temperature
%properties, rather than being calcualated for the adjacent volumes, then
%length-averaged.

P_Ave = Ave_Rho*Ave_Temp*R;

end
```

RapidExpansion

```
function [f_adj] = RapidExpansion(Ave_Vel,Ave_Rho,US_Area,DS_Area,A,L,f_adj)
%RAPIDEXPANSION This function adjusts the friction factor to account for
%the losses associated with a rapid expansion of area in the direction of
%flow.
%   If there is no rapid expansion in the direction of flow, then the f_adj
%   input is returned as output.  Otherwise, the Borda-Carnot sudden
%   expansion equation is applied.  It states that the drop in pressure,
%       Delta_P = rho*A1/A2*(1 - A1/A2)*v^2    <--V1?
%   This equation is converted into an adjusted friction factor, so that
%   when friction is applied in the adjacent volumes, the losses associated
%   with the sudden expansion are also applied.


%% Previous code
    % This was incorporated into friction factor

x = 0.77;

if Ave_Vel > 0

    if DS_Area > US_Area
        f_adj = f_adj + 4*x*(US_Area/DS_Area)*(1 -
US_Area/DS_Area)*sqrt(4*A/pi)/L;
    end
```

```
else

    if DS_Area < US_Area
        f_adj = f_adj + 4*x*(DS_Area/US_Area)*(1 -
DS_Area/US_Area)*sqrt(4*A/pi)/L;
    end

end

%% Current Code
    % Direct Pressure loss in volume

% DeltaP = 0;
%
% if Ave_Vel > 0
%
%     if DS_Area > US_Area
%         DeltaP = Ave_Rho*(US_Area/DS_Area)*(1 - US_Area/DS_Area)*Ave_Vel^2;
%     end
%
% else
%
%     if DS_Area < US_Area
%         DeltaP = Ave_Rho*(DS_Area/US_Area)*(1 - DS_Area/US_Area)*Ave_Vel^2;
%     end
%
% end

end
```

FlowPropsOLD

```
function [MassFlow,MomentumFlow,EnergyFlow,Friction] =
FlowPropsOLD(Ave_Temp,Ave_Rho,Ave_Vel,A,L,f,f_adj,Cv,R,Height)
%FLOWPROPS This function calculates the mass, momentum and energy flows
%between the adjacent volumes.  It also calculates friction.
%   These values represent the mass/momentum/energy leaving the left volume
%   and entering the right volume.  This ensures conservation.


g = 9.81;  % [m/s^2]

MassFlow = Ave_Vel*A*Ave_Rho;
MomentumFlow = MassFlow*Ave_Vel;
EnergyFlow = MassFlow*(Ave_Temp*(Cv+R) + Ave_Vel^2/2 + Height*g);
    %The above and below equations are equivalent, but are both kept for
    %reference.
%EnergyFlow = MassFlow*(T_ave*Cv + v_ave^2/2 + P_ave/rho_ave);
Friction = FrictionCalc(Ave_Temp,Ave_Rho,Ave_Vel,A,L,f,f_adj);
    %The last constant here can be adjusted to change how friction is
    %calculated.  See function help for details.
end
```

extrapolate

```
function [y00] = extrapolate(y10,y21,y01,y02,y22,bound,percent)
%EXTRAPOLATE This function extrapolates by space and time.  It does not
%allow the extrapolated value to exceed a bound by a certain percent.
%The extrapolated bound must be within (percent*bound,bound/percent).


%% Extapolate:

%% Average two first-order extrapolations:  (working, not for D,T,P BC)

% y00 = (2*y10 - y21 + 2*y01 - y02)/2;  %Saving to back up.

%% 1st Order / 1st Order Attempt
    %While estimating y11

% %Estimate y11:
%     %This is the value in the adjacent volume for the previous time step.
%
% y11 = (y21 + y01)/2;
%
%
% %Extrapolate using First-order in space and First-order in time:
%
% y00 = 2*y11 - y22;


%% Estimate y20 by time extrapolation, then find y00 by space extrapolation:
(working, not for D,T,P BC)

y20 = 2*y21 - y22;
y00 = 2*y10 - y20;

%% Define upper and lower bounds, based on sign.

if bound >= 0
    upper = bound/percent;
    lower = bound*percent;
else
    upper = bound*percent;
    lower = bound/percent;
end


%% Coerce to limits if extrapolated value is not within range.

if y00 < lower
    y00 = lower;
elseif y00 > upper
    y00 = upper;
end

end
```

LengthAve

```
function [Ave_Prop,Total] = LengthAve(US_Prop,US_Length,DS_Prop,DS_Length)
%LENGTHAVE This function averages aproperty based on the conditions in the
%adjacent cells.
%   This function is weighted by length such that the resulting property is
%   more similar to the shorter cell (the cell with the closest center).


%Find the total Length:

Total = US_Length + DS_Length;


%Average by length weighting:

Ave_Prop = (DS_Length*US_Prop + US_Length*DS_Prop)/Total;

end
```

FrictionCalc

```
function [Friction] = FrictionCalc(Ave_Temp,Ave_Rho,Ave_Vel,A,L,f,f_adj)
%FRICTIONCALC This function calculates the frictional force exerted in the
%junction, to be used by the adjacent volumes.  This function has the
%option to use different types of friction settings.
%   • If f = 0, Friction = 0, regardless of other parameters.  Use this case
%   if you are using flow without friction.
%   • If f = 1, Friction is calculated from Reynolds number.  Use this case
%   if you are using the smooth pipe calculations.
%   • For all other f, friction is calculated using a constant friction
%   factor (determined by f).


%If f = 0, do not bother with the rest of the calculations:, unless there
%is an adjustment.

if f == 0 && f_adj == 0
    Friction = 0;
else


%Calculate needed properties:

    Dh = sqrt(A*4/pi);
%     mu = 1.983e-5*sqrt(Ave_Temp/300);
% mu = 0.0005
mu = exp(578.919/(Ave_Temp - 137.546) - 3.7188);
    Re = Ave_Rho*abs(Ave_Vel)*Dh/mu;


%Calculate f based on Re, if f = 1:
    if f == 1
%         if Re <= 1189.4
%             f = 64/Re + f_adj;
%         elseif Re <= 49817.9
%             f = 0.316*Re^(-1/4) + f_adj;
%         else
%             f = 0.184*Re^(-1/5) + f_adj;
%         end
f = 0.0791*Re^(-1/4) + f_adj;
    else
        f = f + f_adj;
    end


%Calculate the force due to friction:

    Tau = Ave_Vel^2*Ave_Rho*f/8;
    Friction = -sign(Ave_Vel)*L*Dh*pi*Tau/4;
        %NOTE: the 1/4 is because L refers to the total length of both
        %adjacent volumes.  For this value to be used by volumes, it must
        %represent 1/2 of the length of a volume.

end
```

Volume Block Code

ICs

```
function [Mass,Momentum,Energy,Volume,Height] =
ICs(Temperature,Density,Velocity,Area,Length,Angle,US_Height)
SpHeatV = 724.96;   % [J/kg-K]
g = 9.81;  % [m/s^2]
Height = US_Height + Length*sin(Angle*pi/180);
H = (Height + US_Height)/2;
Volume = Area*Length;
Mass = Volume*Density;
Momentum = Mass*Velocity;
Energy = Mass*(SpHeatV*Temperature + 0.5*Velocity^2 + g*H);
```

MomentumAdj

```
function Force   =
MomentumAdj(US_Press,US_Friction,US_Area,DS_Press,DS_Friction,DS_Area,V_Area,
V_Mass,Vel,L,Angle)
%% MOMENTUMADJ
%This function calculates all the forces applied to the momentum flow in
%the volume cell.


g =  9.81; % [m/s^2]
%% Ratio
%This calculates the ratio of pressure in the x direction to total
%pressure.

US_Dh = sqrt(4*US_Area/pi);
DS_Dh = sqrt(4*DS_Area/pi);
V_Dh = sqrt(4*V_Area/pi);

% US_R = (V_Dh - US_Dh)/sqrt((V_Dh - US_Dh)^2 + 4*L^2);
% DS_R = (DS_Dh - V_Dh)/sqrt((DS_Dh - V_Dh)^2 + 4*L^2);
% US_R = 0;
% DS_R = 0;

x = 0;

%% Changing Area Calculations
%This section calculates the area difference between the current volume and
%adjacent volumes.  If this volume's cross-sectional area is larger, an
%adjustment to the pressure forces needs to be applied.

% if US_Area > 0 && DS_Area > 0
%
%     if US_Area < V_Area
%         US_Diff = V_Area - US_Area;
%         US_Diff = 0;
%     else
%         US_Diff = 0;
%         US_Area = V_Area;
%     end
```

```
%
%     if DS_Area < V_Area
%         DS_Diff = V_Area - DS_Area;
%     else
%         DS_Diff = 0;
%         DS_Area = V_Area;
%     end
%
% else
%     US_Diff = 0;
%     DS_Diff = 0;
% end


%% Pressure Balance

% Pressure = US_Press*US_Area + x*US_Diff*V_Press - DS_Press*DS_Area -
x*DS_Diff*V_Press;
% Pressure = US_Press*US_Area  - DS_Press*DS_Area;
Pressure = US_Area*US_Press + (DS_Area - US_Area)*(US_Press + DS_Press)/2 -
DS_Area*DS_Press;


%% Body Force

Fg = V_Mass*g*sin(pi*Angle/180);


%% Total Force

Force = Pressure + US_Friction + DS_Friction - Fg;


end
```

Volume

```
function [Temperature,Density,Velocity,Pressure] =
Volume(Mass,Momentum,Energy,Volume,US_Height,Height)
SpHeatV = 724.96;   % [J/kg-K]
R = 287.04;
g = 9.81;  % [m/s^2]
H = (US_Height + Height)/2;
Density = Mass/Volume;
Velocity = Momentum/Mass;
Temperature = (Energy/Mass - Velocity^2/2 - H*g)/SpHeatV;
Pressure = Density*Temperature*R;
% mu = 1.983e-5*(abs(Temperature)/300)^(1/2);
% Dh = sqrt(4*Area/pi);
% Re = Density*abs(Velocity)*Dh/mu;
% if Re <= 1189.4
%     f = 64/Re;
% else
%     f = 0.316*Re^(-1/4);
% end
% Tau = Velocity^2*Density*f/8;
% Friction = sign(Velocity)*Length*Dh*pi*Tau;
% US_P = US_VolumeProps.Density*US_VolumeProps.Temperature*R;
% DS_P = DS_VolumeProps.Density*DS_VolumeProps.Temperature*R;
% BodyForces = US_P*(Area*Length +
US_VolumeProps.Area*US_VolumeProps.Length)/(Length + US_VolumeProps.Length) -
DS_P*(Area*Length + DS_VolumeProps.Area*DS_VolumeProps.Length)/(Length +
DS_VolumeProps.Length) - Friction;
```

Simulink Images

JuncVolCombo_SP

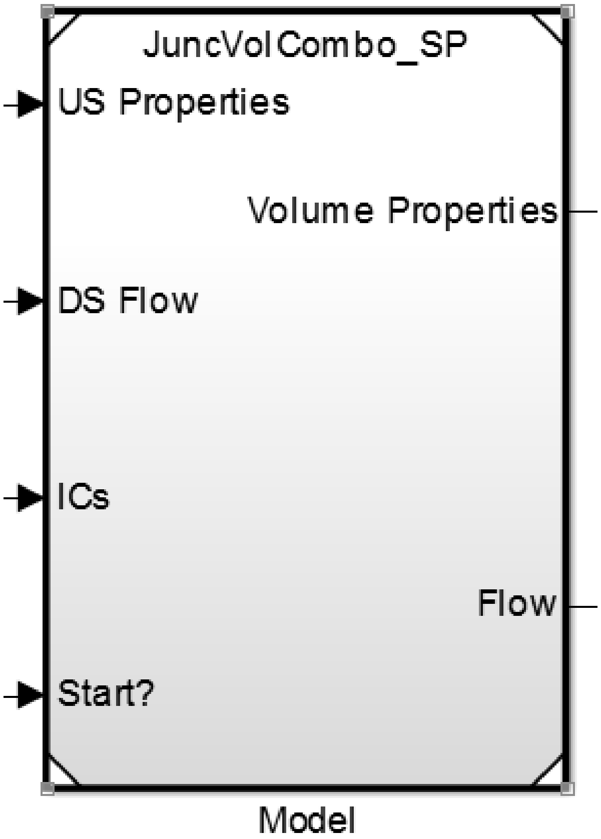

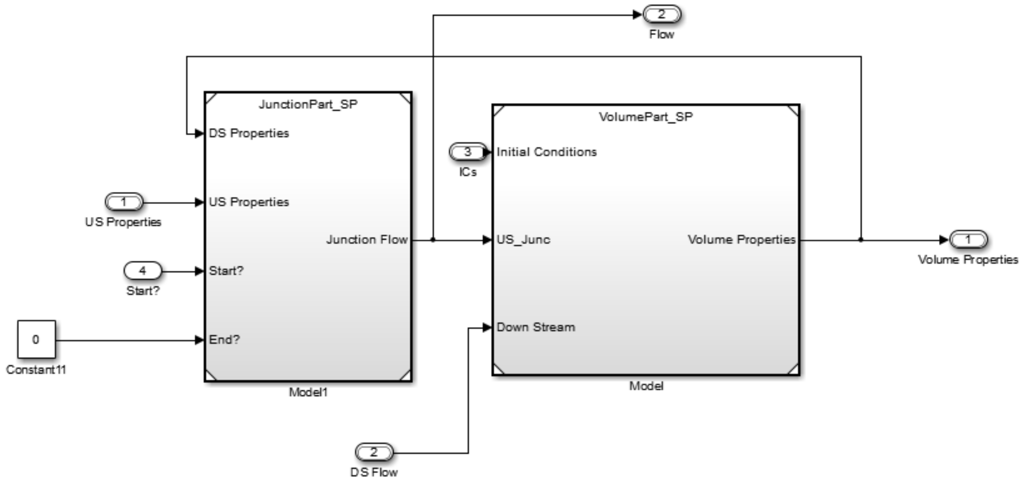

JunctionPart_SP

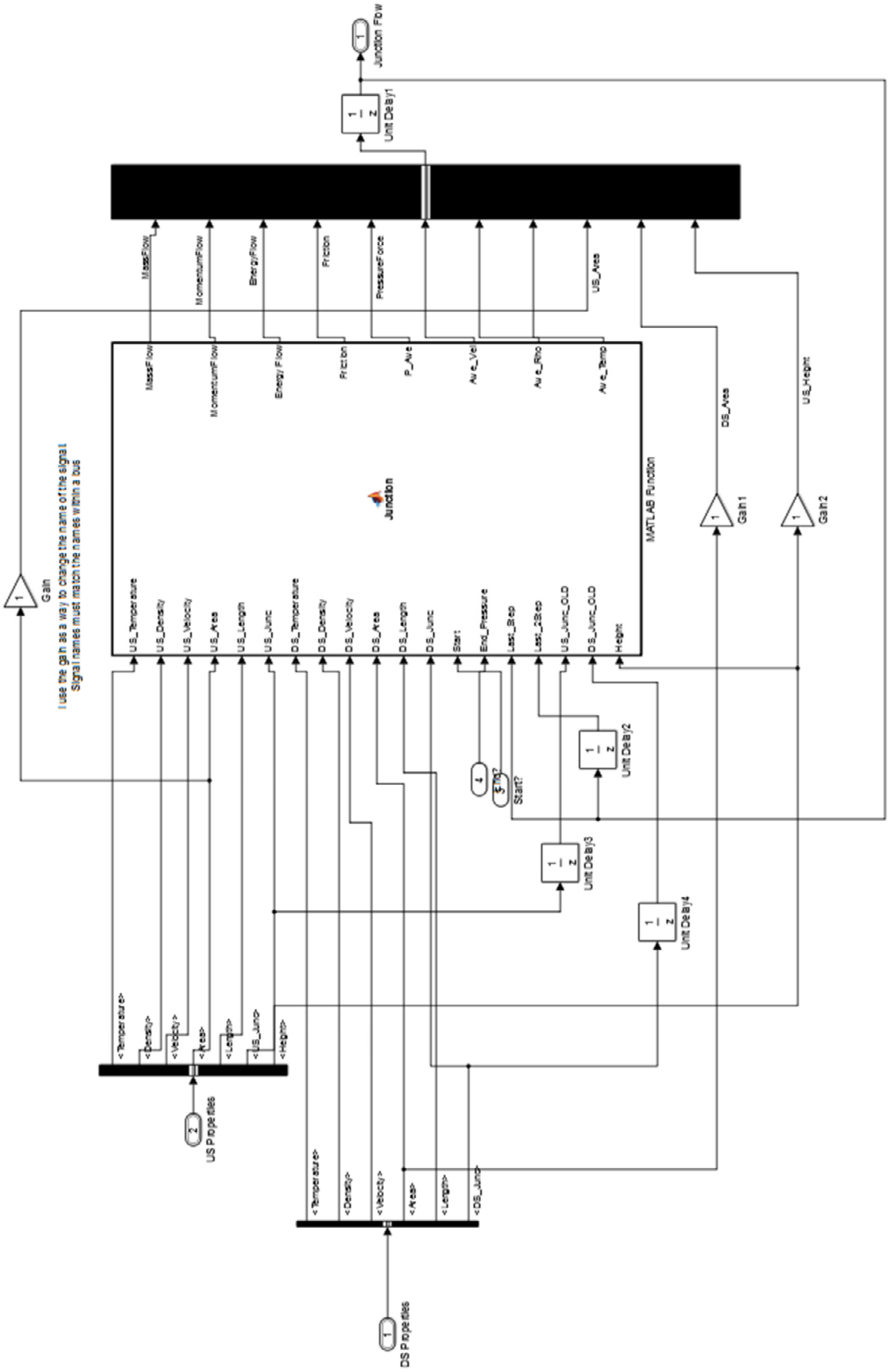

VolumePart_SP

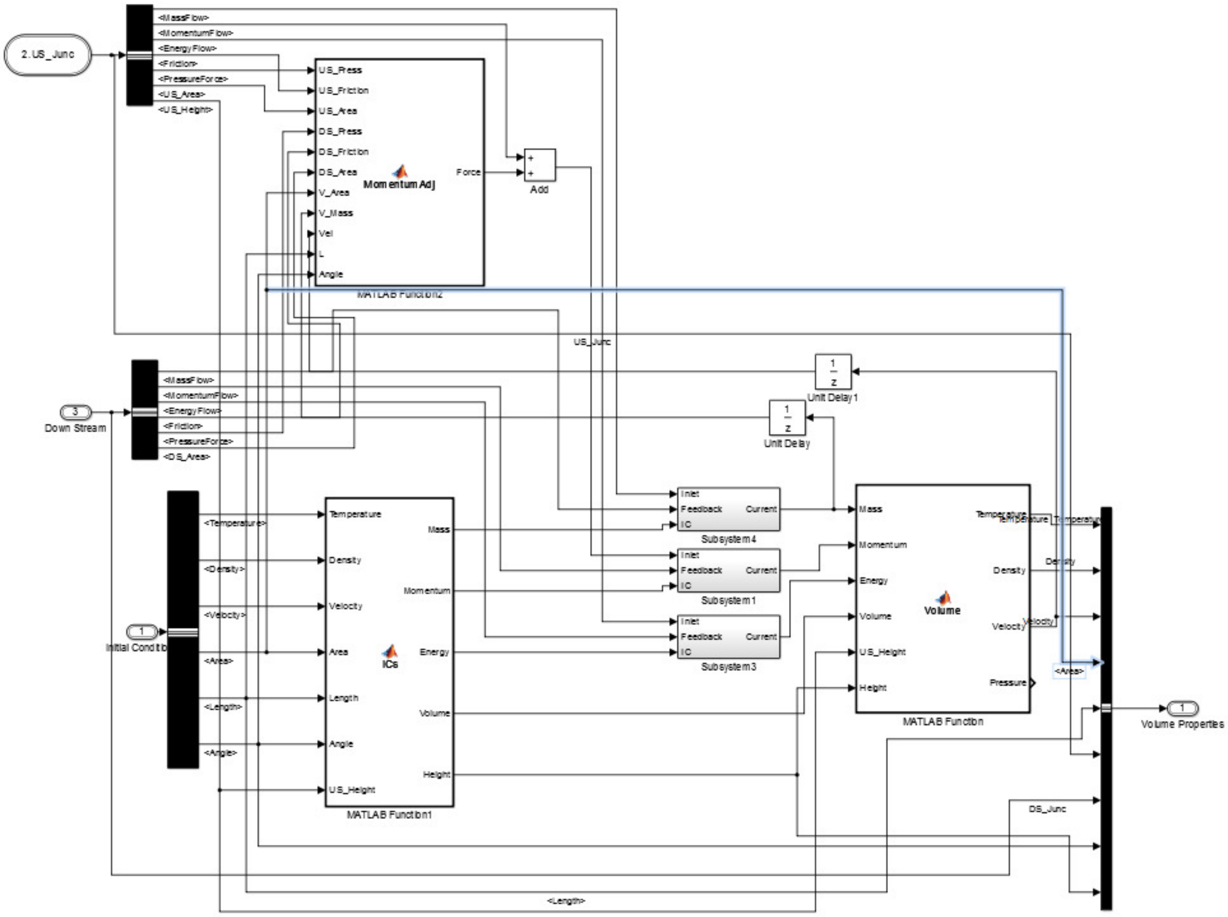

Subsystem (Integrator)

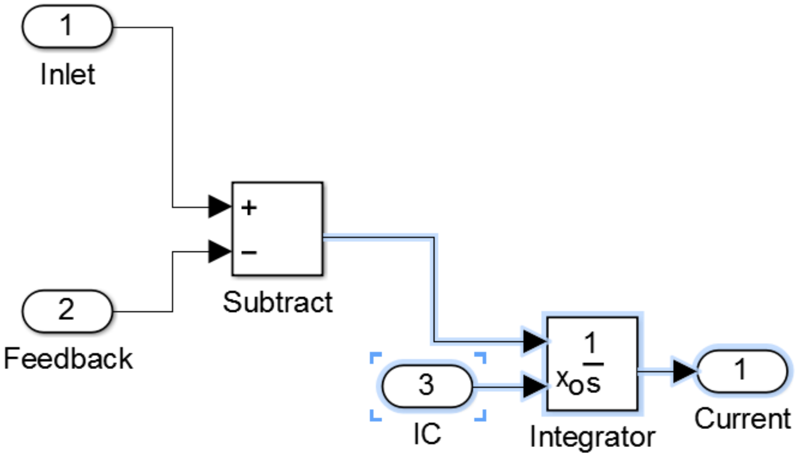

Appendix D: Two Phase Simulation Code

Please note that functions used by both the single phase and two phase simulations are only shown in "Appendix C: Single Phase Simulation Code."

Junction Block Code

Junction_V

```
function
[MassFlow,MomentumFlow,EnergyFlow,Ave_Temp,Ave_Vel,Ave_Rho,P_Ave,Void_Fractio
n] =
Junction_V(US_Temperature,US_Density,US_Velocity,US_Area,US_Length,US_Junc,DS
_Temperature,DS_Density,DS_Velocity,DS_Area,DS_Length,DS_Junc,Start,End_Press
ure,Last_Step,Last_2Step,US_Junc_OLD,DS_Junc_OLD,US_Vol,DS_Vol,Height)
%JUNCTION This is the main function to calculate the flows and state
%between two adjacent volumes (or on a boundary condition).
%   This function finds the average temperature, pressure and velocity
%   between two volumes (or on a boundary condition), then calculates the
%   mass, momentum and energy flows between the two volumes.

%% Constants

rho_water = 1000;  % [kg/m^3]
Cv = 724.96;   % [J/kg-K]
R = 287.04;   % [J/kg-K]
expercent = 0.8;
f = 0;
    %This constant can be adjusted to change how friction is calculated.
    %See the help for the function "FrictionCalc" for details.

US_Void = US_Vol.Void_Fraction;
DS_Void = US_Vol.Void_Fraction;

%% Junction Type Determination

if End_Pressure > 0
    %% Right Boundary Condition

    A = US_Area;
    Total_L = 2*US_Length;

    if End_Pressure == 9999
        [Ave_Temp,Ave_Rho,Ave_Vel,P_Ave,Void_Fraction] =
Outlet(US_Temperature,US_Density,US_Velocity,US_Void,DS_Temperature,DS_Densit
y,DS_Velocity,US_Junc,Last_Step,Last_2Step,US_Junc_OLD,expercent,R);
    else
        [Ave_Temp,Ave_Rho,Ave_Vel,P_Ave,Void_Fraction] =
Intlet(DS_Temperature,DS_Density,DS_Velocity,DS_Void,US_Temperature,US_Densit
y,US_Velocity,US_Junc,Last_Step,Last_2Step,US_Junc_OLD,expercent,R);
    end


elseif Start > 0
    %% Left Boundary Condition
    Total_L = 2*DS_Length;
    A = DS_Area;

    if Start == 9999
        [Ave_Temp,Ave_Rho,Ave_Vel,P_Ave,Void_Fraction] = 
Intlet(US_Temperature,US_Density,US_Velocity,US_Void,DS_Temperature,DS_Densit
y,DS_Velocity,DS_Junc,Last_Step,Last_2Step,DS_Junc_OLD,expercent,R);
    else
        [Ave_Temp,Ave_Rho,Ave_Vel,P_Ave,Void_Fraction] = 
Outlet(DS_Temperature,DS_Density,DS_Velocity,DS_Void,US_Temperature,US_Densit
y,US_Velocity,DS_Junc,Last_Step,Last_2Step,DS_Junc_OLD,expercent,R);
    end



else
    %% Interior Cells

    [Ave_Temp,Ave_Rho,Ave_Vel,P_Ave,A,Total_L,Void_Fraction] = 
Inner(US_Temperature,US_Density,US_Velocity,US_Area,US_Length,US_Void,DS_Temp
erature,DS_Density,DS_Velocity,DS_Area,DS_Length,DS_Void,R);
end
%% Two-phase mixing
    % Now that the average properties are determined, this section the
    % mixture ratio.

% [MassRatio,Mix_v] = 
Mixing(US_Mass_R,US_Density,US_Length,US_Area,DS_Mass_R,DS_Density,DS_Length,
DS_Area,Ave_Rho,A,rho_water);




%% Other Losses
    % These losses are added to the friction factor.

A = Void_Fraction*A;
f_adj = RapidExpansion(Ave_Vel,Ave_Rho,US_Area,DS_Area,A,Total_L,0);

% P_Ave = P_Ave + 2*P_loss;

%% Flow Calculations
    % To be used by adjacent volumes.

[MassFlow,MomentumFlow,EnergyFlow,~] = 
FlowProps(Ave_Temp,Ave_Rho,Ave_Vel,P_Ave,A,Total_L,f,f_adj,Cv,Height,A);


end
```

Junction_L

```
function [MassFlow,MomentumFlow,EnergyFlow,Friction,Ave_Temp,Ave_Vel] = 
Junction_L(US_Temperature,US_Density,US_Velocity,US_Area,US_Length,US_Junc,DS
_Temperature,DS_Density,DS_Velocity,DS_Area,DS_Length,DS_Junc,Start,End_Press
ure,Last_Step,Last_2Step,US_Junc_OLD,DS_Junc_OLD,Ave_P,Void_Fraction,Height)
%JUNCTION_L This is the main function to calculate the flows and state
%between two adjacent volumes (or on a boundary condition).
%   This function finds the average temperature, pressure and velocity
%   between two volumes (or on a boundary condition), then calculates the
%   mass, momentum and energy flows between the two volumes.

%% Constants

C_water = 4180;  % [J/kg-K]
rho_water = 1000;  % [kg/m^3]
expercent = 0.8;
f = 0.02; %0.032;
    %This constant can be adjusted to change how friction is calculated.
    %See the help for the function "FrictionCalc" for details.
VF = 0;  %Void Filler:  Void fraction is already caclulated.  Nearby void
fractions are not needed.


%% Junction Type Determination

if End_Pressure > 0
    %% Right Boundary Condition

    A = US_Area;
    Total_L = 2*US_Length;

    if End_Pressure == 9999
        [Ave_Temp,~,Ave_Vel,~,~] =
Outlet(US_Temperature,US_Density,US_Velocity,VF,DS_Temperature,DS_Density,DS_
Velocity,US_Junc,Last_Step,Last_2Step,US_Junc_OLD,expercent,0);
    else
        [Ave_Temp,~,Ave_Vel,~,~] =
Intlet(DS_Temperature,DS_Density,DS_Velocity,VF,US_Temperature,US_Density,US_
Velocity,US_Junc,Last_Step,Last_2Step,US_Junc_OLD,expercent,0);
    end


elseif Start > 0
    %% Left Boundary Condition

    Total_L = 2*DS_Length;
    A = DS_Area;

    if Start == 9999
        [Ave_Temp,~,Ave_Vel,~] =
Intlet(US_Temperature,US_Density,US_Velocity,VF,DS_Temperature,DS_Density,DS_
Velocity,DS_Junc,Last_Step,Last_2Step,DS_Junc_OLD,expercent,0);
    else
        [Ave_Temp,~,Ave_Vel,~] =
Outlet(DS_Temperature,DS_Density,DS_Velocity,VF,US_Temperature,US_Density,US_
Velocity,DS_Junc,Last_Step,Last_2Step,DS_Junc_OLD,expercent,0);
    end
```

```
else
    %% Interior Cells

    [Ave_Temp,~,Ave_Vel,~,A,Total_L] =
Inner(US_Temperature,US_Density,US_Velocity,US_Area,US_Length,VF,DS_Temperatu
re,DS_Density,DS_Velocity,DS_Area,DS_Length,VF,0);
end
%% Two-phase mixing
    % Now that the average properties are determined, this section the
    % mixture ratio.

% [MassRatio,Mix_v] =
Mixing(US_Mass_R,US_Density,US_Length,US_Area,DS_Mass_R,DS_Density,DS_Length,
DS_Area,Ave_Rho,A,rho_water);



%% Other Losses
    % These losses are added to the friction factor.

Flow_A = (1 - Void_Fraction)*A;
f_adj = RapidExpansion(Ave_Vel,rho_water,US_Area,DS_Area,A,Total_L,0);


%% Flow Calculations
    % To be used by adjacent volumes.

[MassFlow,MomentumFlow,EnergyFlow,Friction] =
FlowProps(Ave_Temp,rho_water,Ave_Vel,Ave_P,Flow_A,Total_L,f,f_adj,C_water,Hei
ght,A);

end
```

Outlet

```
function [Ave_Temp,Ave_Rho,Ave_Vel,Ave_P,Void_Fraction] =
Outlet(IN_Temp,IN_Rho,IN_Vel,IN_Void,OUT_Temp,OUT_Rho,OUT_Vel,IN_Junc,Last_St
ep,Last_2Step,Adj_Junc,expercent,R)
%OUTLET This function calculates the properties of a boundary condition that
%is letting fluid out of the model.
%   This function calculates junction properties with a real volume inlet
%   and a constant outlet.


%Property extrapolation:
% IN_Temp = IN_Temp
% J_TempIN = IN_Junc.Temp
% Last_Temp = Last_Step.Temp
% Last_2Temp = Last_2Step.Temp
% Adj_Temp = Adj_Junc.Temp
% expercent = expercent

Ave_Temp =
extrapolate(IN_Temp,IN_Junc.Temp,Last_Step.Temp,Last_2Step.Temp,Adj_Junc.Temp
,IN_Temp,expercent);
Ave_Vel =
extrapolate(IN_Vel,IN_Junc.Vel,Last_Step.Vel,Last_2Step.Vel,Adj_Junc.Vel,IN_V
el,expercent);


if isfield(IN_Junc,'Rho')
    Ave_Rho =
extrapolate(IN_Rho,IN_Junc.Rho,Last_Step.Rho,Last_2Step.Rho,Adj_Junc.Rho,IN_R
ho,expercent);
    Void_Fraction =
extrapolate(IN_Void,IN_Junc.Void_Fraction,Last_Step.Void_Fraction,Last_2Step.
Void_Fraction,Adj_Junc.Void_Fraction,IN_Void,expercent);
%     disp('The average temperature is')
%     Ave_Temp = Ave_Temp
    %Calculate pressure based on type of boundary condition:
else
    Ave_Rho = IN_Rho;
    Void_Fraction = 0;
%     disp('Liquid Temp:')
%     Ave_Temp = Ave_Temp
end

if OUT_Vel == 0
    Ave_P = OUT_Rho*OUT_Temp*R;
else
    Ave_P = Ave_Rho*Ave_Temp*R;
end


end
```

Inlet

```
function [Ave_Temp,Ave_Rho,Ave_Vel,Ave_P,Void_Fraction] =
Intlet(IN_Temp,IN_Rho,IN_Vel,IN_Void,OUT_Temp,OUT_Rho,OUT_Vel,OUT_Junc,Last_S
tep,Last_2Step,Adj_Junc,expercent,R)
%INLET This function performs calculations for the boundary condition that
%fluid is flowing into.
%   This calculates junction properties from upstream constants and
%   properties from a real downstream cell.


%Pass Constants:

Ave_Temp = IN_Temp;
Ave_Rho = IN_Rho;
Ave_P = IN_Temp*IN_Rho*R;
Void_Fraction = IN_Void;
```

```
%Calculate Velocity based on BC method:

if IN_Vel == 0
    Ave_Vel =
extrapolate(OUT_Vel,OUT_Junc.Vel,Last_Step.Vel,Last_2Step.Vel,Adj_Junc.Vel,OU
T_Vel,expercent);
else
    Ave_Vel = IN_Vel;
    Ave_P = 0;
end

end
```

Inner

```
function [Ave_Temp,Ave_Rho,Ave_Vel,P_Ave,A,L,Void] =
Inner(IN_Temp,IN_Rho,IN_Vel,IN_Area,IN_Length,IN_Void,OUT_Temp,OUT_Rho,OUT_Ve
l,OUT_Area,OUT_Length,OUT_Void,R)
%INNER This function calculates the average properties for a junction with
%two real adjacent volumes.
%   All properties are length-averaged, or calculated from length-averaged
%   properties.

[Ave_Temp,L] = LengthAve(IN_Temp,IN_Length,OUT_Temp,OUT_Length);
[Ave_Rho,~] = LengthAve(IN_Rho,IN_Length,OUT_Rho,OUT_Length);
[Ave_Vel,~] = LengthAve(IN_Vel,IN_Length,OUT_Vel,OUT_Length);
[A,~] = LengthAve(IN_Area,IN_Length,OUT_Area,OUT_Length);
[Void,~] = LengthAve(IN_Void,IN_Length,OUT_Void,OUT_Length);
% IN_Temp
% OUT_Temp
% Ave_Temp


%Pressure is calculated from the length-averaged density and temperature
%properties, rather than being calcualated for the adjacent volumes, then
%length-averaged.

P_Ave = Ave_Rho*Ave_Temp*R;

end
```

FlowProps

```
function [MassFlow,MomentumFlow,EnergyFlow,Friction] =
FlowProps(Ave_Temp,Ave_Rho,Ave_Vel,Ave_P,A,L,f,f_adj,C,Height,Friction_A)
%FLOWPROPS This function calculates the mass, momentum and energy flows
%between the adjacent volumes.  It also calculates friction.
%   These values represent the mass/momentum/energy leaving the left volume
%   and entering the right volume.  This ensures conservation.

g = 9.81;  % [m/s^2]

MassFlow = Ave_Vel*A*Ave_Rho;
```

```
MomentumFlow = MassFlow*Ave_Vel;
% EnergyFlow = MassFlow*(Ave_Temp*(Cv+R) + Ave_Vel^2/2);
    %The above and below equations are equivalent, but are both kept for
    %reference.
EnergyFlow = MassFlow*(Ave_Temp*C + Ave_Vel^2/2 + Ave_P/Ave_Rho + Height*g);
Friction = FrictionCalc(Ave_Temp,Ave_Rho,Ave_Vel,Friction_A,L,f,f_adj);
    %The last constant here can be adjusted to change how friction is
    %calculated.  See function help for details.
end
```

Volume Block Code

ics

```
function [Mass_L,Mom_L,Energy_L,Mass_V,Mom_V,Energy_V,Volume,Height] =
ics(Vapor,Liquid,Void_Fraction,Area,Length,US_Height,Angle)
%ICS This block calculates the initial conditions in terms of initial
%masses, momentums and energies.
%   Should make this only execute once.

%% Constants

Rho_water = 1000;  %[kg/m^3]
C_L = 4180; % J/kg-K
Cv = 724.96;  % [J/kg-K]
g = 9.81;  % [m/s^2]

%% Find Volumes

Volume = Area*Length;
Volume_L = (1 - Void_Fraction)*Volume;
Volume_V = Void_Fraction*Volume;


%% Determine Masses

Mass_L = Volume_L*Rho_water;
Mass_V = Volume_V*Vapor.Rho;


%% Determine Momentums

Mom_L = Mass_L*Liquid.Vel;
Mom_V = Mass_V*Vapor.Vel;


%% Find Volume's Exit Height

Height = US_Height + sin(Angle*pi/180)*Length;


%% Determine Energies

Energy_L = Mass_L*(C_L*Liquid.Temp + 0.5*Liquid.Vel^2 + (Height +
US_Height)*g/2);
Energy_V = Mass_V*(Cv*Vapor.Temp + 0.5*Vapor.Vel^2 + (Height +
US_Height)*g/2);

end
```

flowadjustments

```
function
[Mass_L_IN,Mass_L_OUT,Momentum_L_IN,Momentum_L_OUT,Energy_L_IN,Energy_L_OUT,M
ass_V_IN,Mass_V_OUT,Momentum_V_IN,Momentum_V_OUT,Energy_V_IN,Energy_V_OUT] =
flowadjustments(US_Junction,DS_Junction,VolumeData,Area,Length,Angle)
%FLOWADJUSTMENTS  This function takes the upstream and downstream flows and
%determines the change in mass, momentum and energy for the volume.
%   Inputs are busses that are split once they enter this function.



%% Constants

rho_water = 1000;
R = 287.04;

Vol_Press = VolumeData.Vapor.Press;
Void_Fraction = VolumeData.Void_Fraction;
Vapor_Vel = VolumeData.Vapor.Vel;
Vapor_Temp = VolumeData.Vapor.Temp;
Vapor_Rho = VolumeData.Vapor.Rho;
Liquid_Vel = VolumeData.Liquid.Vel;
Liquid_Temp = VolumeData.Liquid.Temp;

%% Mass Balance
    % This section will contain the logic for mass transfer between liquid
    % and vapor in the future.

Mass_L_IN = US_Junction.MassFlow_L;
Mass_L_OUT = DS_Junction.MassFlow_L;
Mass_V_IN = US_Junction.MassFlow_V;
Mass_V_OUT = DS_Junction.MassFlow_V;




%% Changing Area Calculations
%This section calculates the area difference between the current volume and
%adjacent volumes.  If this volume's cross-sectional area is larger, an
%adjustment to the pressure forces needs to be applied.

US_Area = US_Junction.US_Area;
DS_Area = DS_Junction.DS_Area;
US_Press = US_Junction.Pressure;
DS_Press = DS_Junction.Pressure;
US_VF = US_Junction.Void_Fraction;
DS_VF = DS_Junction.Void_Fraction;
Dh = 2*sqrt(Area/pi);

% if US_Area > 0 && DS_Area > 0
%
%     if US_Area < Area
%         US_Diff = Area - US_Area;
%     else
%         US_Diff = 0;
%         US_Area = Area;
%     end
%
%     if DS_Area < Area
%         DS_Diff = Area - DS_Area;
%     else
%         DS_Diff = 0;
%         DS_Area = Area;
%     end
%
% else
%     US_Diff = 0;
%     DS_Diff = 0;
% end


%% Pressure Calculations

% Pressure = US_Junction.Pressure*US_Area + US_Diff*Vol_Press -
DS_Junction.Pressure*DS_Area - DS_Diff*Vol_Press;
US_V_A = US_VF*US_Area;
DS_V_A = DS_VF*DS_Area;
US_L_A = (1 - US_VF)*US_Area;
DS_L_A = (1 - DS_VF)*DS_Area;
Pressure_Vapor = US_V_A*US_Press + (DS_V_A - US_V_A)*(US_Press + DS_Press)/2
- DS_V_A*DS_Press;
Pressure_Liquid = US_L_A*US_Press + (DS_L_A - US_L_A)*(US_Press + DS_Press)/2
- DS_L_A*DS_Press;

%% Interphase Drag

f_int = 1;
deltaV = Vapor_Vel - Liquid_Vel;
drag = f_int*Void_Fraction*(1 -
Void_Fraction)*rho_water*sign(deltaV)*deltaV^2/Dh;
dragforce = drag*Area*Length;
% dragforce = 10*deltaV;
% Dh_int = sqrt(Void_Fraction*Area*4/pi);
% Tau_int = deltaV^2*Vapor_Rho*f_int/8;
% dragforce = sign(deltaV)*Length*Dh_int*pi*Tau_int;


%% Interphase Heat Transfer

h = 50000;  % [W/m^3-K]
Delta_T = Vapor_Temp - Liquid_Temp;
Q_dot = h*Delta_T*Void_Fraction*(1 - Void_Fraction)*Area*Length;


%% Energy Balance

% Work (rate) Done by friction:
    % W_out,V = V_vap * F_d
    % W_in,L  = V_liq * F_d
    % W_lost  = (V_vap - V_liq) * F_d
    % Assuming energy dissapates into both phases equally, half of "lost"
    % energy stays in the vapor phase.

% Net energy transfered from Vapor to liquid:
W_net = dragforce*(Liquid_Vel + Vapor_Vel)/2;

% Work (rate) Done by expansion (changing volume of a fluid)
    %W = P*dVol/dt
    %dVol_L/dt = m_dot_L/rho_L

Ave_VF = (US_VF + DS_VF)/2;
W_exp = Vol_Press*(Mass_L_IN - Mass_L_OUT)/rho_water +
0.5*R*Vapor_Temp*(Vapor_Rho*(Mass_L_IN - Mass_L_OUT)/rho_water + (Mass_L_IN -
Mass_L_OUT))*(Area*Length)*(1 - 2*Ave_VF);

% This work term matches the kinetic energy transfer due to drag force.
% If energy was kept the same, then internal energy would increase/decrease
% based on the momentum change.  By transfering energy from one phase or
% another, only velocity is affected by friction.

Energy_L_IN = US_Junction.EnergyFlow_L + Q_dot + W_net + W_exp;
Energy_L_OUT = DS_Junction.EnergyFlow_L;
Energy_V_IN = US_Junction.EnergyFlow_V - Q_dot - W_net - W_exp;
Energy_V_OUT = DS_Junction.EnergyFlow_V;


%% Body Forces

Weight_L = rho_water*Area*Length*(1 - Void_Fraction)*sin(Angle*pi/180);
Weight_V = Vapor_Rho*Area*Length*Void_Fraction*sin(Angle*pi/180);


%% Momentum Balance

% massfrac = Void_Fraction*Vapor_Rho/((1-Void_Fraction)*rho_water);

Momentum_L_IN = US_Junction.MomentumFlow_L + Pressure_Liquid +
US_Junction.Friction + DS_Junction.Friction + dragforce - Weight_L;
Momentum_L_OUT = DS_Junction.MomentumFlow_L;
Momentum_V_IN = US_Junction.MomentumFlow_V + Pressure_Vapor - dragforce -
Weight_V;
Momentum_V_OUT = DS_Junction.MomentumFlow_V;


end
```

Volume

```
function
[Vapor_Temp,Vapor_Vel,Vapor_Rho,Vapor_Press,Liquid_Temp,Liquid_Vel,Void_Fract
ion] = Volume(Mass_L,Mom_L,Energy_L,Mass_V,Mom_V,Energy_V,Vol,Height)
%VOLUME This function uses the mass, momentum and energy present within a
```

```
%volume to calculate the properties of the liquid and vapor present.
%   The output is 2 busses.  Vapor contains the vapor properties of the
%   volume (Density, Temperature, Pressure, Velocity) and Liquid contains
%   the liquid properties (Temperature and Velocity).

%% Constants

Rho_L = 1000;  % [kg/m^3]
C_L = 4180;  % [J/kg-K]
Cv = 724.96;  % [J/kg-K]
R = 287.04;  % [J/kg-K]


%% Find Void Fraction

if Mass_L > 0
    Void_Fraction = 1 - Mass_L/(Rho_L*Vol);
else
    Void_Fraction = 1;
end


%% Determine Liquid Properties

[Liquid_Temp,Liquid_Vel] = tempvel(Mass_L,Mom_L,Energy_L,C_L,Height);


%% Determine Vapor Properties

Vapor_Rho = Mass_V/(Void_Fraction*Vol);
[Vapor_Temp,Vapor_Vel] = tempvel(Mass_V,Mom_V,Energy_V,Cv,Height);
Vapor_Press = Vapor_Rho*Vapor_Temp*R;


end
```

---

tempvel

```
function [Temperature,Velocity] = tempvel(Mass,Momentum,Energy,C,Height)
%TEMPVEL This function calculates temperature and velocity.
%   Formulations for liquid and vapor are the same.

g = 9.81;  % [m/s^2]

Velocity = Momentum/Mass;
Temperature = (Energy/Mass - Velocity^2/2 - Height*g)/C;

end
```

Simulink Images

JuncVolCombo

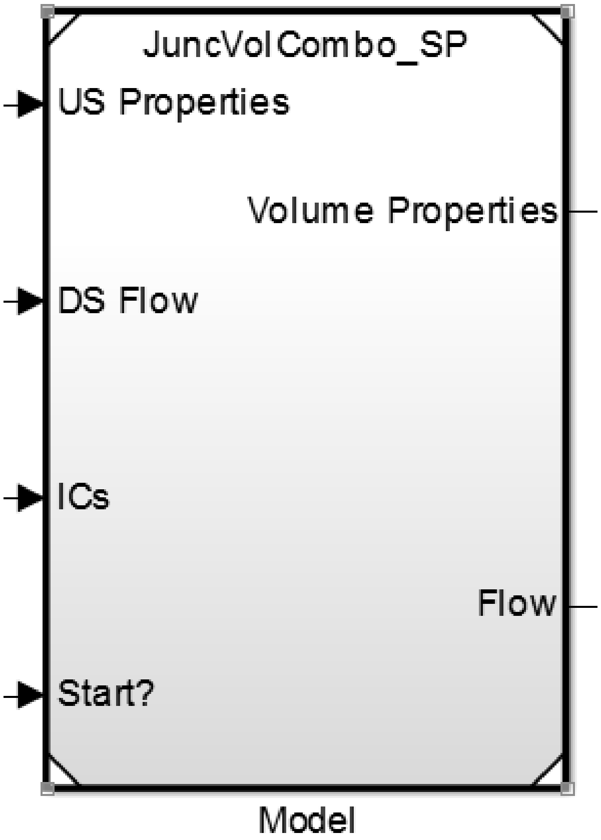

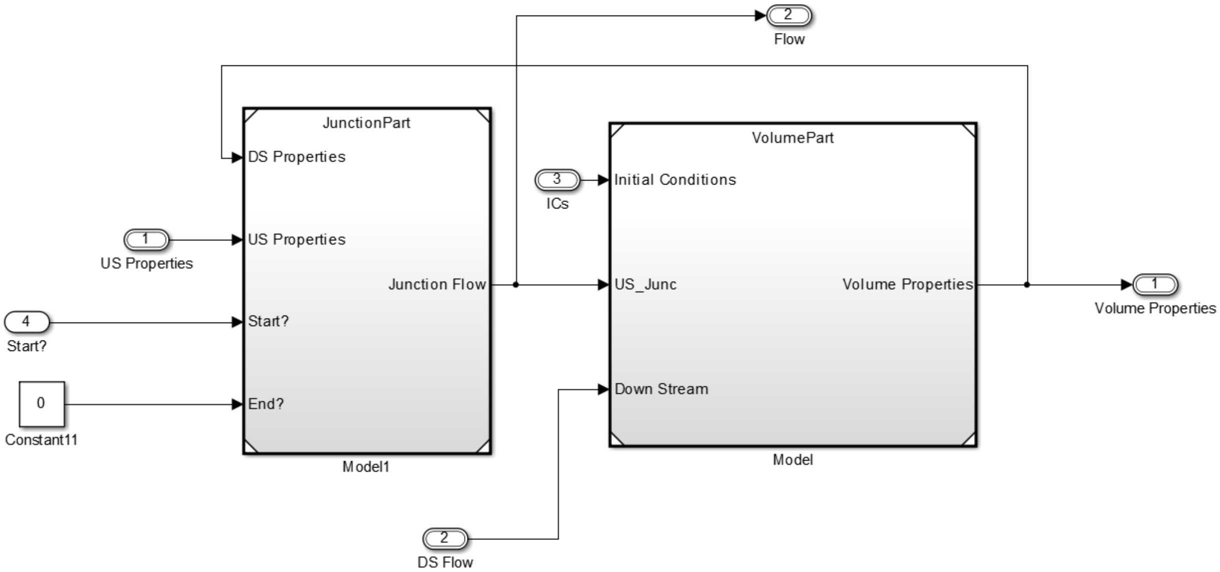

JunctionPart

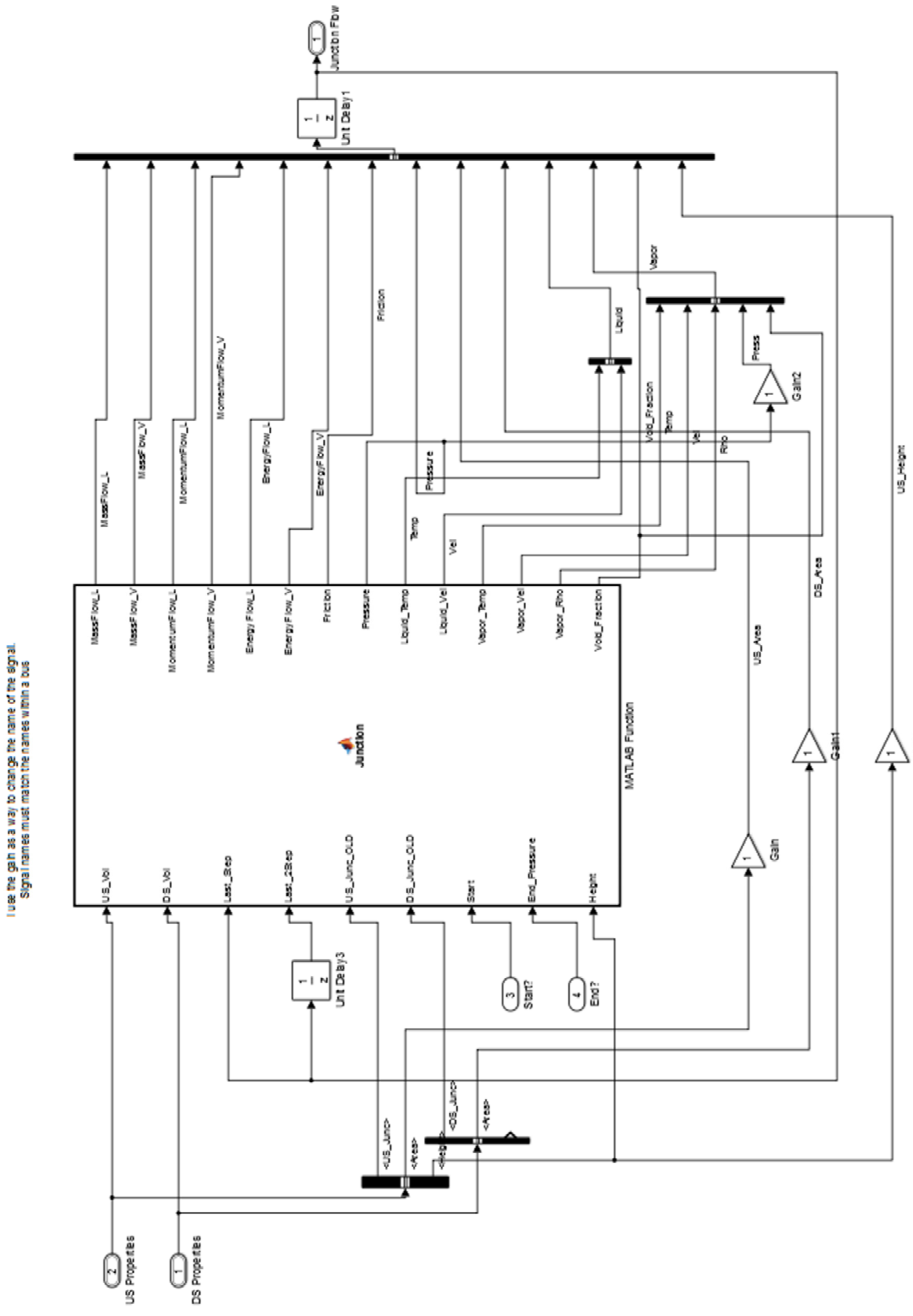
I use the gain as a way to change the name of the signal.
Signal names must match the names within a bus

VolumePart

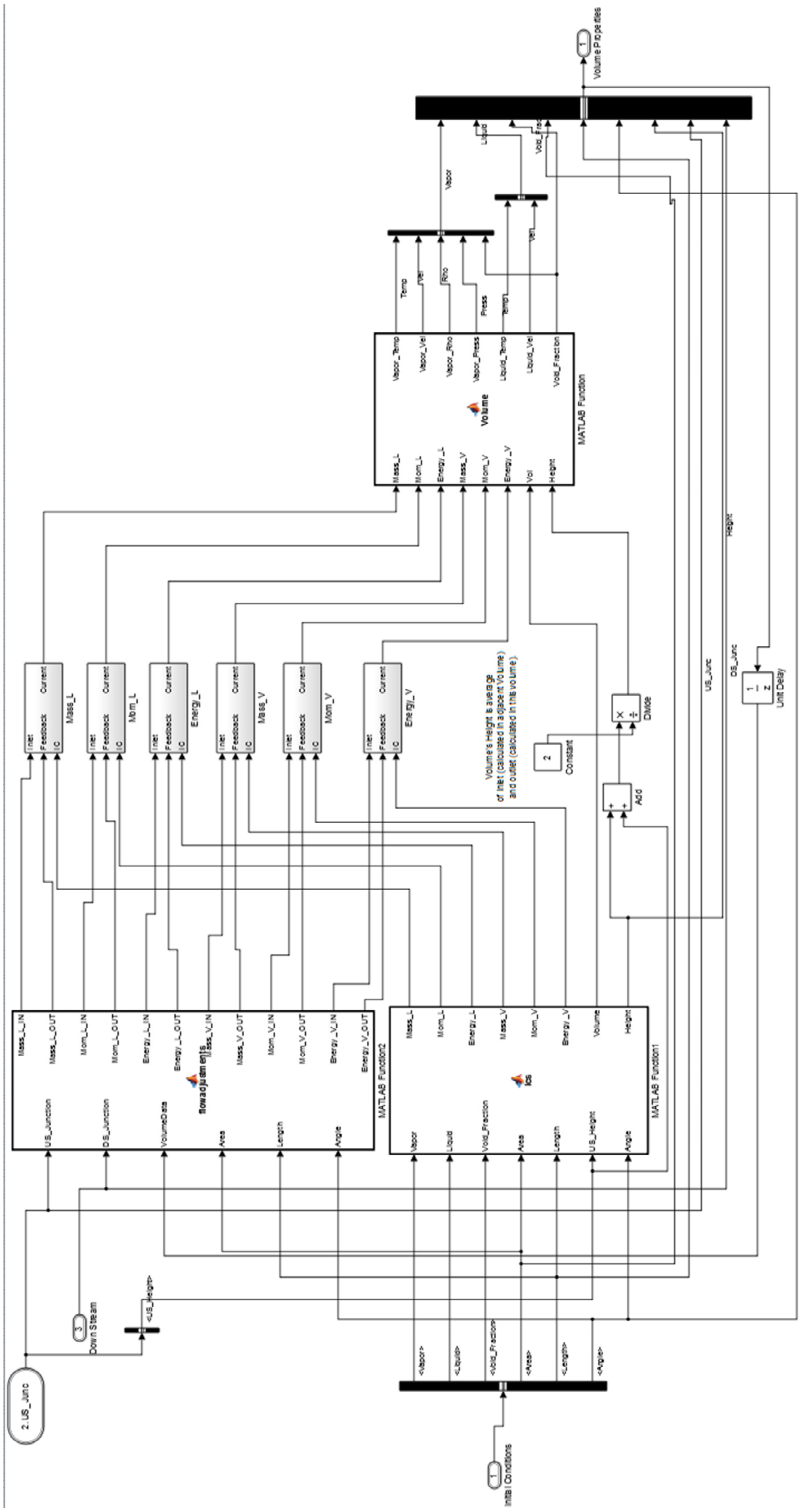

1
Volume Properties
Vapor
Liquid
Void_Frac
Temp
Vel
Rho
Press
Temp
Vel
Mass_L
Mom_L
Energy_L
Mass_V
Mom_V
Energy_V
Vol
Height
Volume
Vapor_Temp
Vapor_Vel
Vapor_Rho
Vapor_Press
Liquid_Temp
Liquid_Vel
Void_Fraction
MATLAB Function
Height
Inlet
Feedback
IC
Current
Mass_L
Mom_L
Energy_L
Mass_V
Mom_V
Energy_V
Volume's Height is average
of inlet (calculated in adjacent Volume)
and outlet (calculated in this volume)
2
Constant
Add
Divide
US_Junc
DS_Junc
1/z
Unit Delay
US_Junction
DS_Junction
VolumeData
Area
Length
Angle
flowadjustments
Mass_L_IN
Mass_L_OUT
Mom_L_IN
Mom_L_OUT
Energy_L_IN
Energy_L_OUT
Mass_V_IN
Mass_V_OUT
Mom_V_IN
Mom_V_OUT
Energy_V_IN
Energy_V_OUT
MATLAB Function2
Vapor
Liquid
Void_Fraction
Area
Length
US_Height
Angle
ics
Mass_L
Mom_L
Energy_L
Mass_V
Mom_V
Energy_V
Volume
Height
MATLAB Function1
2. US_Junc
3
Down Steam
<US_Height>
<Vapor>
<Liquid>
<Void_Fraction>
<Area>
<Length>
<Angle>
1
Initial Conditions